Mechanistic study of oxygen atom transfer catalyzed by rhenium compounds

by

Xiaopeng Shan

A dissertation submitted to the graduate faculty

in partial fulfillment of the requirements for the degree of

DOCTOR OF PHILOSOPHY

Major: Inorganic Chemistry

Program of Study Committee:
James H. Espenson, Major Professor
Douglas K. Finnemore
William S. Jenks
John G. Verkade
Keith Woo

Iowa State University

Ames, Iowa

2003

Graduate College
Iowa State University

This is to certify that the doctoral dissertation of

Xiaopeng Shan

has met the dissertation requirements of Iowa State University

James H. Espenson
Major Professor

Gary J. Miller
For the Major Program

TABLE OF CONTENTS

GENERAL INTRODUCTION

Introduction

Oxygen atom transfer (OAT) catalyzed by transition metal complexes has received extensive attention from inorganic and bioinorganic chemists for decades due to its contribution to biochemistry and industrial applications.[1-3] Molybdenum(IV/VI) and tungsten(IV/VI) complexes have been widely explored because of their important roles in oxo-transferases.[2,4-6] To the contrary, rhenium(V/VII), as a neighbor, only has been explored only to a limited extent.[7]

A rhenium(V) dimer, $\{MeReO(mtp)\}_2$, a model of a proposed intermediate for sulfur transfer reaction, was synthesized from methyltrioxorhenium(VII), abbreviated MTO, and $mtpH_2$, 2-(mercaptomethyl) thiophenol (o-$HSC_6H_4CH_2SH$).[8] Lewis bases, pyridines and phosphanes, were found to monomerize $\{MeReO(mtp)\}_2$, giving rise to MeReO(mtp)L (L = Lewis base).[9-11] All of these rhenium(V) complexes are able to catalyze OAT reactions, especially $MeReO(mtp)PPh_3$, showing remarkable reactivity for reaction between pyridine N-oxides and phsophanes in eq 1.[12-14]

$$PyO + PZ_3 \rightarrow Py + OPZ_3 \qquad (1)$$

A notable feature of these rhenium(V) complexes is the five-coordinate distorted square pyramidal structure in chart 1. The rhenium atom is surrounded by the terminal oxo group at the axial position and a basal plane defined by a methyl, two thiolate and one thioether sulfur atom for the dimer, or a Lewis base for monomers. There is vacant position trans to the terminal oxo group, from which substrates access rhenium as well as the departure of the products.

Chart 1

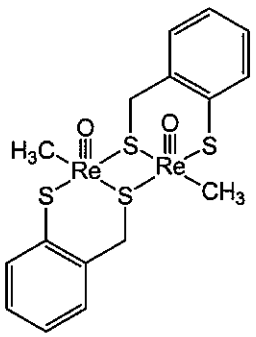	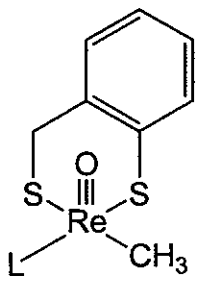
{MeReO(mtp)}$_2$	MeReO(mtp)L

Aside from studies on OAT, in Chapter I, we described an unique methyl transfer from rhenium to thiolate sulfur, which occurs during the oxidation of MeReO(edt)PPh_3 with sulfoxides and the reaction of MTO with 1,2-ethanedithiol as well. Only a few precedents exist for this type of methyl transfer. An example is the conversion of D,L-homocystein, $HS(CH_2)_2CHNH_2CO_2H$, to L-methionine, $MeS(CH_2)_2CHNH_2CO_2H$ with methylcobalamin and methylcobinamide, which is catalyzed by Vitamin B_{12}, modeled by methyl-bis(dimethylglyoximato)cobalt(III) and related complexes which are able to convert thiols to thioethers. The new reactions of rhenium complexes, reported in Chapter I, give sound evidence for the analogous conversion, which affords further mechanistic understanding of methyl transfer. Although the structure of ReO(κ^2-edt)(κ^2-edtMe) was unsolved, evidence from NMR, UV spectra for oxidation products by H_2O_2 and structure of further ligand displacement product of ReO(κ^2-edt)(κ^1-edtMe)TPA all proved that the methyl group, originally on rhenium in MeReO(edt)PPh_3 or MTO, transfers to thiolate sulfur. On the basis of kinetic information and a literature study, a reductive methyl transfer mechanism was proposed.

Often a monoanionic bidentate ligand is employed for the study of the coordination chemistry of rhenium for the radiotherapeutic applications of the β-emitting isotopes ^{186}Re

and ^{188}Re, containing a {$Re^{V}O$} core without methyl group. Typical donor atom pairs are P,O (HPO = phosphinocarboxylic acid); N,O (HNO = e.g., picolinic acid or 8-hydroxyquinoline); and N,S (HNS = 2-mercaptoquinoline). In Chapter II, we described syntheses and characterization of four methyloxorhenium(V) complexes: $MeReO(PA)_2$, $MeReO(HQ)_2$, $MeReO(MQ)_2$, and $MeReO(DPPB)_2$ (in which PAH = 2-picolinic acid, HQH = 8-hydroxyquinoline, MQH = 8-mercaptoquinoline, and DPPBH = diphenylphosphinobenzoic acid). These compounds catalyze the sulfoxidation of thioethers by pyridine N-oxides and sulfoxides. Here we report kinetic and mechanistic studies of the latter reaction. The trapping of a transient dioxorhenium(VII) species was performed.

To extend our exploration of rhenium catalysts, in Chapter III we describe the formation and characterization of three methyl(oxo)rhenium(V) complexes; two contain the anion $MeReO(edt)(SPh)^{-}$ with the cations 2-picolinium and 2,6-lutidinium, and the third is a neutral rhenium compound, MeReO(edt)(tmtu), where edt stands for 1,2-ethanedithiolate and tmtu for 1,1,3,3-tetramethylthiourea. To understand the OAT process catalyzed by $MeReO(mtp)PPh_3$, which is described early, it is important to investigate the steps of OAT from pyridine N-oxides to rhenium catalyst separately, including a study of the intermediates MeReO(edt)PyO from ligand displacement and $MeReO_2$(edt)PyO from oxidation. An especially the striking feature is that nucleophiles assist oxidation by incorporation of a second molecule of pyridine N-oxide in the transition state. The ionic compound was found to be suitable for this purpose because formation of both intermediates can be clearly separated and kinetically investigated. To extend an understanding of ligand displacement, the non-oxidizing ligands pyridines and PPh_3 were employed as well. An unanticipated assistance of ligand displacement of ionic compound by Brønsted bases was discovered and studied.

As an essential step in OAT and an important part of rhenium chemistry, ligand displacement has attracted our attention. In Chapters IV and V, kinetic and equilibrium studies of ligand displacements of MeReO(dithiolato)Py and $ReO(\kappa^2\text{-edt})(\kappa^2\text{-edtMe})$ were performed. In Chapter IV, equilibrium and rate constants have been determined for this family of ligand displacement reactions of previously-prepared five-coordinate, square-pyramidal rhenium(V) complexes:

$$MeReO(dt)Py + PZ_3 = MeReO(dt)(PZ_3) + Py \quad (2)$$

In this equation, PZ_3 denotes a generalized phosphane (Z = aryl, alkyl), often $P(C_6H_4\text{-}4\text{-}Y)_3$ with subsituent Y, Py is a generalized pyridine, $4\text{-}X\text{-}C_5H_4N$ with subsituent X and dt represents either 1,2-ethanedithiolate or 1,3-propanedithiolate. We have evaluated equilibrium constants for reaction 2, and correlated them by a two-variable linear free-energy relationship. The rate constants for eq 2 were also evaluated, but their interpretation was less straightforward. A multiple-substituent correlation analysis, authenticated for certain organic reactions, was not particularly satisfactory. The answer lies in a multiple step mechanism, in which the rate controlling step may vary with the influence of the substituent on the entering ligand.

In Chapter V, we report the kinetics and mechanism of ligand (phosphane) displacement (eq 3) of the thioether sulfur to generate a phosphane-rhenium(V) compound.

$$ReO(\kappa^2\text{-edt})(\kappa^2\text{-edtMe}) + PZ_3 = ReO(\kappa^2\text{-edt})(\kappa^1\text{-edtMe})(PZ_3) \quad (3)$$

Hammett analysis for both equilibrium and rate constants revealed that an early transition state was involved in the reaction. Also, sulfur inversion of the thioether ligand has been observed as a line-broadening effect of proton residual of the methyl on thiolate sulfur. A planar intermediate was proposed for sulfur inversion, derived from the comparison of activation energy parameters of ligand displacement and sulfur inversion.

The study of OAT catalyzed by rhenium(V) complexes revealed that the oxidation of rhenium(V) complexes to rhenium(VII) is an essential step in the catalytic cycle. Steric demand is always an important issue for such catalysts. Different ligands for rhenium(V) complexes have been employed, especially those with "3+1", "3+2" and "3+1+1" coordination shells, where "3", "2", "1" represent tri-, bi-, and mono-dentate ligands. They differ in geometry as well as coordination number. In Chapter VI, we describe the syntheses and characterization of four new rhenium(V) compounds with tridentate chelating ligands: 2-mercaptoethyl thioether, 2-mercaptoethyl ether, thioldiglycolic acid and 2-(salicylideneamino)benzoic acid, abbreviated as HSSSH, HSOSH, HOSOH and HONOH respectively. Compounds MeReO(SSS) and MeReO(SOS) have a five-coordinate distorted pentagonal pyramidal geometry about rhenium. To the contrary, $MeReO(OSO)(PZ_3)$ and $MeReO(ONO)(PPh_3)$ are six-coordinate compounds with distorted octahedral structures. The

oxidation of three of these compounds was investigated and followed different rate laws. These mechanistic differences have been interpreted as reflecting the different steric demands of five- and six-coordination shells.

During the period 1998-2003, around two dozen rhenium complexes were synthesized and characterized in our group. In Chapter VII, we summarized the syntheses of rhenium complexes including some unpublished results. The criteria for syntheses were discussed as well, which lie in two issues. First, rhenium(VII) in MTO needs to be reduced to rhenium(V). Usually thiols, phosphanes and even sulfides were employed as reducing reagent. Second, suitable ligands must be used to stabilize rhenium(V). As is well known, methyldioxorhenium(V) does not persist in solution, but it can be readily oxidized by oxidants such as dioxygen, pyridine N-oxides, sulfoxides, nitrate and even perchlorate etc.[15,16] Without an oxidant, a black precipitate was observed as the product of polymerization of methyldioxorhenium(V).[17]

Dissertation Organization

This dissertation consists of seven Chapters. Chapter I has been published in *Angewandte Chemie International Edition*. Chapter II has been published in *Inorganic Chemistry*. Chapter III has been submitted to *Inorganic Chemistry*. Chapter IV has been submitted to *Dalton transactions*. Chapter V has been published in *Organometallics*. Chapter VI has been published in *Inorganic Chemistry*. Chapter VII contains part of a manuscript submitted to *Inorganic Synthesis*. Each Chapter is self-contained with its own equations, figures, tables, references, and supporting information. Following the last Chapter are general conclusions. Except for the X-ray structural analysis and several synthetic procedures in Chapter VII, all the work in this dissertation was performed by the author of this thesis, Xiaopeng Shan.

References

(1) Bernadou, J.; Meunier, B. *Chem. Commun.* **1998**, 2167-2173.

(2) Young, C. G.; Wedd, A. G. *Chem. Commun.* **1997**, 1251-1257.

(3) Holm, R. H. *Chem. Rev.* **1987**, *87*, 1401-1449.

(4) Hille, R. *Trends Biochem. Sci.* **2002**, *27*, 360-367.

(5) Holm, R. H. *Coord. Chem. Rev.* **1990**, *100*, 183-221.

(6) Arzoumanian, H. *Coord. Chem. Rev.* **1998**, *178-180*, 191-202.

(7) Arias, J.; Newlands, C. R.; Abu-Omar, M. M. *Inorg. Chem.* **2001**, *40*, 2185-2192.

(8) Jacob, J.; Guzei, I. A.; Espenson, J. H. *Inorg. Chem.* **1999**, *38*, 1040-1041.

(9) Lente, G.; Shan, X.; Guzei, I. A.; Espenson, J. H. *Inorg. Chem.* **2000**, *39*, 3572-3576.

(10) Lente, G.; Guzei, I. A.; Espenson, J. H. *Inorg. Chem.* **2000**, *39*, 1311-1319.

(11) Jacob, J.; Lente, G.; Guzei, I. A.; Espenson, J. H. *Inorg. Chem.* **1999**, *38*, 3762-3763.

(12) Wang, Y.; Espenson, J. H. *Inorg. Chem.* **2002**, *41*, 2266-2274.

(13) Wang, Y.; Espenson, J. H. *Org. Lett.* **2000**, *2*, 3525-3526.

(14) Lente, G.; Espenson, J. H. *Inorg. Chem.* **2000**, *39*, 4809-4814.

(15) Abu-Omar, M. M.; Espenson, J. H. *Inorg. Chem.* **1995**, *34*, 6239-6240.

(16) Abu-Omar, M. M.; Appelman, E. H.; Espenson, J. H. *Inorg. Chem.* **1996**, *35*, 7751-7757.

(17) Espenson, J. H.; Yiu, D. T. Y. *Inorg. Chem.* **2000**, *39*, 4113-4118.

CHAPTER I. METHYL TRANSFER FROM RHENIUM TO COORDINATED THIOLATE GROUPS

A communication published in *Angewandte Chemie International Edition*

Xiaopeng Shan, Arkady Ellern and James H. Espenson

A prominent reaction of Vitamin B_{12} is the conversion of D,L-homocystein, $HS(CH_2)_2CHNH_2CO_2H$, to L-methionine, $MeS(CH_2)_2CHNH_2CO_2H$ with methylcobalamin and methylcobinamide.[1-4] Methyl-bis(dimethylglyoximato)cobalt(III) and related complexes also convert thiols to thioethers.[5]

$$Co^{III}\text{–}CH_3 + RSH \rightarrow [Co^{I}]^- + RSCH_3 + H^+ \quad (1)$$

There are, however, a lack of precedents in the literature that do not involve organocobalt complexes. In this work, new reactions of rhenium complexes have been examined, and sound evidence for the analogous conversion has now been obtained.

Chart 1

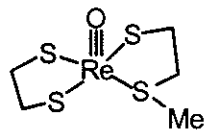

1

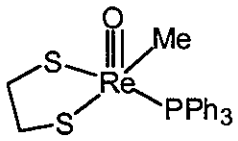

3

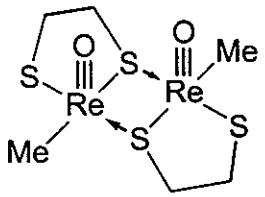

4

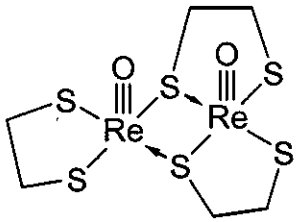

5

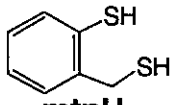

mtpH$_2$

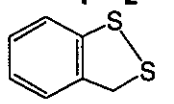

6

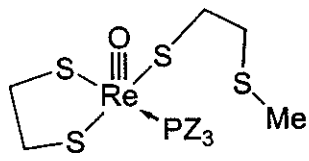

7

$MeReO_3$ (MTO, **2**)[6] reacts with the readily-oxidized $mtpH_2$, 2-(mercaptomethyl)-thiophenol ($mtpH_2$), to yield a disulfide (eq. 2):

$$2\ MeReO_3 + 4\ mtpH_2 \rightarrow \mathbf{4} + 2\ (\mathbf{6}) + 4\ H_2O \quad (2)$$

With 1,2-ethanedithiol, however, a quite different result was obtained. As Re^{VII} was reduced to Re^{V}, one $edtH_2$ molecule was transformed to $HS(CH_2)_2SMe$, which remains coordinated to rhenium(V) through both sulfur atoms in a κ^2 fashion (eq. 3):

$$MeReO_3 + 2\ edtH_2 \rightarrow\ \mathbf{1} + 2\ H_2O \qquad (3)$$

Details of the synthesis and characterization of the dark red compound **1** are given in the Experimental Section. A similar reaction starting with [MeReO(edt)(PPh_3)], **3**,[7] gave the same product in lower yield. Crystals of **1** suitable for x-ray diffraction could not be obtained. We have formulated composition of **1** as ReO(κ^2-edt)(κ^2-edtMe) on the basis of the elemental analysis and spectroscopic data. An alternative formulation as an organorhenium(VII) compound, $MeReO(edt)_2$, could not be ruled out by these data, although there was faint evidence in favor of structure **1**, in that the CH_3 resonance appeared at δ 1.90 ppm, which is further downfield than would be expected for a methyl group coordinated to a Re^{VII} center. Indeed, the proposed mechanism suggests that $MeReO(edt)_2$ lies on the pathway to **1**.

Chemical methods were therefore used to obtain information about the molecular structure of **1**, particularly with respect to whether the Me–Re interaction present in the starting materials is retained. Its reaction of **1** with H_2O_2 in wet acetonitrile gave ReO_4^- ions, which are easily recognized from its characteristic UV spectrum. The same product was obtained from **5**, another compound that lacks a Me–Re bond. In contrast, several compounds that do contain a Me–Re group (**2**, **3** and **4**) clearly reacted with hydrogen peroxide to form [MeReO(κ^2-O_2)$_2$(OH_2)], with a characteristic absorption maximum at 360 nm (ε = 1200). Thus, these results suggest that no Me-Re bond exists in **1**.[8]

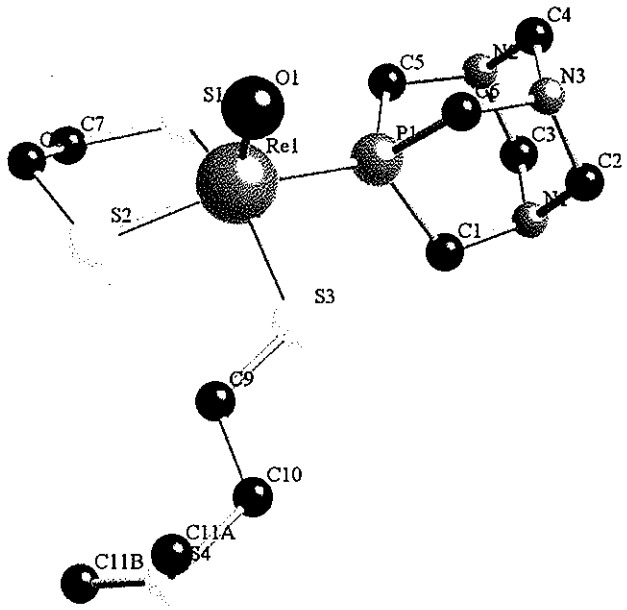

Figure 1. The molecular structure of [ReO(κ^2-edt)(κ^1-edtMe)(PTA)]. The methyl group at S_4 was disordered; the structure was refined at 50% occupancy of the two sites. Selected bond lengths (pm) and angles (°) are: Re–O, 170.05(5); Re–S(3), 230.54(17); Re–P, 242.25(18); S(4)–C(10), 181.0(9); S(4)–C11A, 175.6(17); S(4)–C(11B), 184.0(4). O–Re–S(3), 110.68(19); O–Re–P, 97.3(2); S(2)–Re–P, 153.94(6); S(1)–Re–S(3), 133.58(7); C(10)–S(4)–C(11A), 102.7(7); C(10)–S(4)–C(11B), 104.3(17); C(11A)–S(4)–C(11B), 133.1(14). The structure was drawn with the program CrystalMaker.[14]

The reaction of compound **1** with phosphanes (PZ_3, in general) yields a new series of compounds, [ReO(κ^2-edt)(κ^1-edtMe)(PZ_3)] (**7**) in which the thioether arm has been displaced. One such compound, where PZ_3 = 1,3,5-triaza-phosphaadmantane (PTA),[9] has been characterized crystallographically; the molecular structure is displayed in Figure 1. Phosphanes are generally much stronger Lewis bases than thioethers and will, to a great extent, displace RSR' group. In keeping with this fact, the equilibrium constant for PPh_3 (K_4,

eq. 4) is 6×10^5 (C_6H_6, 25 °C),[10] whereas that for eq. 5 is 8.0 under the same conditions. The large difference in theses values arises from the chelate effect, and illustrates its very substantial importance in this case.

$$MeReO(edt)(Me_2S) + PPh_3 \rightarrow MeReO(edt)PPh_3 + Me_2S \qquad K_4 \ (4)$$

$$\mathbf{1} + PPh_3 = ReO(\kappa^2\text{-edt})(\kappa^1\text{-edtMe})(PPh_3) \qquad K_5 \ (5)$$

The formation of **1**, as shown in reaction (3), follows the net 1:2 stoichiometry given. It is a sequential process that obeys the rate law (eq. 6):

$$d[\mathbf{1}]/dt = k \times [\mathbf{2}] \times [edtH_2] \qquad (6)$$

with $k = 7.3 \times 10^{-2}$ L mol^{-1} s^{-1} (Me_2SO, 25 °C). Clearly the first condensation step is rate determining, as the methylation step occurs more rapidly and is not manifest in the kinetics. The sequential mechanism proposed is given in Scheme 1. The final step appears to involve nucleophilic attack of the coordinated thiolate sulfur on the methyl group of the intermediate. Precedents for this mechanism, aside from those found in organocobalt systems, are rare. While the transfer of a phenyl group to an oxo group of an intermediate species ([$TpRe(O)_2Ph$]$^+$, Tp = hydrotris(1-pyrazoly)borate) represents a distantly related example;[11] a more relevant case is the thermal decomposition of [$MeReO(\kappa^2\text{-}O_2)_2(OH_2)$], which yields MeOOH and $HReO_4$.[12]

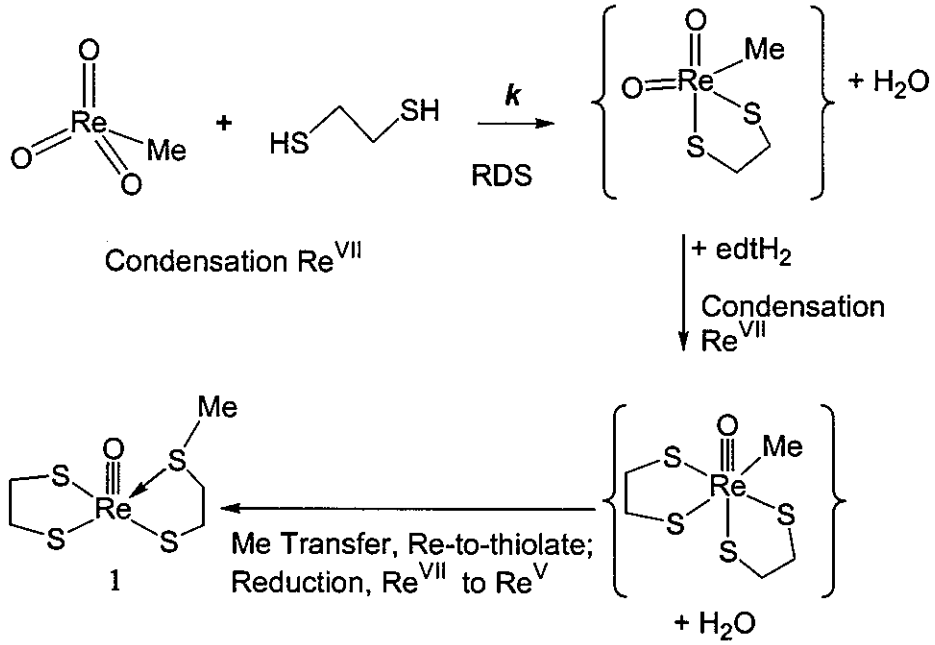

Scheme 1. Proposed mechanism for the formation of **1** (RDS = rate-determining step)

In summary, a novel transformation of MeRe(edt) complex to give a Re(thiolate-methylthioether) complex (**1**) has been discovered and established. This transformation is without precedent, aside from the homocystein-to-methionine transformation found for Vitamin B_{12} and its mimics. Furthermore, the thioether group can be replaced by a phosphane; the derivative with PTA was characterized crystallographically. All of these reactions proceed to equilibrium, but owing to the chelate effect, the equilibrium constants are smaller by a factor of 10^5 than the analogous values of K for the displacement of a nonchelated RSR' group.

Experimental Section

Synthesis of [ReO(κ^2-edt)(κ^2-edtMe)], **1**. Dimethylsulfoxide (0.2 mmol) was added to 5 mL of toluene containing 0.5 mmol of **2**. 1,2-Ethane dithiol (0.5 mmol) was added, whereupon the mixed solution turned red. After 4 h, 10 mL of hexanes was layered on top resulting in a deep red solid (87% yield) which was purified by recrystallization from methylene chloride-hexanes. Elemental analysis, $C_5H_{11}OReS_4$. Found C: 15.16 (14.95 calcd.), H: 2.82 (2.76); S: 32.09 (31.94). ^{1}H NMR: (400 MHz, [D_6]benzene, 25 °C): δ=3.55(m, 1H; CH_2), 3.36(m, 1H; CH), 2.70(m, 1H; CH_2), 2.51(m, 2H, CH_2), 2.11(m, 1H; CH_2), 1.92(m, 1H; CH_2), 1.90(s, 3H, CH_3), 0.84(m, 1H; CH_2); ^{13}C NMR(400 MHz, [D_6]benzene, 25 °C): δ = 45.6, 45.0, 43.5, 36.2, 22.3; UV/Vis (benzene): λ_{max} (ε) = 510 nm (16$\tilde{6}$), 389 nm (3400).

Synthesis of [ReO(κ^2-edt)(κ^1-edtMe)(PTA)]. A 1:1 reaction between **1** and PTA in toluene gave dark, shiny single crystals after recrystallization from toluene-hexanes. Elemental Analysis: $C_{11}H_{23}ON_3PReS_4$. C: 23.57 (23.65 calcd), H: 4.12 (4.15), N: 7.55 (7.52), S: 23.25 (22.96), P: 5.61 (5.54). ^{1}H NMR (400 MHz, [D_6]benzene, 25 °C), δ = 4.34(m, 1H; CH_2), 4.21(m, 7H; CH_2), 3.86(m, 6H; CH_2); 3.43(m, 1H; CH_2), 3.34(m, 1H; CH_2), 3.20(m, 1H; CH_2), 2.97(m, 1H; CH_2), 2.41(m, 2H; CH_2), 1.98(s, 3H; CH_3); ^{13}C NMR(400 MHz, [D_6]benzene, 25 °C): δ = 72.5(d, J(C, P) = 7 Hz), 51.9(d, J(C, P) = 16 Hz), 43.6(d, J(C, P) = 8 Hz), 42.0(s), 37.2(s), 35.5(d, J(C, P) = 9 Hz), 15.3(s); ^{31}P NMR(400 MHz, [D_6]benzene, 25 °C): δ = –74.0; UV/Vis (benzene) λ_{max} (ε) = 386 nm (1900), 318 nm (1600; sh), 262 nm (3$\tilde{8}$).

References:

(1) J. R. Guest, S. Friedman, D. D. Woods, E. L. Smith, *Nature* **1962**, *195*, 340.

(2) J. R. Guest, S. Friedman, M. J. Dilworth, D. D. Woods, *Ann. New York Acad. Sci.* **1964**, *112*, 774.

(3) M. L. Ludwig, R. G. Matthews, *Annu. Rev. Biochem.* **1997**, *66*, 269-313.

(4) R. G. Matthews, *Acc. Chem. Res* **2001**, *34*, 681-689.

(5) G. N. Schrauzer, R. J. Windgassen, *J. Am. Chem. Soc.* **1968**, *89*, 3067.

(6) W. A. Herrmann, R. M. Kratzer, R. W. Fischer, *Angew. Chem. Int. Ed. Engl.* **1997**, *36*, 2652-2654.

(7) G. Lente, X. Shan, I. A. Guzei, J. H. Espenson, *Inorg. Chem.* **2000**, *39*, 3572-3576.

(8) Each compound was treated with 30% hydrogen peroxide to give a final concentration of 38 mM H_2O_2 in acetonitrile. The final spectra from these procedures confirming the two indicated Re(VII) products are given in the Supporting Information.

(9) D. J. Darensbourg, T. J. Decuir, J. H. Reibenspies, *NATO ASI Ser., Ser. 3* **1995**, *5*, 61-80.

(10) This equilibrium constant applies to the analogue of **3**, with mtp instead of edt, where $mtpH_2$ is 2-(mercaptomethyl)thiophenol. The terms contributing to K_1 are given in the Supporting Information.

(11) S. N. Brown, J. M. Mayer, *J. Am. Chem. Soc.* **1996**, *118*, 12119-12133.

(12) W.-D. Wang, J. H. Espenson, *Inorg. Chem.* **1997**, *36*, 5069-5075.

(13) D. Palmer, CrystalMaker, 2.0 ed., Hollywell Press, Bicester, Oxfordshire, **1999**.

Supporting Information

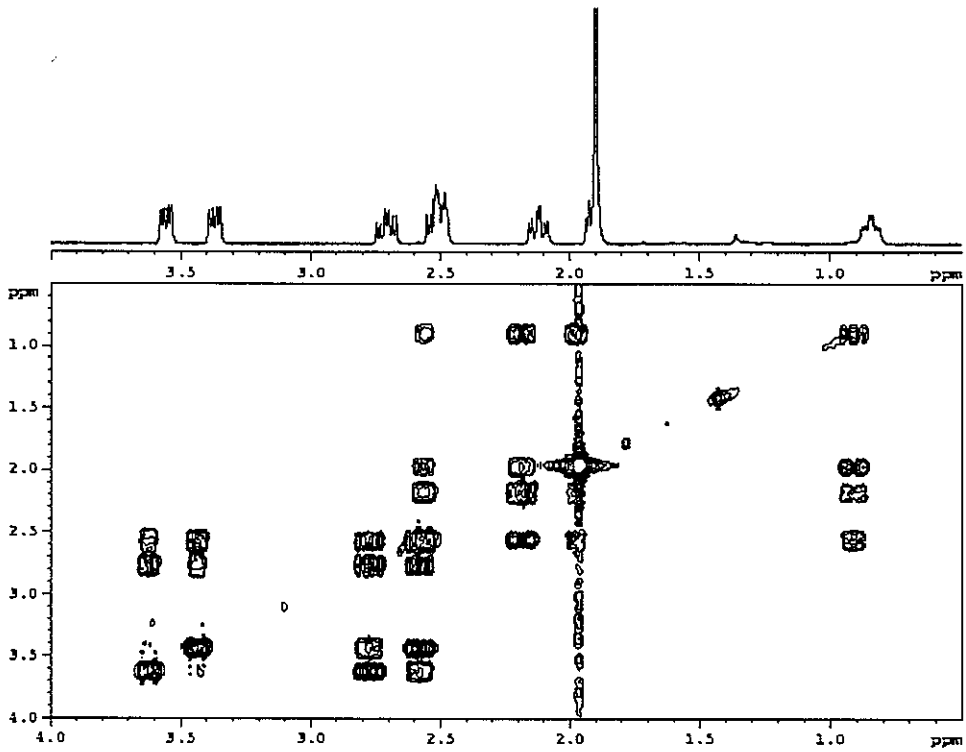

Figure S-1. NMR spectrum of $ReO(\kappa^2\text{-edt})(\kappa^2\text{-edtMe})$

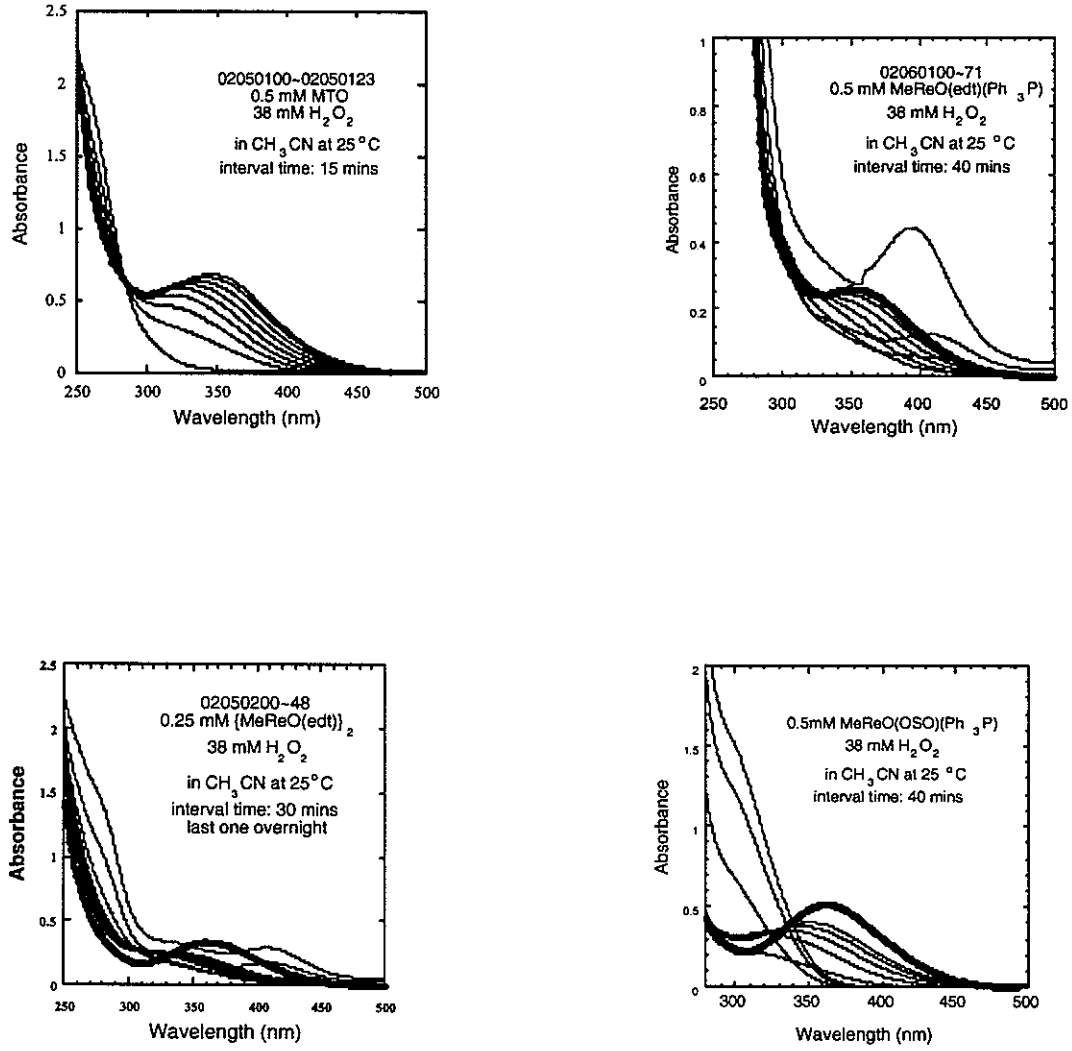

Figure S-2. A. Verification of the formation of [$MeReO(\kappa^2\text{-}O_2)_2(H_2O)$] by its maximum at 360 nm upon addition of H_2O_2 to different compounds containing a Me–Re bond. The final spectrum in each case is shown by the heavy line.

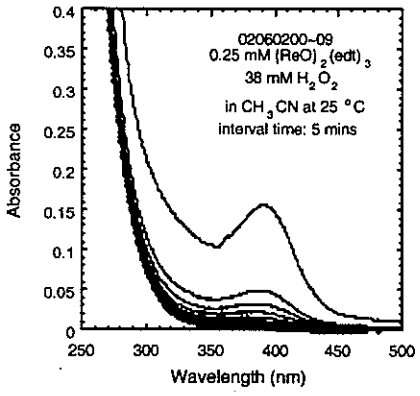

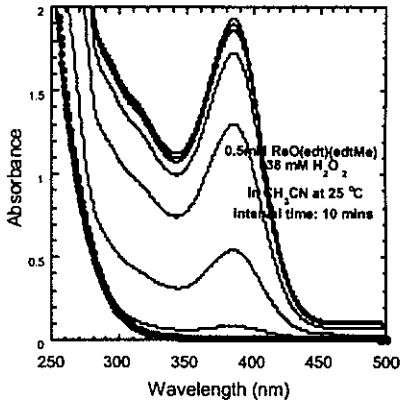

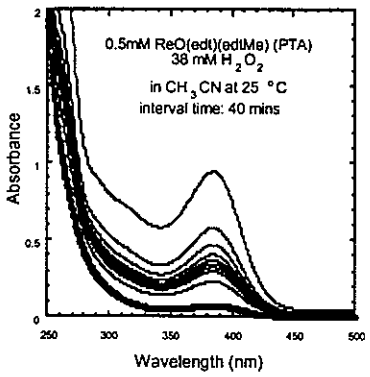

Figure S-2. B. Lack for formation of [MeReO(κ^2-O_2)$_2$(H_2O)] upon addition of H_2O_2 to a compound lacking a Me–Re bond (left), to the compound under investigation, ReO(κ^2-edt)(κ^2-edtMe), and to [ReO(κ^2-edt)(κ^1-edtMe)(PTA)].

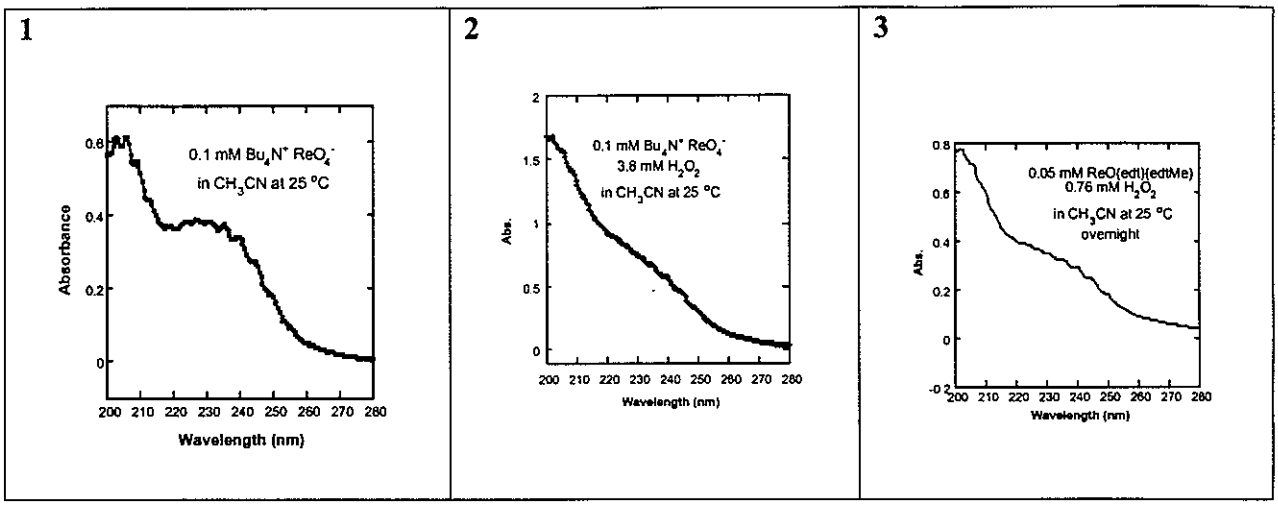

Figure S-2. C. Verification of ReO_4^- from the reactions of $\{ReO\}_2(edt)_3$ and $ReO(\kappa^2\text{-edt})(\kappa^2\text{-edtMe})$ with H_2O_2. The UV spectrum is characteristic of ReO_4^- treated with peroxide. (1) ReO_4^- alone; (2) ReO_4^- with H_2O_2; (3) 1 with H_2O_2

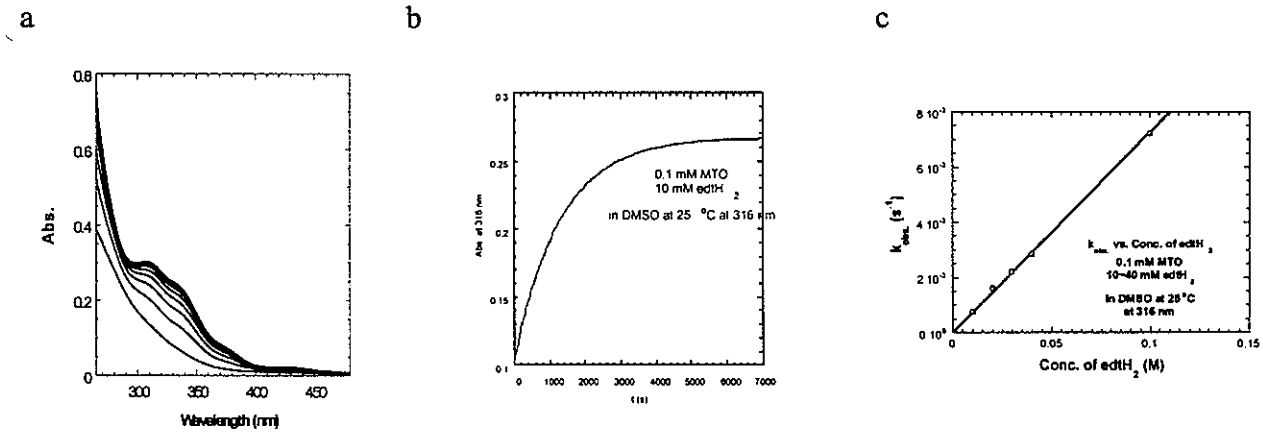

Figure S-3. Kinetic data for the reaction between $MeReO_3$ and $edtH_2$. (a) repetitive scans; (b) absorbance-time data; (c) plot of k_Ψ against $[edtH_2]$.

Table S–1. Crystallographic data for ReO(edt)(edtMe)(PTA)

Part A. Crystal data and structure refinement for ReO(edt)(edtMe)(PTA).

Identification code	ReO(edt)(edtMe)(PTA)
Empirical formula	$C_{11}H_{23}N_3OPReS_4$

Formula weight	558.73	
Temperature	293(2) K	
Wavelength	0.71073 Å	
Crystal system	Triclinic	
Space group	P-1	
Unit cell dimensions	a = 6.4459(4) Å	α= 89.6710(10)°.
	b = 10.6334(7) Å	β= 84.4990(10)°.
	c = 13.4904(8) Å	γ = 77.3490(10)°.
Volume	897.94(10) $Å^3$	
Z	2	
Density (calculated)	2.067 Mg/m^3	
Absorption coefficient	7.321 mm^{-1}	
F(000)	544	
Crystal size	0.20 × 0.18 × 0.05 mm^3	
Theta range for data collection	1.96 to 28.27°.	
Index ranges	$-8 \le h \le 5$, $-13 \le k \le 13$, $-17 \le l \le 17$	
Reflections collected	6486	
Independent reflections	3977 [R(int) = 0.0636]	
Completeness to theta = 28.27°	89.2 %	
Absorption correction	Empirical	
Max. and min. transmission	0.69 and 0.40	
Refinement method	Full-matrix least-squares on F^2	
Data / restraints / parameters	3977 / 0 / 192	
Goodness-of-fit on F^2	1.060	
Final R indices [I>2sigma(I)]	R1 = 0.0570, wR2 = 0.1637	
R indices (all data)	R1 = 0.0580, wR2 = 0.1653	
Largest diff. peak and hole	2.777 and -1.652 $e.Å^{-3}$	

$R1 = \Sigma \, | \, |F_o| - |F_c| \, | \, / \, \Sigma \, |F_o|$ and $wR2 = \{ \, \Sigma \, [\, w(F_o^2 - F_c^2)^2 \,] \, / \, \Sigma \, [\, w(F_o^2)^2 \,] \, \}^{1/2}$

Part B. Atomic coordinates ($\times 10^4$) and equivalent isotropic displacement parameters ($Å^2 \times 10^3$) for ReO(edt)(edtMe)(PTA). U(eq) is defined as one third of the trace of the orthogonalized U_{ij} tensor.

	x	y	z	U(eq)
Re(1)	1012(1)	3752(1)	8352(1)	15(1)
S(1)	-2138(3)	3148(2)	8799(1)	22(1)
S(2)	2425(3)	1573(2)	8115(1)	23(1)
S(3)	2738(3)	4151(2)	6845(1)	23(1)
S(4)	7940(4)	1716(3)	4887(2)	38(1)
P(1)	-1434(3)	5764(2)	8049(1)	16(1)
C(1)	-1843(12)	6386(7)	6786(5)	24(2)
C(2)	-2071(13)	8586(7)	7326(6)	25(2)
C(3)	-5266(11)	7784(7)	7362(6)	22(1)
C(4)	-4099(12)	8383(7)	8888(6)	23(2)
C(5)	-4221(10)	6141(7)	8603(5)	19(1)
C(6)	-476(11)	7110(7)	8565(5)	20(1)
C(7)	-1601(13)	1371(7)	8799(7)	28(2)
C(8)	655(12)	832(7)	8957(6)	23(1)
C(9)	4931(14)	2817(9)	6412(6)	31(2)
C(10)	5790(15)	3029(10)	5364(6)	35(2)
C(11A)	10080(30)	1933(17)	5532(13)	55(6)
C(11B)	6640(60)	350(40)	4770(30)	87(10)
N(1)	-3129(11)	7704(6)	6829(5)	23(1)
N(2)	-5235(10)	7500(6)	8428(5)	21(1)
N(3)	-1956(10)	8351(6)	8396(5)	22(1)
O(1)	2136(9)	4286(5)	9311(4)	26(1)

Atom C11 was refined as disordered by two positions C11A and C11B with occupancy factors 0.5.

Part C. Bond lengths [Å] and angles [°] for ReO(edt)(edtMe)(PTA).

Re(1)-O(1)	1.700(5)	P(1)-C(1)	1.845(7)
Re(1)-S(1)	2.2868(17)	C(1)-N(1)	1.462(10)
Re(1)-S(3)	2.3054(17)	C(2)-N(3)	1.470(10)
Re(1)-S(2)	2.3081(18)	C(2)-N(1)	1.473(10)
Re(1)-P(1)	2.4225(18)	C(3)-N(2)	1.470(10)
S(1)-C(7)	1.845(8)	C(3)-N(1)	1.477(10)
S(2)-C(8)	1.830(7)	C(4)-N(3)	1.468(9)
S(3)-C(9)	1.823(9)	C(4)-N(2)	1.483(9)
S(4)-C(11A)	1.756(17)	C(5)-N(2)	1.477(9)
S(4)-C(10)	1.810(9)	C(6)-N(3)	1.480(10)
S(4)-C(11B)	1.84(4)	C(7)-C(8)	1.477(11)
P(1)-C(5)	1.838(7)	C(9)-C(10)	1.502(11)
P(1)-C(6)	1.843(7)		

O(1)-Re(1)-S(1)	114.66(19)	C(5)-P(1)-Re(1)	122.1(2)
O(1)-Re(1)-S(3)	110.68(19)	C(6)-P(1)-Re(1)	109.3(3)
S(1)-Re(1)-S(3)	133.58(7)	C(1)-P(1)-Re(1)	122.8(2)
O(1)-Re(1)-S(2)	108.6(2)	N(1)-C(1)-P(1)	111.0(5)
S(1)-Re(1)-S(2)	85.06(6)	N(3)-C(2)-N(1)	113.7(6)
S(3)-Re(1)-S(2)	89.85(6)	N(2)-C(3)-N(1)	114.0(6)
O(1)-Re(1)-P(1)	97.3(2)	N(3)-C(4)-N(2)	113.8(6)
S(1)-Re(1)-P(1)	81.19(6)	N(2)-C(5)-P(1)	110.5(5)
S(3)-Re(1)-P(1)	83.86(6)	N(3)-C(6)-P(1)	110.3(5)
S(2)-Re(1)-P(1)	153.94(6)	C(8)-C(7)-S(1)	110.3(5)
C(7)-S(1)-Re(1)	108.1(3)	C(7)-C(8)-S(2)	110.4(5)
C(8)-S(2)-Re(1)	103.2(3)	C(10)-C(9)-S(3)	110.9(6)
C(9)-S(3)-Re(1)	112.7(3)	C(9)-C(10)-S(4)	112.8(7)
C(11A)-S(4)-C(10)	102.7(7)	C(1)-N(1)-C(2)	111.3(6)
C(11A)-S(4)-C(11B)	133.1(14)	C(1)-N(1)-C(3)	111.9(6)
C(10)-S(4)-C(11B)	104.3(13)	C(2)-N(1)-C(3)	108.3(6)

C(5)-P(1)-C(6)	100.1(3)	C(3)-N(2)-C(5)	112.2(6)
C(5)-P(1)-C(1)	99.3(3)	C(3)-N(2)-C(4)	108.4(6)
C(6)-P(1)-C(1)	98.9(3)	C(5)-N(2)-C(4)	110.8(6)
C(2)-N(3)-C(4)	110.0(6)	C(4)-N(3)-C(6)	111.0(6)
C(2)-N(3)-C(6)	111.0(6)		

Part D. Anisotropic displacement parameters ($Å^2 \times 10^3$) for ReO(edt)(edtMe)(PTA). The anisotropic displacement factor exponent takes the form: $-2\pi^2[h^2 a^{*2} U_{11} + ... + 2 h k a^* b^* U_{12}]$

	U_{11}	U_{22}	U_{33}	U_{23}	U_{13}	U_{12}
Re(1)	15(1)	17(1)	15(1)	1(1)	-1(1)	-7(1)
S(1)	17(1)	20(1)	29(1)	3(1)	0(1)	-9(1)
S(2)	24(1)	18(1)	26(1)	2(1)	5(1)	-5(1)
S(3)	24(1)	24(1)	20(1)	4(1)	4(1)	-4(1)
S(4)	28(1)	55(2)	28(1)	-11(1)	4(1)	-5(1)
P(1)	16(1)	17(1)	16(1)	1(1)	-2(1)	-6(1)
C(1)	26(4)	22(4)	20(3)	1(3)	-1(3)	-1(3)
C(2)	27(4)	21(4)	28(4)	7(3)	-1(3)	-11(3)
C(3)	18(3)	24(4)	24(4)	3(3)	-8(3)	-3(3)
C(4)	23(4)	21(4)	25(4)	-7(3)	4(3)	-9(3)
C(5)	12(3)	21(3)	24(3)	2(3)	-2(2)	-5(2)
C(6)	20(3)	19(3)	24(3)	0(3)	1(3)	-12(3)
C(7)	29(4)	18(4)	39(5)	4(3)	-3(3)	-11(3)
C(8)	21(3)	18(3)	28(4)	5(3)	2(3)	-6(3)
C(9)	34(4)	34(4)	22(4)	8(3)	6(3)	-3(3)
C(10)	33(4)	49(5)	18(4)	4(3)	6(3)	-2(4)
N(1)	22(3)	25(3)	21(3)	2(2)	-2(2)	-6(2)
N(2)	18(3)	26(3)	20(3)	-2(2)	-2(2)	-10(2)
N(3)	22(3)	21(3)	23(3)	0(2)	0(2)	-10(2)
O(1)	28(3)	29(3)	24(3)	2(2)	-4(2)	-14(2)

Re(1)	15(1)	17(1)	15(1)	1(1)	-1(1)	-7(1)
S(1)	17(1)	20(1)	29(1)	3(1)	0(1)	-9(1)

Part E. Hydrogen coordinates ($\times 10^4$) and isotropic displacement parameters ($Å^2 \times 10^3$) for ReO(edt)(edtMe)(PTA).

	x	y	z	U(eq)
H(1A)	-468	6369	6419	28
H(1B)	-2556	5834	6436	28
H(2A)	-633	8499	7005	29
H(2B)	-2839	9465	7238	29
H(3A)	-6123	8645	7288	26
H(3B)	-5953	7184	7051	26
H(4A)	-4948	9256	8872	27
H(4B)	-3979	8157	9581	27
H(5A)	-5008	5579	8313	23
H(5B)	-4262	5989	9314	23
H(6A)	-376	6993	9274	24
H(6B)	937	7120	8250	24
H(7A)	-2525	1089	9323	34
H(7B)	-1907	1058	8167	34
H(8A)	984	-93	8838	27
H(8B)	884	988	9642	27
H(9A)	6064	2739	6847	38
H(9B)	4432	2020	6439	38
H(10A)	6303	3821	5344	42
H(10B)	4640	3130	4936	42
H(11A)	9867	1669	6210	82
H(11B)	10146	2826	5522	82
H(11C)	11389	1422	5219	82

H(11D)	5751	509	4227	130
H(11E)	5790	267	5374	130

Derivation S-1. Evaluation of K for the equilibrium

Reaction	K	Ref
$MeReO(mtp)SMe_2 + PPh_3 = MeReO(mtp)PPh_3 + Me_2S$	K_1	
Given these data:		
$\{MeReO(mtp)\}_2 + 2\ Py = 2\ MeReO(mtp)Py$	$K_2 = 1.74 \times 10^2$	1
$\{MeReO(mtp)\}_2 + 2\ Me_2S = 2\ MeReO(mtp)SMe_2$	$K_3 = 4.2 \times 10^{-4}$	2
$MeReO(mtp)Py + PPh_3 = MeReO(mtp)PPh_3 + Py$	$K_4 = 9.0 \times 10^2$	1

$$K_1 = K_4 \times \sqrt{\frac{K_2}{K_3}} = 6 \times 10^5$$

(1) Lente, G.; Guzei, I. A.; Espenson, J. H. *Inorg. Chem.* 2000, 39, 1311-1319.

(2) Shan, X.; Espenson, J. H., unpublished results.

CHAPTER II. METHYLOXORHENIUM(V) COMPLEXES WITH TWO BIDENTATE LIGANDS: SYNTHESES AND REACTIVITY STUDIES

A manuscript published in *Inorganic Chemistry*

Xiaopeng Shan, Arkady Ellern, James H. Espenson

Abstract

Four new methyloxorhenium(V) complexes were synthesized: $MeReO(PA)_2$ (**1**), $MeReO(HQ)_2$ (**2**), $MeReO(MQ)_2$ (**3**), and MeReO(diphenylphosphinobenzoate)$_2$ (**4**) (in which PAH = 2-picolinic acid, HQH = 8-hydroxyquinoline and MQH = 8-mercaptoquinoline). Although only one geometric structure has been identified crystallographically for **1**, **2** and **3**, two isomers of **3** and **4** in solution were detected by NMR spectroscopy. These compounds catalyze the sulfoxidation of thioethers by pyridine N-oxides and sulfoxides. The rate law for the reaction between pyridine N-oxides and thioethers, catalyzed by **1**, shows a first-order dependence on the concentrations of pyridine N-oxide and **1**. The second order rate constants of series of para substituted pyridine N-oxides fall in the range of 0.27–7.5 L mol^{-1} s^{-1}. Correlation of these rate constants by the Hammett LFER method gave a large negative reaction constant, $\rho = -5.2$. The next and rapid step does not influence the kinetics, but it could be explored with competition experiments carried out with a pair of methyl aryl sulfides, $MeSC_6H_4$-*p*-Y. The value of each rate was expressed relative to the reference compound that has Y = H. A Hammett analysis of k_Y/k_H gave $\rho = -1.9$. Oxygen-18 labeled **1** was used in a single turnover experiment for 4-picoline N-oxide and dimethyl sulfide. No ^{18}O labeled DMSO was found. We suggest that the reaction proceeds by way of two intermediates that were not observed during the reaction. The first intermediate contains an opened PA-chelate ring; this allows the pyridine N-oxide to access the primary coordination sphere of rhenium. The second intermediate is a *cis*-dioxorhenium(VII) species, which the thioether then attacks. Oxygen-18 experiments were used to show that the two oxygens of this intermediate are not equivalent; only the "new" oxygen is attacked by, and transferred to, SR_2. Water inhibits the reaction because it hydrolyzes the rhenium(VII) intermediate.

Introduction

Certain aspects of the coordination chemistry of rhenium have been widely developed because of the radiotherapeutic applications of the β-emitting isotopes ^{186}Re and ^{188}Re.[1-3] Most of these rhenium complexes contain a {$Re^{V}O$} core.[4-7] Often a monoanionic bidentate ligand is present. Typical donor atom pairs such as P,O (HPO = phosphinocarboxylic acid),[8,9] N,O (HNO = e.g., picolinic acid or 8-hydroxyquinoline),[10-13] and N,S (HNS = 2-mercaptoquinoline).[12] Molybdenum complexes have been extensively investigated owing to interest in their oxotransferase activity,[14-18] In comparison, only a few rhenium complexes have been investigated.[19-23] This research focuses on compounds containing a methyl(oxo)-rhenium(V) core, {$MeRe^{v}O$}.[24-27]

We have now extended our exploration of rhenium catalysts[28-33] by the preparation and characterization of four new [2+2]methyl-oxorhenium compounds, Chart 1. These reactions are catalyzed by them:

$$RSR' + XC_5H_4NO \xrightarrow{[Re]} RS(O)R' + C_5H_4N \quad (1)$$

$$R_2S + R'_2SO \rightleftharpoons R_2S(O) + R'_2S \quad (2)$$

Chart 1. Structural Formulas of [2+2] Methyloxorhenium(V) Compounds

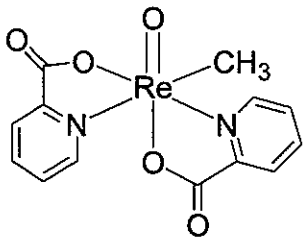

MeReO(PA)$_2$ **1**

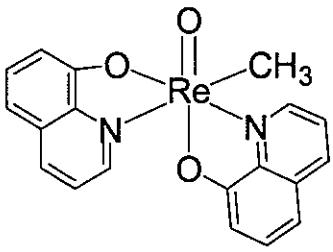

MeReO(HQ)$_2$ **2**

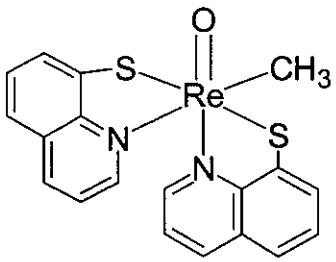

MeReO(MQ)$_2$ **3a**

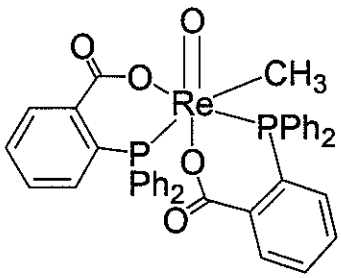

MeReO(diphenylphosphinobenzoate)$_2$ **4a**

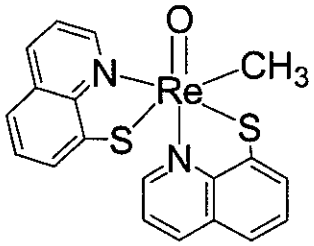

MeReO(MQ)$_2$ **3b**

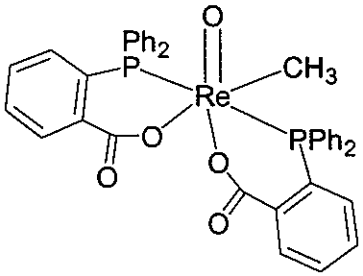

MeReO(diphenylphosphinobenzoate)$_2$ **4b**

Kinetic studies were carried out with **1**, the most effective catalyst. Our goal has been to identify the steps in the mechanism, including the formulation of chemically-reasonable reaction intermediates. This includes the trapping of a transient dioxorhenium(VII) species.

Experimental Section

Reagents and Instrumentation. Methyltrioxorhenium(VII), CH_3ReO_3 or MTO, was prepared from sodium perrhenate, tetramethyl tin and chlorotrimethylsilane.[34] The chelating

ligands were purchased from commercial sources and used as received. Anhydrous methylene chloride was the solvent for UV/Visible spectrophotometry. D_1-chloroform for NMR studies was dried over 4A molecular sieves (Fisher) for 24 h at 200 °C.

UV/Vis data were obtained with a Shimadzu Model 2501 spectrophotometer. Least-squares kinetic fits were carried out with KaleidaGraph software. Bruker DRX-400 MHz and AC200 spectrometers were used to record ^1H, ^{13}C and ^{31}P NMR spectra. The chemical shift for ^1H was defined relative to that of the residual $CHCl_3$ in the solvent, δ 7.27 ppm. Infrared spectra were recorded by a Nicolet-500 spectrometer. GC-MS spectra were recorded by Finnegan MAT MAGNUM mass spectrometer. Elemental analysis was performed by Desert Analytics Laboratory.

Syntheses. Compounds **1-3** were prepared from MTO (50 mg, 0.2 mmol), the bidentate ligand (0.4 mmol), and the reducing agent triphenylphosphine (53 mg, 0.2 mmol) in 20 mL of CH_2Cl_2. After stirring the mixture for 12 h, 20 mL of hexanes was layered the top of the resulting solution and the mixture placed in a freezer at ca. –12 °C. After 24 h a black powder had deposited; it was filtered and rinsed with hexanes. A crystal suitable for x-ray diffraction analysis was obtained by recrystallization from methylene chloride-hexanes. Dimethyl sulfide (19 mg, 0.3 mmol) could also be used as the reducing agent for the preparation of **1** provided anhydrous sodium sulfate was added as a drying agent to complete the reaction. If the acidic form of the monoanionic ligand is written as H(X,Y), where X and Y are the donor atoms, the chemical equation for the syntheses is

$$MeReO_3 + 2\ H(X,Y) + PPh_3/Me_2S \rightarrow MeRe(O)(X,Y)_2 + H_2O + Ph_3PO/Me_2SO \qquad (3)$$

1 was obtained in 83% yield from triphenylphosphine, 53% from dimethyl sulfide. NMR ^1H: δ 8.84 (d, 1H), 8.52 (d, 1H), 8.44 (m, 1H), 8.29 (m, 1H), 8.19 (d, 1H), 7.77 (m, 3H), 4.43 (s, 3H); ^{13}C: 180, 163, 153, 150, 148, 146, 143, 130, 126, 125, 53, 29, 11. IR ($CHCl_3$): 1003 cm^{-1} and, for the ^{18}O-labeled compound, 951 cm^{-1}. The two agree precisely with the predicted $(18/16)^{1/2}$ ratio. UV-Vis ($CHCl_3$), λ_{max}/nm (log ε/L mol^{-1} cm^{-1}): 568 (2.3), 396.5 (3.83) and 260 (4.14). Elemental Analysis: $C_{13}H_{11}N_2O_5Re$, Found (Calcd.) C 33.85 (33.84), H 2.48 (2.40), N 6.06 (6.07).

2 was obtained in 80% yield. NMR ^1H: δ 8.56 (d, 1H), 8.36 (m, 1H), 8.21 (m, 1H), 7.66 (m, 4H), 7.40 (m, 3H), 7.07 (d, 1H) 6.46 (d, 1H), 4.53 (s, 3H). ^{13}C: too insoluble. IR ($CHCl_3$):

980 cm^{-1}. UV-Vis ($CHCl_3$), λ_{max}/nm (log ε/L mol^{-1} cm^{-1}): 470 (sh), 417 (3.70) and 360 (sh). Elemental Analysis: $C_{19}H_{15}N_2O_3Re$, Found (Calcd.): C 44.64 (45.14), H 2.92 (2.99), N 5.29 (5.54).

3 was obtained in 50% yield. Two sets of ^1H NMR resonance peaks were found in solution with a ratio 3:1. Two geometric isomers were assigned to these peaks according to the x-ray structure and an earlier study of pyridine exchange reactions.[35] In solution, the major species is **3a**, NMR ^1H: δ 10.88 (d, 1H), 8.39 (d, 1H), 8.34 (d, 2H), 8.06 (d, 2H), 7.80 (t, 1H), 7.74 (d, 1H), 7.58 (m, 1H), 7.74 (d, 1H), 7.41 (t, 1H), 6.95 (d, 1H), 6.75 (m, 1H), 4.95 (s, 3H). The minor solution species is **3b**. Only three peaks are available due to broadening and overlap with peaks from **3a**. NMR ^1H: δ 9.40 (s, 1H), 8.65 (s, 1H), 5.14 (s, 3H) ppm. ^{13}C: too insoluble. IR ($CHCl_3$): **3a**, 985.46 cm^{-1}; **3b**, 999 cm^{-1}. UV-Vis ($CHCl_3$), λ_{max}/nm (log ε/L mol^{-1} cm^{-1}): 699 (2.6), 432 (3.78) and 267.5 (4.43). Elemental Analysis: $C_{19}H_{15}N_2OReS_2$, Found (Calcd.): C 42.16 (42.44), H 2.54 (2.81), N 5.13 (5.21), S 11.37 (11.93).

4 was prepared by adding MTO (50 mg, 0.2 mmol) into 20 mL of CH_2Cl_2 containing 2-diphenylphosphinobenzoic acid (184 mg, 0.6 mmol), which served both as the reducing agent and the new ligand. The color of the solution changed to violet. After 12 h stirring the mixture was layered with hexanes and put into the freezer. A dark powder was isolated by filtration 24 h later and rinsed with hexanes. It consisted of two geometric isomers, **4a** and **4b**, in a total yield of 65%. The two could not be separated, but their NMR spectra in $CDCl_3$ were resolved and assigned as explained later. **4a** ^1H NMR: δ 6.5–8.5 (m, 14H), 3.39 (t, 3H); ^{31}P NMR: –0.34 (d, J_{PP} = 9 Hz), –3.07 (d, J_{PP} = 9 Hz); **4b**: 6.5–8.5 (m, 14H), 4.12 (t, 3H); ^{31}P NMR: 6.64 (d, J_{PP} = 262 Hz), –5.28 (d, J_{PP} = 262 Hz).

X-ray studies. Crystals for **1**, **2** and **3a** were selected under ambient conditions. Each crystal was mounted and centered in the X-ray beam by use of a video camera. The crystal evaluation and data collection were performed on a Bruker CCD-1000 diffractometer with Mo K_α (λ = 0.71073 Å) radiation and a detector-to-crystal distance of 4.98 cm. The initial cell constants were obtained from three series of ω scans at different starting angles. Each series consisted of 30 frames collected at intervals of 0.3° in a 10° range about ω with the exposure time of 10 s per frame. The reflections were successfully indexed by an automated indexing routine built into the SMART program. The final cell constants were calculated

from a set of strong reflections from the actual data collection. The data were collected using the full sphere routine for high redundancy. The data were corrected for Lorentz and polarization effects. The absorption correction was based on fitting a function to the empirical transmission surface as sampled by multiple equivalent measurements[36] using SADABS software.[37]

The position of the heavy atom was found by the Patterson method. The remaining atoms were located in an alternating series of least-squares cycles and difference Fourier maps. All non-hydrogen atoms were refined in full-matrix an isotropic approximation. All hydrogen atoms were placed at calculated idealized positions and were allowed to ride on the neighboring atoms with relative isotropic displacement coefficients. The ORTEP diagrams were drawn at 50% probability level.

Kinetics. Reactions of pyridine N-oxides and dimethyl sulfide were monitored by following the decrease in absorbance from 275 to 310 nm according to which pyridine N-oxide was being studied. Owing to the large values of their molar absorptivities, a cell with a path length of 0.05 cm in a cylindrical cell holder thermostated at 25.0 ± 0.2 °C was used. Dimethyl sulfide was added in at least ten-fold excess, allowing the absorbance–time data to be fitted to pseudo-first-order kinetics, according to eq 2.

$$\mathrm{Abs}_t = \mathrm{Abs}_\infty + (\mathrm{Abs}_0 - \mathrm{Abs}_\infty) \times \exp(-k_{obs} t) \tag{4}$$

Competition kinetics. A different aspect of the reaction scheme was studied by this method. A pair of methyl aryl sulfides with different para substituents at concentrations ten times higher than that of 4-picoline N-oxide. The concentrations of the two starting sulfides and of the sulfoxides formed were determined by NMR spectroscopy 15 min after the beginning of the reaction. The rate constant ratio for $MeSC_6H_4Y$ as compared to MeSPh is given simply as the product of two concentration ratios at a given time because the sulfide concentrations are nearly invariant during the initial reaction period.

$$\frac{k_Y}{k_H} = \frac{d[MeS(O)C_6H_4Y] / dt}{d[MeS(O)Ph] / dt} = \frac{[MeS(O)C_6H_4Y]_t}{[MeS(O)Ph]_t} \times \frac{[MeSPh]_0}{[MeSC_6H_4Y]_0} \tag{5}$$

Oxygen-18 labeling. Equilibration between MTO and 30 times the molar ratio of $H_2{}^{18}O$ (90% enrichment) was allowed to proceed for 20 min in anhydrous methylene chloride,

which was sufficient for oxygen exchange between MTO and water.[38] The resulting solution was vacuum dried. The same procedure was repeated three times, yielding a sample of $MeRe^{18}O_3$, enriched to ca. 50% ^{18}O content. It used to prepare **1** by the PPh_3 method. The ^{18}O content of **1** was ca. 50% by IR spectroscopy. A reaction was carried out in anhydrous methylene chloride with 4-picoline N-oxide (10 mM), dimethyl sulfide (20 mM) and **1** (10 mM) to guarantee the formation of enough sulfoxides. The isotopic content of the resulting solution was determined by GC-MS.

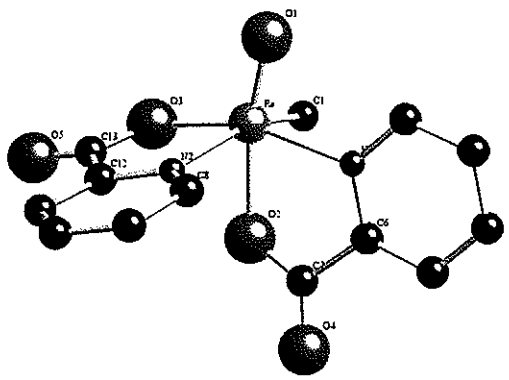

1

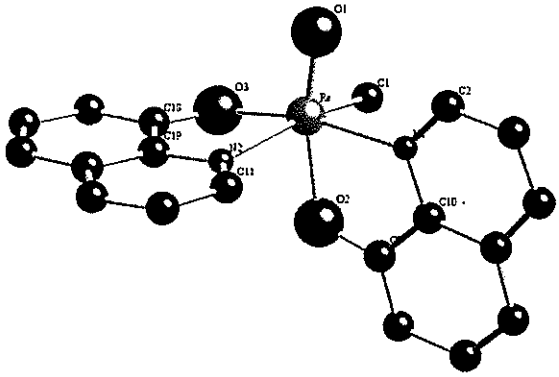

2

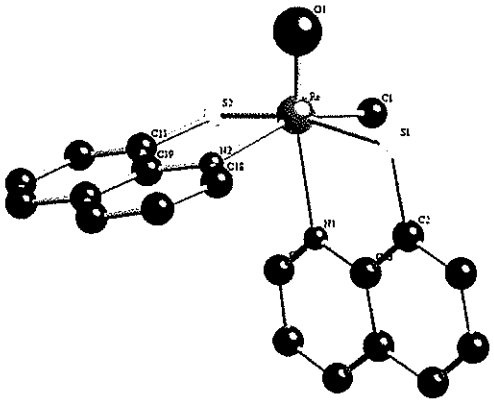

3a

Figure 1. Crystallographically-determined molecular structures of compounds **1**, **2** and 3a. Table 2 shows the selected bond lengths and angles.

Table 1. Experimental Data for the X-ray Diffraction Studies of **1**, **2**, and **3a**.

Compound	**1**	**2**	**3a**
empirical formula	$C_{13}H_{11}N_2O_5Re$	$C_{19}H_{15}N_2O_3Re$	$C_{19}H_{15}N_2OReS_2$
formula wt	461.44	505.53	537.65
a, Å	28.466(7)	9.233(2)	8.4428(14)
b, Å	7.0933(17)	9.724(2)	9.1357(15)
c, Å	15.186(4)	10.780(2)	12.531(2)
α, deg		101.054(3)	85.504(3)
β, deg	111.892(4)	103.955(3)	89.214(3)
γ, deg		112.402(4)	64.825(3)
volume, Å3	2845.3(12)	823.8(3)	871.8(3)
Z	8	2	2
space group	C2/c	P-1	P-1
temp, K	298(2)	298(2)	298(2)
Wavelength	0.71073 Å	0.71073 Å	0.71073 Å
ρ_{calcd}, g cm-3	2.154	2.038	2.048
μ, mm-1	8.564	7.396	7.218
R indices	R1 = 0.0821,	R1 = 0.0354	R1 = 0.0681
(all data)a	wR2 = 0.1686	wR2 = 0.0832	wR2 = 0.1566

[a] $R1 = \Sigma \, | \, |F_o| - |F_c| \, | \, / \, \Sigma \, |F_o|$; $wR2 = \{ \, \Sigma \, [\, w(F_o^2 - F_c^2)^2 \,] \, / \, \Sigma \, [\, w(F_o^2)^2 \,] \, \}^{1/2}$.

Table 2. Selected Bond lengths (pm) and Angles[a] (deg) of **1**, **2** and **3a** Complexes.

	1	**2**	**3a**
Re–O(1)	166.2(8)	167.7(4)	167.4(8)
Re–C(1)	211.1(13)	211.1(6)	211.3(12)
Re–N(1)	211.3(9)	212.5(4)	238.3(9)
Re–N(2)	216.3(9)	220.1(4)	214.8(9)
Re–O(2)	210.0(7)	203.7(4)	
Re–O(3)	201.4(8)	198.6(4)	
Re–S(1)			244.7(3)
Re–S(2)			231.3(3)
O(1)–Re–C(1)	98.8(5)	97.9(3)	102.5(4)
O(1)–Re–N(1)	90.9(4)	87.47(17)	*165.6(4)*
O(1)–Re–N(2)	103.9(4)	99.02(17)	103.6(4)
C(1)–Re–N(1)	88.6(5)	89.3(2)	78.8(4)
C(1)–Re–N(2)	156.3(4)	81.66(15)	153.6(4)
N(2)–Re–N(1)	97.9(3)	100.12(16)	76.9(3)
O(1)–Re–O(2)	*165.3(4)*	*162.86(17)*	-
N(1)–Re–O(3)	159.4(4)	166.48(15)	-
C(1)–Re–O(2)	84.1(5)	84.8(2)	-
S(1)–Re–N(2)	-	-	95.9(3)
S(1)–Re–S(2)	-	-	165.66(10)
C(1)–Re–S(2)	-	-	87.2(4)

[a] Italicized entries: *trans*-[Oxo-Re-donor atom] angles

Results

Structures. Table 1 shows the crystallographic parameters for **1**, **2** and **3a**, and Figure 1 displays their molecular structures drawn by the program CrystalMaker.[39] In all three compounds the rhenium(V) atom occupies the center of a distorted octahedron defined by its axial ligands, the terminal oxo group and one donor atom of one bidentate ligand. The three remaining donor atoms and the methyl group occupy the equatorial plane. Table 2 lists the

important bond distances and angles. In all of these compounds the Re ≡ O distances are virtually identical at 167 pm, as are the Re–C distances at 211 pm. The values of ν(Re–O) from the IR studies fall in the range 985-1003 cm^{-1} for **1-4**, relatively insensitive to the ligand environment. In every case, the donor atom trans to the terminal oxo group lies at a longer distance than its counterpart in the equatorial plane; this comes as no surprise, reflecting extensive π back-bonding from oxo to rhenium(V). In keeping with that, the *trans*(O≡ Re–donor atom) angles lie in the range 162.9–165.5°, notably less than 180°.

All of **1–4** should exist as four geometrical isomers. No evidence for structures of **1** or **2**, other than the ones characterized, was obtained. Even the solution NMR in deuterated chloroform from the original preparation prior to product isolation showed the single isomer. Two isomers in ca. 3:1 ratio were found for **3** in solution, but only the major one, **3a**, was isolated. The minor isomer, **3b**, is characterized by δ(Me–Re) 5.14. The hydrogen signals from the MQ ligand are somewhat broadened, which is not the case for **3a** or free MQH. This suggests an internal process, and brings to mind the exchange between Py and five-coordinate MeReO(edt)Py ($edtH_2$ = 1,2-ethane dithiol). For it, the transition state is six-coordinate and features a turnstile rotation that interchanges the Me group and the two Py ligands.[35,40] Such an exchange, if it occurs within **3b**, could well give rise to signal broadening.

Compound **4** exists as ca. equimolar amounts of two isomers, the structures of which are presented in Chart 1. The basis for these assignments is the widely different coupling constants in the ^{31}P NMR spectra. J_{P-P} = 9 Hz in **4a** and 262 Hz in **4b**. According to the literature[41-43] the very high coupling constant suggests a structure for **4b** in which the two phosphorus donor atoms lie trans to one another.

The donor atoms are N and O for PA and HQ; we surmise the heterocyclic nitrogen is the more weakly bound when both are equatorial; consequently **1** and **2** adopt structures with an axial O-donor atom. Whatever atom is trans to the oxo group is the most weakly bound of all, irrespective of the inherent Lewis basicity. The same rule applies to ligand MQ, which gives rise to the minor isomer **3b**, because a thiolate sulfur is a better Lewis base than a ring nitrogen. In that sense, **3a** is similar insofar as the MQ ligand that spans an axial and an equatorial position. The two isomers differ only in regards to the orientation of the in-plane

ligand, which may be a factor of less consequence. Again, the two isomers of **4** differ in the same way as do the two isomers of **3**. Both isomers of **4** have an O-donor atom trans to the oxo group; that donor is a weaker Lewis base than a phosphine towards Re(V). The comparable abundances of **4a** and **4b** may reflect the steric influence of the bulky phosphine ligand.

Oxygen atom transfer: Sulfoxide to sulfide. The following nearly isoenergetic reaction,[19] occurred when any of the compounds **1–4** was used in catalytic quantity with a 10-fold excess of dimethyl sulfide:

$$Ph_2SO + Me_2S \rightarrow Ph_2S + Me_2SO \quad (6)$$

Unlike some oxorhenium(V) compounds that catalyze this reaction efficiently, such as $[(hoz)_2Re(O)(OH_2)][OTf]$[19] and MeReO(dithiolatte)PPh_3,[32,33] none of these compounds led to a rapid reaction for reasons that will be presented later. We therefore turned our attention to a catalytic system where efficient reactions could be observed.

Oxygen atom transfer: pyridine N-oxides to thioethers. Kinetic studies of these reactions in anhydrous methylene chloride were carried out:

$$XC_5H_4NO + RSR' \rightarrow XC_5H_4N + RS(O)R' \quad (7)$$

Studies were limited to catalyst **1** because **2** and **3** react more slowly and **4** is not available as a single compound. A sample repetitive scan spectrum (X = 4-Me; Me_2S) is presented in Figure 2.

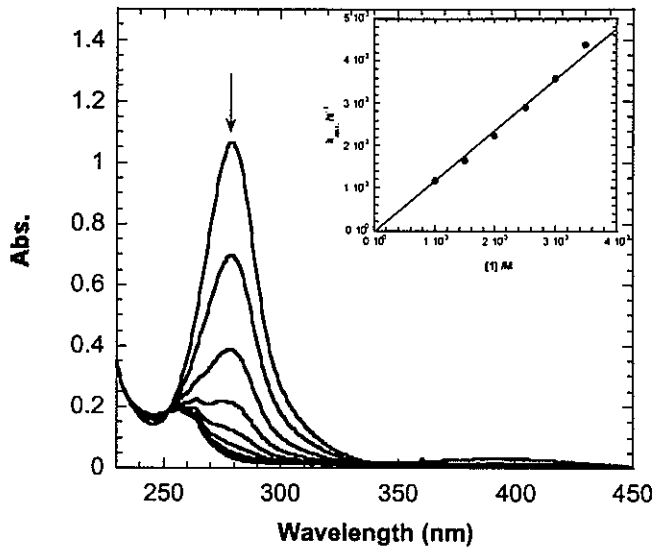

Figure 2. Repetitive scans of 10 mM 4-picoline N-oxide, 100 mM dimethyl sulfide and 2 mM **1** in anhydrous methylene chloride at 25 °C. The inset shows the plot of k_{cat} against the concentration of the catalyst.

The absorbance-time decrease, which shows the greatest amplitude at 279 nm, follows first-order kinetics. The values of k_{obs} so obtained are linear functions of the total catalyst concentration, designated as $[1]_T$, to reflect the fact that at various points during the cycle **1** exists in different forms present at low concentrations.

$$-\frac{d[XC_5H_4NO]}{dt} = k_{cat}[XC_5H_4NO][1]_T \qquad (8)$$

The kinetic determinations employed a ≥10-fold excess of sulfide over pyridine N-oxide. Varying the sulfide concentration gave the same rate constant, k_{cat} = 1.23 ± 0.01 (10 mM Me_2S) and 1.20 ± 0.05 L mol^{-1} s^{-1} (100 mM Me_2S). Different thioethers also gave the same value of k_{cat}/L mol^{-1} s^{-1}: 1.20 ± 0.05 (Me_2S), 1.22 ± 0.01 (pentamethylene sulfide) and 1.28 ± 0.07 (*tert*-butyl methyl sulfide. For a range of pyridine N-oxides, the identity of X exerts a strong influence on the value of k_{cat}, as can be seen from Table 3.

Table 3. Kinetics of Sulfoxidation Reactions Catalyzed by **1**

Part A. UV spectra of XC_5H_4NO and k_{cat} [b]

X	λ_{max}/nm ($\varepsilon/10^4$ L mol^{-1}cm^{-1})	k_{cat}/L mol^{-1} s^{-1}
4-MeO	280 (0.415)	7.5
4-Me	279 (1.07)	1.23
2-Me	272 (1.04)	0.57
3-Me	278 (0.920)	0.43
4-Ph	310 (1.54)	0.36
4-H	277 (0.615)	0.27

Part B. Relative Rate Constants for **5** and methyl aryl sulfides [c]

Y	k_Y/k_H
4-MeO	5.1
4-Me	2.4
4-H	1.00 (rel.)
4-Cl	0.44
4-Br	0.37
4-HO_2C	0.18
4-MeC(O)	0.11
4-CN	0.078

[a] In anhydrous dichloromethane at 25 °C; [b] Conditions: 10 mM XC_5H_4NO, 100 mM Me_2S, 2–8 mM **1**; [c] At 25 °C in D_1-chloroform with 10 mM 4-MeC_5H_4NO, 2 mM **1**, and 50 mM each of MeSPh and $MeSC_6H_4Y$.

Competition experiments. The foregoing reveals that the sulfide enters the catalytic cycle at a stage later than the step(s) that determine the rate and the value of k_{cat}. That is, RSR' reacts with an active rhenium intermediate in a fast subsequent step. To evaluate the effects of thioethers it was therefore useful to take the thioethers in pairs, for which purpose

$MeSC_6H_4Y$ and MeSPh were employed. The design of the experiment is presented in this diagram:

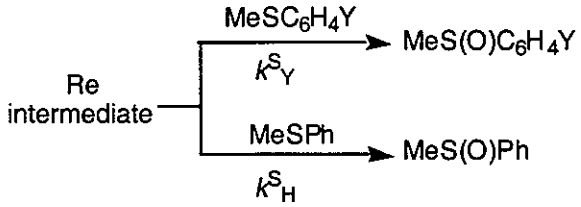

The NMR data were analyzed to determine the ratio k^S_Y/k^S_H for the different aryl groups on sulfide according to eq 5. Table 3B presents the results of such determinations. For reasons to be presented later, it was deemed essential to determine the same ratio for two other pyridine N-oxides. These data are also given in Table 3.

Oxygen-18 labeling. Stoichiometric amounts of **1** and 4-picoline N-oxide and twice as much Me_2S were employed in the case where $MeRe^{18}O(PA)_2$ was employed in anhydrous dichloromethane. The solution was analyzed by GC-MS after two h reaction time. Although ample $Me_2S^{16}O$ was detected, $Me_2S^{18}O$ proved absent.

Discussion

Thermochemical and electronic considerations. Sulfoxide-to-sulfide transfer of an oxygen atom is nearly isoenergetic;. $\Delta G° = -2.9$ kJ for reaction 6 between diphenyl sulfoxide and dimethyl sulfide in methylene chloride.[19] The use of pyridine N-oxides provides a system with a considerably greater driving force. From thermochemical data for C_5H_4NO and Me_2S,[44-47] we estimate $\Delta G° \cong \Delta H° = -63$ kJ mol^{-1}.

The value of k_{cat} depends strongly on the electronic properties of the substituent on the pyridine N-oxide ring. For the five entries in 3 with substituents in the 4- and 3-positions, an analysis according to Hammett's method gives $\rho_{cat} = -5.2$ in Figure 3. This is an exceptionally negative value, most reasonably interpreted in terms of two composite effects that enter in the same direction. More will be said about this in what follows.

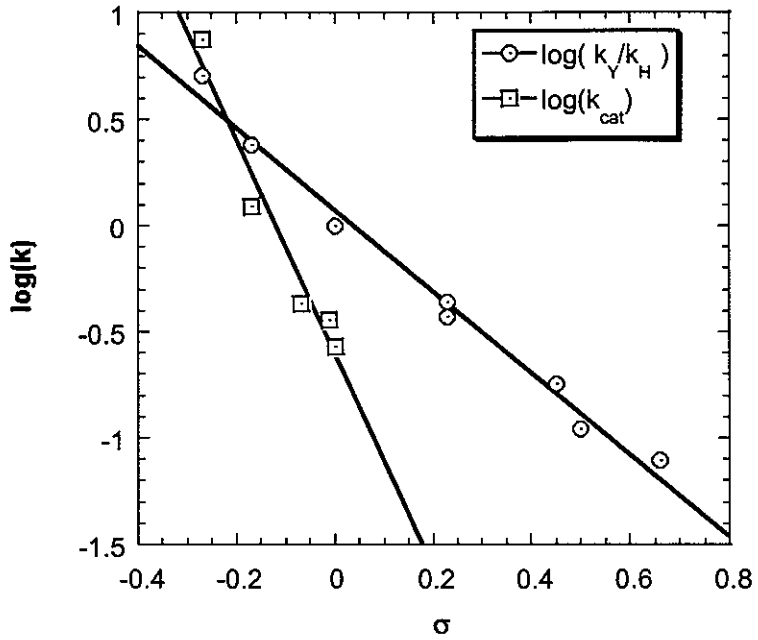

Figure 3. LFER correlations. (1) of k_{cat} values for reactions between XC_5H_4NO and 100 mM Me_2S in presence of 2~8 mM **1** in anhydrous CH_2Cl_2 at 25 °C; (2) of relative rate constants k_Y/k_H determined by competition kinetics for reactions of $MeSC_6H_4Y$ reactions between 10 mM 4-picoline N-oxide and 50 mM each of $MeSC_5H_4Y$ and 50 mM $C_6H_5SCH_3$ in the presence of 2 mM **1** in $CDCl_3$ at 25 °C.

A similar analysis was carried out on the rate constant ratio k^S_Y/k^S_H. The fact that this quantity is a ratio and not an absolute rate constant does not compromise the answer in the least. From the data in Table 3, we find $\rho_S = -1.9$, as shown in Figure 3.

Substrate binding. It seems self-evident that activation of a pyridine N-oxide requires its coordination to rhenium(V) for the catalyst to exert its effect. In systems studied earlier, this has not appeared to pose a significant part of the overall barrier, because five-coordinate catalysts such as MeReO(dithiolate)PPh_3 permit its ready entry. For **1**, however, one must propose either that PyO attacks **1** as it is, giving rise to a seven-coordinate intermediate, or that ring-opening of one arm of one PA ligand precedes entry of PyO. We surmise the N donor atom is preferentially released to avoid the presumably unfavorable $[Re]^+O^-$ in dichloromethane.

We have argued strongly against any dissociative process for complexes such as MeReO(dithiolate)L.[35,40] Thus it seems we must also consider direct ligand displacement as the route to **5**. We discount this mechanism, however; because the parent is not a *five-coordinate* complex from which ligand dissociation becomes unlikely, but a *six-coordinate* one in which the weakness of a rhenium–ligand trans to the oxo group has been well established.

By whichever pathway the **1** = **5** reaction occurs, the net process is an equilibrium that can be represented by an equilibrium constant K_{15}, the value of which varies with the X-group of XC_5H_4NO according to its Lewis basicity. Because this step remains at equilibrium, its mechanism, while of intrinsic interest in its own right, remains immaterial in the kinetic analysis. Stronger Lewis bases are more strongly coordinated in **5**, which provides one factor contributing to the negative reaction constant ρ_{cat} found for k_{cat}. That contribution is designated ρ_{15}, and it is one component of ρ_{cat}.

The rate-controlling step (RCS). The rate law indicates that the thioether is not involved in the mechanism until after the RCS, because the rate remains independent of variations in the concentration and identity of RSR'. We therefore conclude that intermediate **5** undergoes unimolecular cleavage of the N–O bond of coordinated pyridine N-oxide:

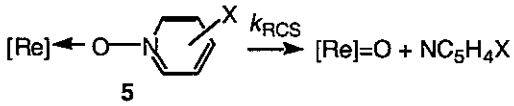

5

The experimental rate constant k_{cat} is therefore a composite: $k_{cat} = K_{15} \times k_{RCS}$. The large negative reaction constant $\rho_{cat} = -5.2$ allows us to argue that the substituent effects on each component must have the same sign, lest cancellation of the effects take place. Because K_{15} represents a Lewis acid-base equilibrium, ρ_{15} will therefore be negative, as argued previously. The negative reaction constant ρ_{RCS} indicates that electron flow from the oxygen of the coordinate pyridine N-oxide provides the principal barrier at the transition state:

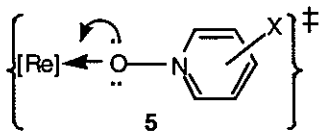

5

The thioether step and its oxo-group selectivity. A direct reaction occurs between intermediate **6** and RSR'. Because it occurs rapidly compared to the RCS, kinetic competition

experiments were employed. The rate constants relative to MeSPh are given in Table 3B. The reaction constant is $\rho_S = -1.9$, which indicates nucleophilic attack of the thioether on one oxygen of dioxorhenium(VII) intermediate **6**. This forms the next intermediate, **7**, that might best be viewed as being or becoming a sulfoxide complex of rhenium(V).

What is astonishing, however, is the high selectivity the thioether exhibits as to which of the two oxo groups of **6** it attacks. Data obtained with the catalyst **1** as $MeRe(^{18}O)(PA)_2$ (oxygen-18 content, 50%) gave, in combination with an equimolar quantity of 4-$MeC_5H_4N^{16}O$ and dimethyl sulfide, only $Me_2S^{16}O$. Had the thioether reacted non-selectively, the enrichment level of the sulfoxide would have corresponded to 25% $Me_2S^{18}O$.

Examination of the plausible structure of **6** is helpful in this regard. As shown in Scheme 1, intermediate **7a** appears to be a dead-end because displacement of sulfoxide by the dangling pyridine arm of PA is impossible. On the other hand, unimolecular displacement within **7b** restores **1** directly and forms $Me_2S^{16}O$ exclusively.

Scheme 1: Oxo-group selectivity at the thioether step

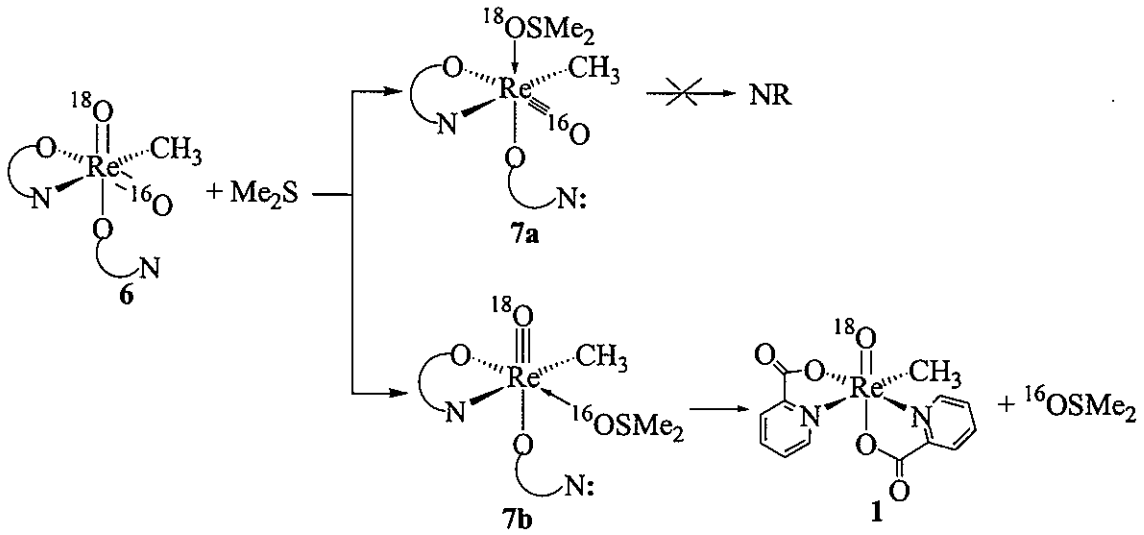

Conclusion. Four new rhenium(V) complexes with monoanionic bidentate ligands, PA, HQ, MQ, and DPPB, were synthesized and characterized. All of them catalyze oxygen atom transfer from milder oxidants, pyridine N-oxides or sulfoxides, to thioethers. Based on

kinetic and mechanistic studies, a multi-step mechanism has been proposed with involvement of several unobserved but plausible intermediates to account for the reaction at each stage.

References

(1) Blower, P. J.; Prakash, S. *Perspectives on Bioinorganic Chemistry* **1999**, *4*, 91-143.

(2) Hashimoto, K.; Yoshihara, K. *Top. Curr. Chem.* **1996**, *176*, 275-291.

(3) Blaeuenstein, P. *New J. Chem.* **1990**, *14*, 405-407.

(4) Bandoli, G.; Tisato, F.; Refosco, F.; Gerber, T. I. A. *Revs. Inorg. Chem.* **1999**, *19*, 187-210.

(5) Romão, C. C.; Kühn, F. E.; Herrmann, W. A. *Chem. Rev.* **1997**, *97*, 3197-3246.

(6) Herrmann, W. A.; Kuehn, F. E. *Acc. Chem. Res.* 1997; Vol. 30, p 169-180.

(7) Herrmann, W. A. *J. Organomet. Chem.* **1986**, *300*, 111-137.

(8) Correia, J. D. G.; Domingos, A.; Santos, I.; Bolzati, C.; Refosco, F.; Tisato, F. *Inorg. Chim. Acta* **2001**, *315*, 213-219.

(9) Bolzati, C.; Tisato, F.; Refosco, F.; Bandoli, G.; Dolmella, A. *Inorg. Chem.* **1996**, *35*, 6221-6229.

(10) Harris, T. A.; McKinney, T. M.; Wu, W.; Fanwick, P. E.; Walton, R. A. *Polyhedron* **1996**, *15*, 3289-3298.

(11) Dorsett, T. E.; Walton, R. A. *J. Organomet. Chem.* **1976**, *114*, 127-134.

(12) Leeaphon, M.; Rohl, K.; Thomas, R. J.; Fanwick, P. E.; Walton, R. A. *Inorg. Chem.* **1993**, *32*, 5562-5568.

(13) Wilcox, B. E.; Heeg, M. J.; Deutsch, E. *Inorg. Chem.* **1984**, *23*, 2962-2967.

(14) Coucouvanis, D. *Acc. Chem. Res.* **1991**, *24*, 1-8.

(15) Holm, R. H.; Berg, J. M. *Acc. Chem. Res.* **1986**, *19*, 363-370.

(16) Holm, R. H. *Coord. Chem. Rev.* **1990**, *100*, 183-221.

(17) Thapper, A.; Lorber, C.; Fryxelius, J.; Behrens, A.; Nordlander, E. *J. Inorg. Bioch.* **2000**, *79*, 67-74.

(18) Young, C. G. *J. Biol. Inorg. Chem* **1997**, *2*, 810-816.

(19) Arias, J.; Newlands, C. R.; Abu-Omar, M. M. *Inorg. Chem.* **2001**, *40*, 2185-2192.

(20) Huang, R.; Espenson, J. H. *J. Mol. Catal. A:* **2001**, *168*, 39-46.

(21) Arterburn, J. B.; Perry, M. C. *Organic Letters* **1999**, *1*, 769-771.

(22) Abu-Omar, M. M.; Khan, S. I. *Inorg. Chem.* **1998**, *37*, 4979-4985.

(23) Arterburn, J. B.; Nelson, S. L. *J. Org. Chem.* **1996**, *61*, 2260-2261.

(24) Espenson, J. H.; Shan, X.; Wang, Y.; Huang, R.; Lahti, D. W.; Dixon, J.; Lente, G.; Ellern, A.; Guzei, I. A. *Inorg. Chem.* **2002**, *41*, 2583-2591.

(25) Jacob, J.; Guzei, I. A.; Espenson, J. H. *Inorg. Chem.* **1999**, *38*, 3266-3267.

(26) Jacob, J.; Guzei, I. A.; Espenson, J. H. *Inorg. Chem.* **1999**, *38*, 1040-1041.

(27) Lente, G.; Shan, X.; Guzei, I. A.; Espenson, J. H. *Inorg. Chem.* **2000**, *39*, 3572-3576.

(28) Jacob, J.; Lente, G.; Guzei, I. A.; Espenson, J. H. *Inorg. Chem.* **1999**, *38*, 3762-3763.

(29) Lente, G.; Guzei, I. A.; Espenson, J. H. *Inorg. Chem.* **2000**, *39*, 1311-1319.

(30) Lente, G.; Jacob, J.; Guzei, I. A.; Espenson, J. H. *Inorg. React. Mechs.* **2000**, *2*, 169-177.

(31) Lente, G.; Espenson, J. H. *Inorg. Chem.* **2000**, *39*, 4809-4814.

(32) Wang, Y.; Espenson, J. H. *Inorg. Chem.* **2002**, *41*, 2266-2274.

(33) Wang, Y.; Espenson, J. H. *Organic Letters* **2000**, *2*, 3525-3526.

(34) Herrmann, W. A.; Kratzer, R. M.; Fischer, R. W. *Angew. Chem., Int. Ed.* **1997**, *36*, 2652-2654.

(35) Espenson, J. H.; Shan, X.; Lahti, D. W.; Rockey, T. M.; Saha, B.; Ellern, A. *Inorg. Chem.* **2001**, *40*, 6717-6724.

(36) Blessing, R. H. *Acta Cryst. Sect. A* **1995**, *51*, 33-38.

(37) All software and sources of the scattering factors are contained in the SHELXTL (version 5.1) program library (G. Sheldrick, B. A. X.-R. S., Madison, WI)..

(38) Herrmann, W. A.; Kuchler, J. G.; Weichselbaumer, G.; Herdtweck, E.; Kiprof, P. *J. Organomet. Chem.* **1989**, *372*, 351-370.

(39) Palmer, D.; CrystalMaker, 2.0 ed.; Hollywell Press: Bicester, Oxfordshire, 1999.

(40) Lahti, D. W.; Espenson, J. H. *J. Amer. Chem. Soc.* **2001**, *123*, 6014-6024.

(41) Bennett, M. A.; Robertson, G. B.; Rokicki, A.; Wickramasinghe, W. A. *J. Am. Chem. Soc.* **1988**, *110*, 7098-7105.

(42) Cotton, F. A.; Dikarev, E. V.; Herrero, S. *Inorg. Chem.* **2000**, *39*, 609-616.

(43) Cowan, R. L.; Trogler, W. C. *J. Am. Chem. Soc.* **1989**, *111*, 4750-4761.

(44) Shaofeng, L.; Pilcher, G. *J. Chem. Thermo.* **1988**, *20*, 463-465.

(45) Ribeiro da Silva, M. D. M. C.; Agostinha, M.; Matos, R.; Vaz, M. C.; Santos, L. M. N. B. F.; Pilcher, G.; Acree, W. E., Jr.; Powell, J. R. *J. Chem. Thermo.* **1998**, *30*, 869-878.

(46) Jenks, W. S.; Matsunaga, N.; Gordon, M. *J. Org. Chem.* **1996,** *61*, 1275-1283.

(47) Mackle, K. *Tetrahedron* 1963, *19*, 1159-1170.

Supporting Information

S-1. Crystal data for compound **1**.

Part A. Crystal data and structure refinement for **1**.

Identification code	1	
Empirical formula	$C_{13}H_{11}N_2O_5Re$	
Formula weight	461.44	
Temperature	298(2) K	
Wavelength	0.71073 Å	
Crystal system	Monoclinic	
Space group	C2/c	
Unit cell dimensions	a = 28.466(7) Å	α= 90°.
	b = 7.0933(17) Å	β= 111.892(4)°.
	c = 15.186(4) Å	γ = 90°.
Volume	2845.3(12) $Å^3$	
Z	8	
Density (calculated)	2.154 Mg/m^3	
Absorption coefficient	8.564 mm^{-1}	
F(000)	1744	
Crystal size	0.4 × 0.4 × 0.1 mm^3	
Theta range for data collection	2.72 to 26.38°.	
Index ranges	$-35 \le h \le 35, -8 \le k \le 8, -18 \le l \le 18$	
Reflections collected	11350	
Independent reflections	2900 [R(int) = 0.1399]	
Completeness to theta = 26.38°	99.6 %	
Absorption correction	Empirical	
Max. and min. transmission	1 and 0.38	
Refinement method	Full-matrix least-squares on F^2	
Data / restraints / parameters	2900 / 0 / 190	
Goodness-of-fit on F^2	0.978	

Final R indices [I>2sigma(I)]	R1 = 0.0656, wR2 = 0.1567
R indices (all data)	R1 = 0.0821, wR2 = 0.1686
Largest diff. peak and hole	3.453 and -4.686 e.Å^{-3}

$R1 = \Sigma \, | \, |F_o| - |F_c| \, | \, / \, \Sigma \, |F_o|$ and $wR2 = \{ \, \Sigma \, [\, w(F_o^2 - F_c^2)^2 \,] \, / \, \Sigma \, [\, w(F_o^2)^2 \,] \, \}^{1/2}$

Part B. Atomic coordinates ($\times 10^4$) and equivalent isotropic displacement parameters (Å$^2 \times 10^3$) for **1**. U(eq) is defined as one third of the trace of the orthogonalized U_{ij} tensor.

	x	y	z	U(eq)
Re	4062(1)	1212(1)	10101(1)	35(1)
C(1)	4738(5)	2510(20)	10999(9)	61(3)
C(2)	4313(5)	2244(19)	8360(8)	52(3)
C(3)	4319(6)	3420(30)	7628(9)	72(5)
C(4)	4124(5)	5220(20)	7536(10)	68(4)
C(5)	3905(5)	5803(19)	8145(10)	59(4)
C(6)	3906(4)	4612(15)	8867(8)	42(3)
C(7)	3657(4)	5083(16)	9551(9)	45(3)
C(8)	2952(5)	693(17)	8615(9)	48(3)
C(9)	2428(5)	370(20)	8335(10)	61(3)
C(10)	2237(5)	-90(20)	9005(10)	62(3)
C(11)	2553(6)	-152(18)	9965(11)	57(3)
C(12)	3068(4)	232(13)	10190(8)	36(2)
C(13)	3445(5)	171(17)	11185(9)	50(3)
N(1)	4099(4)	2849(12)	8966(6)	39(2)
N(2)	3257(3)	647(12)	9523(6)	35(2)
O(1)	4312(4)	-626(13)	9754(7)	60(2)
O(2)	3730(3)	3807(9)	10200(6)	43(2)
O(3)	3923(3)	526(12)	11268(6)	51(2)
O(4)	3416(4)	6532(13)	9466(10)	83(4)

O(5)	3335(4)	-160(16)	11858(7)	74(3)

Part C. Bond lengths [Å] and angles [°] for **1**.

Re-O(1)	1.662(8)	C(6)-C(7)	1.495(16)
Re-O(3)	2.014(8)	C(7)-O(4)	1.215(14)
Re-O(2)	2.100(7)	C(7)-O(2)	1.297(13)
Re-C(1)	2.111(13)	C(13)-O(5)	1.198(13)
Re-N(1)	2.113(9)	C(13)-O(3)	1.343(14)
Re-N(2)	2.163(9)	C(13)-C(12)	1.492(17)
C(2)-N(1)	1.350(14)	C(12)-N(2)	1.346(13)
C(2)-C(3)	1.393(18)	C(12)-C(11)	1.402(18)
C(3)-C(4)	1.38(2)	C(11)-C(10)	1.40(2)
C(4)-C(5)	1.36(2)	C(10)-C(9)	1.357(18)
C(5)-C(6)	1.384(16)	C(9)-C(8)	1.410(17)
C(6)-N(1)	1.351(15)	C(8)-N(2)	1.328(15)

O(1)-Re-O(3)	109.7(4)	O(4)-C(7)-O(2)	126.4(12)
O(1)-Re-O(2)	165.3(4)	O(4)-C(7)-C(6)	120.7(11)
O(3)-Re-O(2)	84.7(3)	O(2)-C(7)-C(6)	112.9(10)
O(1)-Re-C(1)	98.8(5)	O(5)-C(13)-O(3)	122.3(12)
O(3)-Re-C(1)	88.2(4)	O(5)-C(13)-C(12)	123.5(12)
O(2)-Re-C(1)	84.1(5)	O(3)-C(13)-C(12)	114.2(9)
O(1)-Re-N(1)	90.9(4)	N(2)-C(12)-C(11)	122.3(11)
O(3)-Re-N(1)	159.4(4)	N(2)-C(12)-C(13)	115.5(10)
O(2)-Re-N(1)	74.8(3)	C(11)-C(12)-C(13)	122.2(11)
C(1)-Re-N(1)	88.6(5)	C(10)-C(11)-C(12)	117.0(12)
O(1)-Re-N(2)	103.9(4)	C(9)-C(10)-C(11)	120.5(13)
O(3)-Re-N(2)	77.7(3)	C(10)-C(9)-C(8)	119.1(13)
O(2)-Re-N(2)	75.8(3)	N(2)-C(8)-C(9)	121.3(11)

C(1)-Re-N(2)	156.3(4)	C(6)-N(1)-C(2)	119.1(10)
N(1)-Re-N(2)	97.9(3)	C(6)-N(1)-Re	117.2(7)
N(1)-C(2)-C(3)	119.8(13)	C(2)-N(1)-Re	123.6(8)
C(4)-C(3)-C(2)	120.6(13)	C(8)-N(2)-C(12)	119.8(10)
C(5)-C(4)-C(3)	119.0(13)	C(8)-N(2)-Re	127.0(8)
C(4)-C(5)-C(6)	119.2(14)	C(12)-N(2)-Re	113.2(7)
N(1)-C(6)-C(5)	122.2(11)	C(7)-O(2)-Re	120.4(7)
N(1)-C(6)-C(7)	114.1(9)	C(13)-O(3)-Re	119.2(7)
C(5)-C(6)-C(7)	123.5(12)		

Part D. Anisotropic displacement parameters ($Å^2 \times 10^3$) for **1**. The anisotropic displacement factor exponent takes the form: $-2\pi^2[\, h^2 a^{*2} U_{11} + \ldots + 2\, h\, k\, a^* b^* U_{12}\,]$

	U_{11}	U_{22}	U_{33}	U_{23}	U_{13}	U_{12}
Re	32(1)	33(1)	46(1)	1(1)	21(1)	5(1)
C(1)	40(8)	80(10)	59(7)	-5(7)	15(6)	2(6)
C(2)	50(8)	62(8)	51(6)	-16(6)	28(6)	-6(6)
C(3)	73(11)	113(14)	43(7)	-19(8)	35(7)	-45(10)
C(4)	57(10)	87(12)	62(9)	16(8)	25(7)	-18(9)
C(5)	47(8)	48(7)	74(9)	19(6)	15(7)	-12(6)
C(6)	44(7)	36(6)	51(6)	-2(5)	21(5)	-12(5)
C(7)	36(7)	36(6)	68(7)	6(5)	28(6)	-2(5)
C(8)	51(8)	43(6)	60(7)	-3(5)	33(6)	-2(5)
C(9)	38(7)	77(10)	66(8)	-2(7)	17(6)	-3(7)
C(10)	47(8)	61(8)	79(9)	-5(7)	24(7)	-2(6)
C(11)	66(9)	33(6)	87(9)	2(6)	45(8)	5(6)
C(12)	42(6)	22(5)	51(6)	3(4)	24(5)	9(4)
C(13)	60(8)	47(7)	59(7)	12(6)	38(6)	9(6)
N(1)	41(5)	37(5)	37(4)	-8(4)	13(4)	-4(4)
N(2)	39(5)	29(4)	45(5)	4(4)	24(4)	6(4)

O(1)	64(6)	39(4)	92(7)	-1(4)	45(5)	13(4)
O(2)	40(5)	37(4)	60(5)	-5(3)	29(4)	2(3)
O(3)	48(5)	55(5)	52(4)	13(4)	22(4)	2(4)
O(4)	69(7)	41(5)	166(12)	26(6)	73(8)	17(5)
O(5)	75(7)	89(8)	74(6)	27(6)	45(5)	6(6)

Part E. Hydrogen coordinates ($\times 10^4$) and isotropic displacement parameters ($Å^2 \times 10^3$) for **1**.

	x	y	z	U(eq)
H(1A)	5017	2039	10856	91
H(1B)	4792	2242	11648	91
H(1C)	4712	3853	10900	91
H(2)	4457	1049	8431	62
H(3)	4456	2980	7198	87
H(4)	4142	6016	7064	82
H(5)	3758	6990	8078	70
H(8)	3086	945	8155	58
H(9)	2215	457	7700	73
H(10)	1894	-354	8824	75
H(11)	2427	-438	10433	69

S-2. Crystal data for compound **2**.

Part A. Crystal data and structure refinement for **2**.

Identification code	2
Empirical formula	$C_{19}H_{15}N_2O_3Re$
Formula weight	505.53
Temperature	298(2) K
Wavelength	0.71073 Å
Crystal system	Triclinic

Space group	P-1	
Unit cell dimensions	a = 9.233(2) Å	α= 101.054(3)°.
	b = 9.724(2) Å	β= 103.955(3)°.
	c = 10.780(2) Å	γ = 112.402(4)°.
Volume	823.8(3) $Å^3$	
Z	2	
Density (calculated)	2.038 Mg/m^3	
Absorption coefficient	7.396 mm^{-1}	
F(000)	484	
Crystal size	0.36 × 0.28 × 0.25 mm^3	
Theta range for data collection	2.05 to 28.24°.	
Index ranges	$-11 \le h \le 11, -12 \le k \le 12, -14 \le l \le 14$	
Reflections collected	7383	
Independent reflections	3718 [R(int) = 0.0338]	
Completeness to theta = 28.24°	91.3 %	
Absorption correction	Empirical	
Max. and min. transmission	1 and 0.644	
Refinement method	Full-matrix least-squares on F^2	
Data / restraints / parameters	3718 / 0 / 226	
Goodness-of-fit on F^2	1.019	
Final R indices [I>2sigma(I)]	R1 = 0.0323, wR2 = 0.0819	
R indices (all data)	R1 = 0.0354, wR2 = 0.0832	
Largest diff. peak and hole	2.355 and -1.956 $e.Å^{-3}$	

$R1 = \Sigma \, | \, |F_o| - |F_c| \, | \, / \, \Sigma \, |F_o|$ and $wR2 = \{ \, \Sigma \, [\, w(F_o^2 - F_c^2)^2 \,] \, / \, \Sigma \, [\, w(F_o^2)^2 \,] \, \}^{1/2}$

Part B. Atomic coordinates (× 10^4) and equivalent isotropic displacement parameters ($Å^2$ ×

10^3) for **2**. U(eq) is defined as one third of the trace of the orthogonalized U_{ij} tensor.

	x	y	z	U(eq)
Re	2291(1)	-850(1)	2890(1)	28(1)
C(1)	-193(8)	-1670(8)	2859(7)	53(2)
C(2)	3624(7)	1864(7)	5578(5)	35(1)
C(3)	3918(8)	3299(7)	6365(5)	44(1)
C(4)	3421(8)	4254(7)	5806(6)	46(1)
C(5)	2631(7)	3768(6)	4393(6)	37(1)
C(6)	2057(8)	4633(7)	3661(7)	47(1)
C(7)	1377(8)	4047(7)	2297(6)	46(1)
C(8)	1195(7)	2604(7)	1550(6)	39(1)
C(9)	1718(6)	1717(6)	2239(5)	32(1)
C(10)	2420(6)	2309(6)	3655(5)	30(1)
C(11)	5888(7)	1100(6)	2683(5)	38(1)
C(12)	7200(7)	1239(7)	2212(6)	44(1)
C(13)	7016(7)	1(8)	1236(6)	43(1)
C(14)	5528(7)	-1401(7)	720(5)	36(1)
C(15)	5201(8)	-2784(8)	-255(6)	44(1)
C(16)	3717(8)	-4061(7)	-666(6)	45(1)
C(17)	2424(7)	-4088(6)	-183(5)	36(1)
C(18)	2699(6)	-2753(6)	780(5)	29(1)
C(19)	4252(6)	-1416(6)	1231(4)	28(1)
N(1)	2897(5)	1350(5)	4245(4)	31(1)
N(2)	4449(5)	-184(5)	2205(4)	29(1)
O(1)	3070(5)	-1308(5)	4236(4)	39(1)
O(2)	1649(5)	346(4)	1677(3)	35(1)
O(3)	1528(4)	-2701(4)	1299(4)	33(1)

Part C. Bond lengths [Å] and angles [°] for **2**.

Re-O(1)	1.677(4)	C(9)-O(2)	1.325(6)
Re-O(2)	2.037(4)	C(9)-C(10)	1.409(7)
Re-O(3)	1.986(4)	C(10)-N(1)	1.369(6)
Re-C(1)	2.111(6)	C(11)-N(2)	1.322(7)
Re-N(1)	2.125(4)	C(11)-C(12)	1.394(9)
Re-N(2)	2.201(4)	C(12)-C(13)	1.362(9)
C(2)-N(1)	1.330(6)	C(13)-C(14)	1.403(8)
C(2)-C(3)	1.373(8)	C(14)-C(19)	1.411(7)
C(3)-C(4)	1.357(9)	C(14)-C(15)	1.415(8)
C(4)-C(5)	1.414(8)	C(15)-C(16)	1.347(9)
C(5)-C(10)	1.401(7)	C(16)-C(17)	1.406(8)
C(5)-C(6)	1.417(8)	C(17)-C(18)	1.391(7)
C(6)-C(7)	1.356(9)	C(18)-O(3)	1.344(6)
C(7)-C(8)	1.403(9)	C(18)-C(19)	1.408(7)
C(8)-C(9)	1.385(7)	C(19)-N(2)	1.354(6)

O(1)-Re-O(3)	106.04(17)	N(1)-C(10)-C(5)	123.0(5)
O(1)-Re-O(2)	162.86(17)	N(1)-C(10)-C(9)	114.3(4)
O(3)-Re-O(2)	90.91(15)	C(5)-C(10)-C(9)	122.7(5)
O(1)-Re-C(1)	97.9(3)	N(2)-C(11)-C(12)	122.6(5)
O(3)-Re-C(1)	88.7(2)	C(13)-C(12)-C(11)	119.2(5)
O(2)-Re-C(1)	84.8(2)	C(12)-C(13)-C(14)	120.4(5)
O(1)-Re-N(1)	87.47(17)	C(13)-C(14)-C(19)	116.4(5)
O(3)-Re-N(1)	166.48(15)	C(13)-C(14)-C(15)	125.9(5)
O(2)-Re-N(1)	75.59(15)	C(19)-C(14)-C(15)	117.7(5)
C(1)-Re-N(1)	89.3(2)	C(16)-C(15)-C(14)	120.3(5)
O(1)-Re-N(2)	99.02(17)	C(15)-C(16)-C(17)	122.8(5)
O(3)-Re-N(2)	78.20(15)	C(18)-C(17)-C(16)	118.7(5)
O(2)-Re-N(2)	81.66(15)	O(3)-C(18)-C(17)	121.9(5)
C(1)-Re-N(2)	160.9(2)	O(3)-C(18)-C(19)	118.9(4)

N(1)-Re-N(2)	100.12(16)	C(17)-C(18)-C(19)	119.1(5)
N(1)-C(2)-C(3)	122.9(5)	N(2)-C(19)-C(18)	115.7(4)
C(4)-C(3)-C(2)	120.7(5)	N(2)-C(19)-C(14)	122.8(5)
C(3)-C(4)-C(5)	119.0(5)	C(18)-C(19)-C(14)	121.5(5)
C(10)-C(5)-C(4)	116.9(5)	C(2)-N(1)-C(10)	117.4(5)
C(10)-C(5)-C(6)	117.3(5)	C(2)-N(1)-Re	127.8(4)
C(4)-C(5)-C(6)	125.7(6)	C(10)-N(1)-Re	114.8(3)
C(7)-C(6)-C(5)	119.4(6)	C(11)-N(2)-C(19)	118.6(5)
C(6)-C(7)-C(8)	123.5(5)	C(11)-N(2)-Re	130.8(4)
C(9)-C(8)-C(7)	118.4(5)	C(19)-N(2)-Re	110.1(3)
O(2)-C(9)-C(8)	125.5(5)	C(9)-O(2)-Re	118.8(3)
O(2)-C(9)-C(10)	115.9(4)	C(18)-O(3)-Re	115.7(3)
C(7)-C(9)-C(10)	118.6(5)		

Part D. Anisotropic displacement parameters ($Å^2 \times 10^3$) for **2**. The anisotropic displacement factor exponent takes the form: $-2\pi^2[h^2 a^{*2} U_{11} + ... + 2 h k a^* b^* U_{12}]$

	U_{11}	U_{22}	U_{33}	U_{23}	U_{13}	U_{12}
Re	29(1)	25(1)	33(1)	9(1)	11(1)	14(1)
C(1)	38(3)	52(4)	70(4)	13(3)	27(3)	20(3)
C(2)	36(3)	40(3)	33(2)	11(2)	11(2)	23(2)
C(3)	47(3)	43(3)	36(3)	6(2)	12(2)	21(3)
C(4)	54(3)	32(3)	48(3)	5(2)	20(3)	19(3)
C(5)	40(3)	27(3)	51(3)	15(2)	21(2)	17(2)
C(6)	52(3)	33(3)	71(4)	24(3)	26(3)	28(3)
C(7)	47(3)	43(3)	66(4)	36(3)	24(3)	27(3)
C(8)	32(3)	43(3)	49(3)	25(2)	14(2)	19(2)
C(9)	30(2)	32(3)	38(2)	16(2)	12(2)	15(2)
C(10)	27(2)	29(3)	40(2)	13(2)	14(2)	16(2)
C(11)	37(3)	26(3)	42(3)	13(2)	7(2)	10(2)

C(12)	32(3)	39(3)	55(3)	21(3)	11(2)	9(3)
C(13)	29(3)	50(4)	56(3)	24(3)	19(2)	18(3)
C(14)	33(3)	46(3)	39(2)	21(2)	15(2)	23(2)
C(15)	48(3)	57(4)	47(3)	19(3)	26(3)	35(3)
C(16)	58(4)	40(3)	45(3)	9(2)	25(3)	29(3)
C(17)	39(3)	28(3)	39(2)	7(2)	10(2)	16(2)
C(18)	33(2)	28(2)	32(2)	12(2)	13(2)	18(2)
C(19)	31(2)	28(2)	31(2)	13(2)	10(2)	16(2)
N(1)	31(2)	32(2)	33(2)	12(2)	12(2)	18(2)
N(2)	29(2)	27(2)	34(2)	15(2)	10(2)	14(2)
O(1)	51(2)	33(2)	48(2)	22(2)	20(2)	28(2)
O(2)	38(2)	34(2)	33(2)	10(1)	8(1)	20(2)
O(3)	28(2)	25(2)	41(2)	6(1)	12(1)	8(2)

Part E. Hydrogen coordinates ($\times 10^4$) and isotropic displacement parameters ($Å^2 \times 10^3$) for **2**.

	x	y	z	U(eq)
H(1A)	-205	-1616	3755	79
H(1B)	-838	-2737	2281	79
H(1C)	-665	-1031	2527	79
H(2)	3948	1224	5996	42
H(3)	4464	3620	7290	52
H(4)	3598	5214	6344	55
H(6)	2147	5596	4110	56
H(7)	1010	4633	1833	55
H(8)	735	2251	615	47
H(11)	6030	1944	3359	45
H(12)	8190	2165	2560	53
H(13)	7881	86	910	51

H(15)	6014	-2813	-613	53
H(16)	3541	-4963	-1295	54
H(17)	1404	-4982	-503	43

S-3. Crystal data for compound **3a**.

Part A. Crystal data and structure refinement for **3a**.

Identification code	3a	
Empirical formula	$C_{19}H_{15}N_2OReS_2$	
Formula weight	537.65	
Temperature	298(2) K	
Wavelength	0.71073 Å	
Crystal system	Triclinic	
Space group	P-1	
Unit cell dimensions	a = 8.4428(14) Å	α= 85.504(3)°.
	b = 9.1357(15) Å	β= 89.214(3)°.
	c = 12.531(2) Å	γ = 64.825(3)°.
Volume	871.8(3) $Å^3$	
Z	2	
Density (calculated)	2.048 Mg/m^3	
Absorption coefficient	7.218 mm^{-1}	
F(000)	516	
Crystal size	0.3 × 0.3 × 0.2 mm^3	
Theta range for data collection	1.63 to 28.26°.	
Index ranges	$-10 \le h \le 11, -11 \le k \le 11, -16 \le l \le 16$	
Reflections collected	7758	
Independent reflections	3926 [R(int) = 0.0273]	
Completeness to theta = 28.26°	90.8 %	
Absorption correction	Empirical	
Max. and min. transmission	1 and 0.52	

Refinement method	Full-matrix least-squares on F^2
Data / restraints / parameters	3926 / 0 / 226
Goodness-of-fit on F^2	1.099
Final R indices [I>2sigma(I)]	R1 = 0.0633, wR2 = 0.1540
R indices (all data)	R1 = 0.0681, wR2 = 0.1566
Largest diff. peak and hole	6.437 and -2.618 e.Å^{-3}
	(both about 0.6A from Re atom)

$R1 = \Sigma \, | \, |F_o| - |F_c| \, | \, / \, \Sigma \, |F_o|$ and $wR2 = \{ \, \Sigma \, [\, w(F_o^2 - F_c^2)^2 \,] \, / \, \Sigma \, [\, w(F_o^2)^2 \,] \, \}^{1/2}$

Part B. Atomic coordinates ($\times 10^4$) and equivalent isotropic displacement parameters (Å^2 $\times$ 10^3) for **3a**. U(eq) is defined as one third of the trace of the orthogonalized U_{ij} tensor.

	x	y	z	U(eq)
Re	59(1)	7351(1)	7378(1)	33(1)
S(1)	451(4)	4579(4)	7159(3)	44(1)
S(2)	378(4)	9740(3)	7405(2)	38(1)
C(1)	-238(16)	7815(16)	5697(10)	45(3)
C(2)	2586(14)	3606(13)	6737(8)	33(2)
C(3)	3275(16)	2003(14)	6506(10)	42(3)
C(4)	5006(18)	1167(15)	6199(10)	48(3)
C(5)	6082(15)	1938(15)	6104(10)	44(3)
C(6)	5455(13)	3581(14)	6306(8)	34(2)
C(7)	6489(14)	4441(16)	6218(9)	41(3)
C(8)	5801(15)	6022(16)	6422(9)	41(3)
C(9)	4033(15)	6783(15)	6726(10)	40(2)
C(10)	3680(13)	4427(12)	6636(7)	29(2)
C(11)	1460(14)	9439(13)	8640(8)	34(2)
C(12)	1886(18)	10603(16)	9031(10)	48(3)
C(13)	2760(20)	10314(19)	10019(11)	56(3)
C(14)	3167(19)	8940(20)	10632(11)	57(4)

C(15)	2766(17)	7683(17)	10271(9)	46(3)
C(16)	3150(20)	6190(20)	10863(11)	61(4)
C(17)	2690(20)	5080(20)	10479(12)	63(4)
C(18)	1897(18)	5395(16)	9462(10)	48(3)
C(19)	1925(14)	7952(14)	9261(9)	36(2)
N(1)	3019(11)	6033(10)	6836(7)	30(2)
N(2)	1518(12)	6781(11)	8862(7)	37(2)
O(1)	-1993(10)	7806(10)	7764(7)	43(2)

Part C. Bond lengths [Å] and angles [°] for **3a**.

Re-O(1)	1.674(8)	C(7)-C(8)	1.353(18)
Re-C(1)	2.113(12)	C(8)-C(9)	1.414(16)
Re-N(2)	2.148(9)	C(9)-N(1)	1.304(14)
Re-S(2)	2.313(3)	C(10)-N(1)	1.373(13)
Re-N(1)	2.383(9)	C(11)-C(12)	1.383(15)
Re-S(1)	2.447(3)	C(11)-C(19)	1.412(16)
S(1)-C(2)	1.733(11)	C(12)-C(13)	1.40(2)
S(2)-C(11)	1.750(11)	C(13)-C(14)	1.33(2)
C(2)-C(3)	1.380(15)	C(14)-C(15)	1.43(2)
C(2)-C(10)	1.416(15)	C(15)-C(16)	1.41(2)
C(3)-C(4)	1.396(18)	C(15)-C(19)	1.412(16)
C(4)-C(5)	1.365(19)	C(16)-C(17)	1.35(2)
C(5)-C(6)	1.407(17)	C(17)-C(18)	1.398(19)
C(6)-C(7)	1.400(16)	C(18)-N(2)	1.336(15)
C(6)-C(10)	1.435(14)	C(19)-N(2)	1.383(15)

O(1)-Re-C(1)	102.5(4)	C(7)-C(8)-C(9)	119.0(11)
O(1)-Re-N(2)	103.6(4)	N(1)-C(9)-C(8)	123.4(11)
C(1)-Re-N(2)	153.6(4)	N(1)-C(10)-C(2)	119.5(9)

O(1)-Re-S(2)	105.2(3)	N(1)-C(10)-C(6)	120.8(9)
C(1)-Re-S(2)	87.2(4)	C(2)-C(10)-C(6)	119.7(10)
N(2)-Re-S(2)	82.3(3)	C(12)-C(11)-C(19)	118.6(11)
O(1)-Re-N(1)	165.6(4)	C(12)-C(11)-S(2)	122.4(10)
C(1)-Re-N(1)	78.8(4)	C(19)-C(11)-S(2)	119.0(8)
N(2)-Re-N(1)	76.9(3)	C(11)-C(12)-C(13)	120.7(13)
S(2)-Re-N(1)	89.1(2)	C(14)-C(13)-C(12)	121.8(12)
O(1)-Re-S(1)	89.0(3)	C(13)-C(14)-C(15)	120.1(12)
C(1)-Re-S(1)	88.3(4)	C(16)-C(15)-C(19)	117.6(12)
N(2)-Re-S(1)	95.9(3)	C(16)-C(15)-C(14)	124.1(12)
S(2)-Re-S(1)	165.66(10)	C(19)-C(15)-C(14)	118.3(12)
N(1)-Re-S(1)	76.6(2)	C(17)-C(16)-C(15)	120.5(13)
C(2)-S(1)-Re	104.2(4)	C(16)-C(17)-C(18)	119.4(13)
C(11)-S(2)-Re	101.2(4)	N(2)-C(18)-C(17)	122.5(13)
C(3)-C(2)-C(10)	118.1(10)	N(2)-C(19)-C(11)	118.5(10)
C(3)-C(2)-S(1)	121.0(9)	N(2)-C(19)-C(15)	121.1(11)
C(10)-C(2)-S(1)	120.9(8)	C(11)-C(19)-C(15)	120.4(11)
C(2)-C(3)-C(4)	122.4(12)	C(9)-N(1)-C(10)	118.9(9)
C(5)-C(4)-C(3)	120.2(11)	C(9)-N(1)-Re	122.3(8)
C(4)-C(5)-C(6)	120.4(11)	C(10)-N(1)-Re	118.7(6)
C(7)-C(6)-C(5)	123.1(10)	C(18)-N(2)-C(19)	118.7(10)
C(7)-C(6)-C(10)	117.7(10)	C(18)-N(2)-Re	122.1(8)
C(5)-C(6)-C(10)	119.2(10)	C(19)-N(2)-Re	118.9(7)
C(8)-C(7)-C(6)	120.1(10)		

Part D. Anisotropic displacement parameters ($Å^2 \times 10^3$) for **3a**. The anisotropic displacement factor exponent takes the form: $-2\pi^2[\, h^2 a^{*2} U_{11} + \ldots + 2\, h\, k\, a^* b^* U_{12}\,]$

	U_{11}	U_{22}	U_{33}	U_{23}	U_{13}	U_{12}

Re	31(1)	32(1)	36(1)	-4(1)	-1(1)	-12(1)
S(1)	33(1)	38(1)	68(2)	-16(1)	8(1)	-19(1)
S(2)	45(2)	32(1)	35(1)	0(1)	-4(1)	-15(1)
C(1)	37(6)	54(7)	42(6)	-16(5)	1(5)	-15(5)
C(2)	30(5)	37(5)	29(5)	-4(4)	-1(4)	-11(4)
C(3)	44(6)	37(6)	45(6)	-8(5)	4(5)	-16(5)
C(4)	52(7)	35(6)	47(7)	-9(5)	0(6)	-6(5)
C(5)	33(6)	44(6)	44(6)	-7(5)	3(5)	-4(5)
C(6)	28(5)	45(6)	21(4)	-1(4)	-3(4)	-10(4)
C(7)	27(5)	61(7)	33(5)	-3(5)	1(4)	-16(5)
C(8)	31(5)	58(7)	41(6)	-1(5)	-1(5)	-26(5)
C(9)	37(6)	46(6)	44(6)	-6(5)	0(5)	-23(5)
C(10)	29(5)	34(5)	21(4)	-1(4)	-5(4)	-9(4)
C(11)	37(5)	36(5)	33(5)	-11(4)	7(4)	-18(4)
C(12)	62(8)	49(7)	45(7)	-18(6)	13(6)	-32(6)
C(13)	65(9)	71(9)	50(7)	-26(7)	12(6)	-44(8)
C(14)	57(8)	86(11)	37(6)	-22(7)	6(6)	-36(8)
C(15)	45(7)	64(8)	28(5)	-3(5)	2(5)	-23(6)
C(16)	64(9)	79(10)	32(6)	11(6)	-5(6)	-27(8)
C(17)	74(10)	68(9)	46(7)	21(7)	-9(7)	-33(8)
C(18)	58(8)	48(7)	43(6)	10(5)	3(6)	-30(6)
C(19)	32(5)	42(6)	33(5)	-6(4)	3(4)	-14(5)
N(1)	28(4)	31(4)	31(4)	-2(3)	-1(3)	-12(3)
N(2)	37(5)	38(5)	34(5)	3(4)	1(4)	-17(4)
O(1)	35(4)	49(5)	46(5)	-17(4)	10(3)	-17(4)

Part E. Hydrogen coordinates ($\times 10^4$) and isotropic displacement parameters ($Å^2 \times 10^3$) for **3a**.

	x	y	z	U(eq)
H(1A)	-432	8917	5502	67
H(1B)	-1221	7648	5460	67
H(1C)	803	7092	5365	67
H(3)	2560	1459	6556	51
H(4)	5428	82	6060	58
H(5)	7237	1373	5903	53
H(7)	7651	3925	6019	49
H(8)	6481	6601	6364	50
H(9)	3569	7874	6855	49
H(12)	1589	11588	8631	58
H(13)	3060	11104	10254	67
H(14)	3714	8795	11297	68
H(16)	3727	5970	11524	73
H(17)	2892	4124	10888	75
H(18)	1626	4606	9194	57

CHAPTER III. LIGAND DISPLACEMENT AND OXIDATION REACTIONS OF METHYLOXORHENIUM(V) COMPLEXES

A manuscript submitted to *Inorganic Chemistry*

Xiaopeng Shan, Arkady Ellern, Ilia A. Guzei, James H. Espenson

Abstract

Compounds containing the anion $MeReO(edt)(SPh)^-$ (**3**) were prepared with the counter-cations 2-picolinium ($\mathbf{PicH^+3^-}$) and 2,6-lutidinium ($\mathbf{LutH^+3^-}$), where edt is 1,2-ethanedithiolate, were synthesized. $\mathbf{PicH^+3^-}$ and MeReO(edt)(tmtu) (**4**) were crystallographically characterized (tmtu is 1,1,3,3-tetramethylthiourea). The rhenium atom in these compounds exists in a five-coordinate distorted square pyramid. In the solid state, $\mathbf{PicH^+3^-}$ contains an anion with a hydrogen bonded (N–H···S) interaction to the cation. Displacement of PhSH by PPh_3 followed second-order kinetics, whereas with pyridines the reaction was second-order with respect to [Py] and first-order in [$\mathbf{PicH^+3^-}$] in chloroform. To account for this unusual kinetics, the structure formula of $\mathbf{PicH^+3^-}$ in chloroform was proposed to be the molecular species MeReO(edtH)SPh, which can react with a Brönsted base to accelerate ligand displacement. When $PicH^+3^-$ reacts with pyridine N-oxides, a three-stage reaction was observed, consistent with ligand replacement of SPh^- by PyO, N–O bond cleavage of the PyO assisted by another PyO, and eventual decomposition of $MeReO_2(edt)PyO$ to $MeReO_3$. Each of first two steps showed a large substituent effects, $\rho = -5.3$ and $\rho = -4.3$.

Introduction

Our exploration of oxorhenium(V) catalysts[1-7] for oxygen atom transfer (OAT) reactions has been extended. The stoichiometric reactions and certain mechanistic aspects are analogous to those catalyzed by molybdenum oxotranferases.[8-10] Three new methyl(oxo)rhenium(V) complexes have been prepared and characterized; two contain the anion $MeReO(edt)(SPh)^-$ (**3**) with the cations 2-picolinium ($\mathbf{PicH^+3^-}$) and 2,6-lutidinium ($\mathbf{LutH^+3^-}$), and the third is a neutral rhenium compound, MeReO(edt)(tmtu) (**4**), where edt

stands for 1,2-ethanedithiolate and tmtu for 1,1,3,3-tetramethylthiourea. Their structural formulas are shown in Chart 1.

Chart 1. Structural formulas of **1-4**

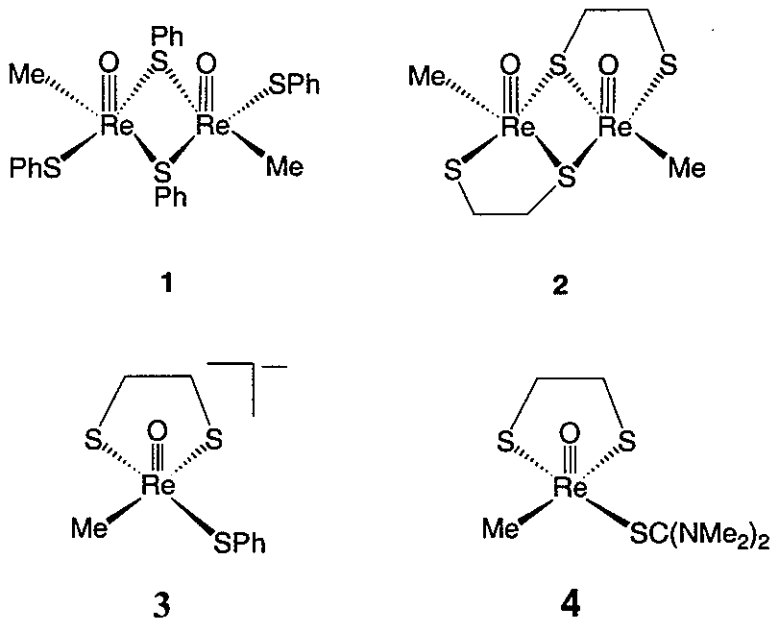

Our goal has been to characterize the steps of OAT from pyridine N-oxides to triphenylphosphine, eq 1, including a study of the intermediates MeReO(edt)PyO from ligand displacement and $MeReO_2$(edt)PyO from oxidation, especially the striking feature that nucleophiles assist oxidation by incorporation of a second molecule of pyridine N-oxide in the transition state. To extend understanding of ligand displacement, the non-oxidizing ligands pyridines and PPh_3 were employed as well. An unanticipated assistance of ligand displacement of **3** by Brønsted bases was discovered and studied.

$$PyO + PPh_3 \rightarrow Py + Ph_3PO \qquad (1)$$

Experimental Section

Reagents and instrumentation. {MeReO(edt)}$_2$ (**2**) was synthesized from 1,2-ethanedithiol and {MeReO(benzenethiolate)}$_2$ (**1**),[11] the later prepared according to the literature.[12] Other chemical reagents were purchased from Aldrich and used as received. Acetonitrile-d_3, benzene-d_6 and chloroform-d_1 were employed as solvents for NMR

spectroscopy. Chloroform from Fisher Scientific was used as solvent for UV/Visible and IR spectrophotometry and for kinetics.

UV/Visible spectra and kinetic data were obtained with Shimadzu Model 3101 and OLIS RSM stopped-flow spectrophotometers. A circulating water thermostatic system controlled the temperature variation to within ±0.2 °C was used for the stopped-flow instrument and an electronic thermostatic holder that maintained the temperature of the cell to ±0.2 °C was used for the UV/visible spectrophotometer. IR spectra were collected with a Nicolet-500 spectrometer. A Bruker DRX-400 MHz spectrophotometer was used to record ^{1}H and ^{13}C NMR spectra. The chemical shift for ^{1}H was calculated relative to the residual proton of the solvent, δ 1.94 for acetonenitrile-d_3, 7.16 for benzene-d_6, and 7.27 for chloroform-d_1. Elemental analyses were performed by Desert Analytics Laboratory.

Kinetics. Reactions of **2**, **PicH$^+$3$^-$**, **LutH$^+$3$^-$**, **4** with PPh_3 and pyridines were followed by the increase in absorbance from 380 to 420 nm from the products MeReO(edt)PPh_3 and MeReO(edt)Py. The concentrations of the ligands were in at least 10-fold excess over rhenium. Thus the absorbance-time data could be fitted to pseudo-first-order kinetics,

$$Abs_t = Abs_\infty + (Abs_0 - Abs_\infty) \times e^{-k\Psi \cdot t} \quad (2)$$

Reactions of **2**, **3** and **4** with pyridine N-oxides were monitored by the change in absorbance from 400 to 500 nm according to the identities of pyridine N-oxides and rhenium compounds. In most case, the concentrations of pyridine N-oxides were at least 100 times larger than those of rhenium compounds. Multiple-phase absorbance changes were observed; reactions with **2** and **3** displayed a three-stage absorbance change: a fast rise and fall followed by a slow decrease. Kinetic traces of the first and second phases can be fitted to consecutive pseudo-first-order kinetics,

$$Abs_t = Abs_\infty + \alpha \times e^{-k\alpha \cdot t} + \beta \times e^{-k\beta \cdot t} \quad (3)$$

The third phase was too sluggish to be studied. In contrast, reaction with compound **4** was a simplified version of reactions with **2** and **3**; only two-stage absorbance change was observed: a fast rise and slow decrease, the former can be fitted to eq 5 and the latter, which spans almost same period of time as the third stage of reactions of **2** and **3**, is not suitable for kinetic study.

Preparation of Salts of MeReO(edt)(SPh)$^-$ (3). 1,2-Ethanedithiol (18.8 mg, 16.8 μL, 0.2 mmol) was added to a mixture of **1** (87 mg, 0.1 mmol) and 2-picoline for PicH$^+$**3**$^-$ or 2,6-lutidine for **LutH**$^+$**3**$^-$ (0.2 mmol) in 20 mL of toluene. The resulting solution was stirred for 2 h as a dark red solid deposited. The product was collected by filtration, rinsed by hexanes, and dried under vacuum.

PicH$^+$**3**$^-$ was obtained in 97% yield. A crystal suitable for x-ray diffraction analysis was obtained by recrystallization from methylene chloride-hexanes. NMR (acetonitrile-d_3) ^{1}H: δ 8.48 (d, 1H), 8.41 (m, 1H), 7.81 (m, 2H), 7.57 (m, 2H), 7.23 (t, 2H), 7.10 (t, 1H), 2.88 (m, 1H), 2.73 (s, 3H), 2.67 (m, 2H), 2.49 (m, 1H), 2.18 (s, 3H); ^{13}C: 150.0, 147.0, 133.9, 128.3, 127.5, 124.8, 124.7, 43.6, 43.4, 19.3, 7.2. IR ($CHCl_3$): 1003 cm^{-1}. UV-Vis($CHCl_3$), λ_{max}/nm (log ε): 337(sh), 397(3.48). Elemental analysis: $C_{15}H_{20}NOReS_3$, Found (Calcd.) C: 35.30 (35.14), H: 4.05 (3.93), N: 2.71 (2.73), S: 19.08 (18.76).

LutH$^+$**3**$^-$ was obtained in 90% yield. NMR (acetonitrile-d_3) ^{1}H: δ 8.26 (t, 1H), 7.57 (m, 4H), 7.23 (m, 2H), 7.11 (m, 1H), 2.88 (m, 1H), 2.69 (m, 2H), 2.67 (s, 6H), 2.17 (s, 3H); ^{13}C: 146.5, 133.9, 127.4, 125.0, 124.7, 43.6, 43.4, 18.8, 6.5. UV-Vis($CHCl_3$), λ_{max}/nm (log ε): 337(sh), 369(3.48).

Preparation of MeReO(edt)(tmtu) (4). Tetramethylthiourea (24.6 mg, 0.2 mmol) was mixed with **2** (61.9 mg, 0.1 mmol) in 20 mL of toluene. After stirring the mixture for 4 h, color of the solution changed from brown to violet and 20 mL of hexanes was layered on the top. After one day, black crystals appeared; they were filtered and rinsed by hexanes. The yield was 76%. Crystal suitable for x-ray diffraction analysis were obtained. NMR (benzene-d_6) ^{1}H: δ 3.58 (m, 1H), 3.25 (s, 3H), 3.13 (m, 1H), 3.04 (m, 1H), 2.69 (m, 1H), 2.38 (sb, 12H); ^{13}C: 46.2, 43.2, 6.8. IR ($CHCl_3$): 976 cm^{-1}. UV-Vis($CHCl_3$), λ_{max}/nm (log ε/L mol^{-1} cm^{-1}): 300(sh). Elemental analysis: $C_7H_{19}N_2ORES_3$, Found (Calcd.) C: 21.71 (21.76), H: 4.12 (4.34), N: 6.34 (6.34), S: 21.80 (21.78).

X-ray Crystallography. Crystals of **PicH**$^+$**3**$^-$ and **4**, selected under ambient conditions, were mounted and centered in the X-ray beam by using a video camera. The crystal evaluation and data collection were performed on a Bruker CCD-1000 diffractometer with Mo K_α (λ = 0.71073 Å) radiation and the detector to crystal distance of 4.90 cm. The cell constants were calculated from a set of certain amount of strong reflections from the actual

data collection. The data were collected by using the full sphere routine. This data set was corrected for Lorentz and polarization effects. The absorption correction was based on fitting a function to the empirical transmission surface as sampled by multiple equivalent measurements[13] using SADABS software.[14]

The position of the Re atom was found by the Patterson method. The remaining atoms were located in an alternating series of least-squares cycles and difference Fourier maps. All non-hydrogen atoms were refined in full-matrix anisotropic approximation. All hydrogen atoms were placed in the structure factor calculation at idealized positions and were allowed to ride on the neighboring atoms with relative isotropic displacement coefficients.

Results

Structures. Table 1 shows the crystallographic parameters for **PicH$^+$3$^-$** and **4** and Figure 1 depicts their molecular structures. In both compounds, the rhenium(V) atom lies in the center of a distorted square pyramid defined by the apical terminal oxo group and a basal plane occupied by a methyl group and three sulfur atoms from edt and SPh or tmtu. Important bond lengths and angles are summarized in Table 2. Irrespective of the negative charge on **PicH$^+$3$^-$**, the Re≡O distances are identical at 169 pm for **PicH$^+$3$^-$** and **4**, as are the values of ν(Re–O) from the IR studies, which fall in the narrow range of 976-1003 cm^{-1}, indicating that the ionic charge does not influence the Re≡O bond. Re–C distances differ slightly, 215 pm in **PicH$^+$3$^-$** and 213 pm in **4**. Also, the chemical shifts of ^{13}C for CH_3, δ 7.2 for **PicH$^+$3$^-$**, 6.8 for **4**; the CH_3 ^{1}H resonance is more sensitive to the ligand environment, being δ 2.38 for PicH$^+$**3**$^-$ and 3.25 for **4**.

Table 1. Experimental Data for the X-ray Diffraction Studies of **PicH$^+$3$^-$** and **4**.

	PicH$^+$3$^-$	**4**
Empirical formula	$C_{15}H_{20}NOReS_3$	$C_7H_{19}N_2OReS_3$
formula weight	512.72	441.64
a, Å	7.3826(5)	8.7615(12)
b, Å	9.7701(6)	16.426(3)
c, Å	12.8309(8)	10.0210(15)
α, deg	94.362(1)	
β, deg	102.414(1)	93.768(4)
γ, deg	99.639(1)	
V, Å^3	885.02(10)	1439.1(4)
Z	2	4
space group	P-1	P2(1)
T, K	173(2)	293(2)
Wavelength, Å	0.71073	0.71073
ρ_{calcd}, g cm^{-3}	1.924	2.038
μ, mm^{-1}	7.216	8.859
R indices	R1 = 0.0237,	R1 = 0.0340
(all data)[a]	wR2 = 0.0575	wR2 = 0.0711

[a] $R1 = \Sigma \, | \, |F_0| - |F_c| \, | \, / \, \Sigma \, |F_0|$; $wR2 = \{ \, \Sigma \, [\, w(F_0^2 - F_c^2)^2 \,] \, / \, \Sigma \, [\, w(F_0^2)^2 \,] \, \}^{1/2}$.

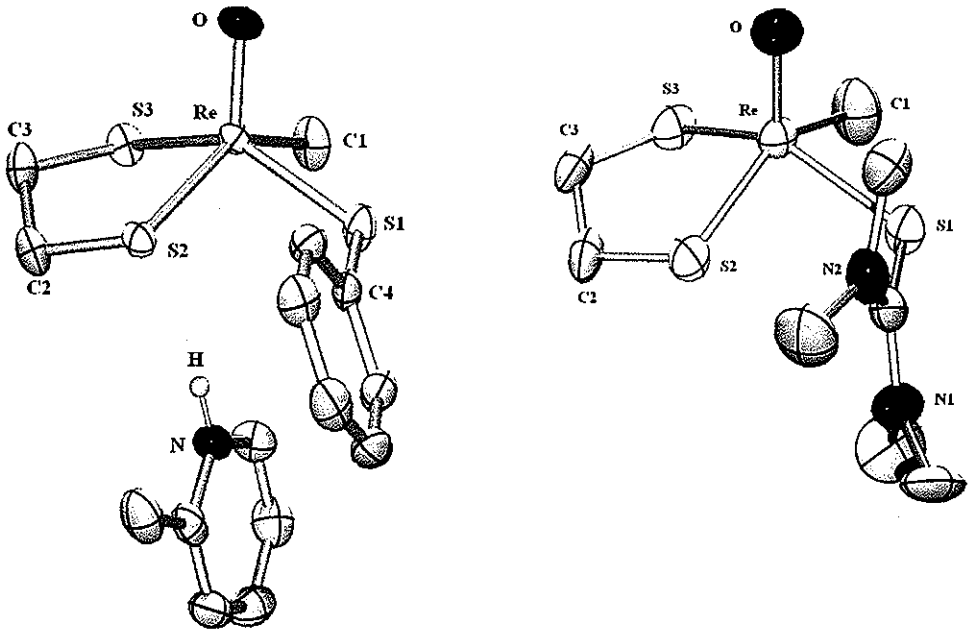

Figure 1. Crystallographically-determined structures of **PicH$^+$3$^-$** and **4**.

Table 2. Selected Bond Lengths (pm) and Angles (deg) of **PicH$^+$3$^-$** and **4**.

	PicH$^+$3$^-$	**4**
Re–O	169.2(3)	168.0(8)
Re–C(1)	215.4(4)	212.8(11)
Re–S(1)	233.49(10)	236.6(3)
Re–S(2)	232.49(9)	230.2(3)
Re–S(3)	229.65(9)	226.4(3)
O–Re–C(1)	107.14(16)	107.6(4)
O–Re–S(1)	109.48(10)	107.4(3)
O–Re–S(3)	108.59(10)	109.2(3)
C(1)–Re–S(2)	139.72(14)	137.3(3)
S(1)–Re–S(3)	140.85(4)	142.54(11)

It is worth noting that **PicH$^+$3$^-$** is a salt in the solid state. The 2 pm elongations of Re–S(2) and Re–S(3) can be attributed to the negative charge on PicH$^+$3$^-$. Based on the

orientation of N–H and the N···S(2) nonbonded distance, 319 pm, we assume a hydrogen bond (N–H···S) interaction between N and S(2). Raper and co-workers discovered a such interaction between a bridging thionate sulfur and a thioamide nitrogen in a copper complex with a N···S distance of 349 pm.[15] Francois and co-workers found two types of N–H···S hydrogen bonds in $(TACN)_2Fe_2S_6$: a "strong" interaction with d_{SH} = 231 pm and a "weak" interaction with d_{SH} = 265 pm.[16] In our case, the calculated position of H gives an angle of 170.3° for N–H···S(2) and d_{SH} = 232 pm. Compared with the literature values, we conclude that a "strong" hydrogen bond interaction exists in **PicH$^+$3$^-$**.

Reactions with PPh_3. PPh_3 reacts with **PicH$^+$3$^-$** and **4** to yield $MeReO(edt)PPh_3$, eq 4-5. The product was identified by ^1H NMR.[17] The reaction of PicH$^+$**3**$^-$ gave rise to benzenethiol and 2-picoline (2-Pic) according to the (aqueous) acidity of PhSH and 2-picolinium (2-PicH$^+$): pK_a = 6.62 for PhSH and pK_a = 6.00 for 2-PicH$^+$; the reaction of **4** generates free tmtu (eq 5).

$$PicH^+\mathbf{3}^- + PPh_3 \rightarrow MeReO(edt)PPh_3 + PhSH + 2\text{-}Pic \quad (4)$$

$$\mathbf{4} + PPh_3 \rightarrow MeReO(edt)PPh_3 + tmtu \quad (5)$$

Both reactions are first-order with respect to the concentrations of rhenium complexes and PPh_3. The second-order rate constants are 2.57 ± 0.02 L mol^{-1} s^{-1} for PicH$^+$**3**$^-$ and (8.20 ± 0.06) × 10^{-2} L mol^{-1} s^{-1} for **4** (Figure 2) in chloroform at 25.0 °C. The thirty-fold slower reaction of **4** can be attributed to the steric hindrance of tmtu. Both rate constants are relatively small compared with the reaction of MeReO(edt)Py with PPh_3, with k = 127 L mol^{-1} s^{-1} in C_6H_6.[18]

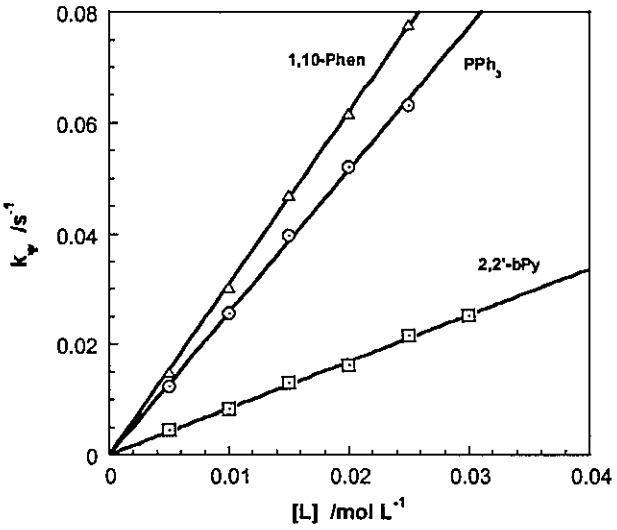

(a)

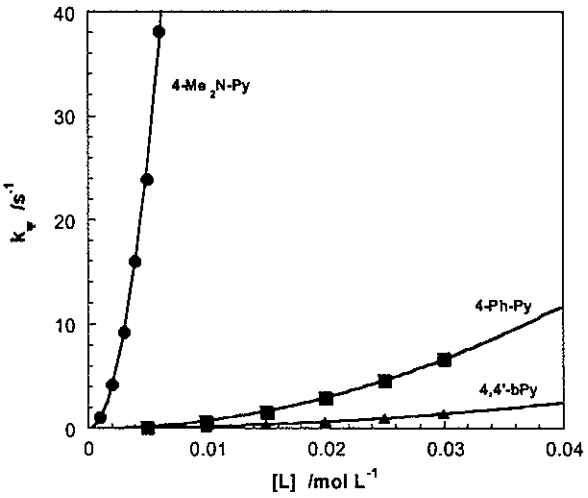

(b)

Figure 2. Plots of the pseudo-first-order rate constants in $CHCl_3$ at 25 °C for the reactions of **PicH$^+$3$^-$** against the concentrations of ligands; (a) PPh_3, 2,2'-bpy, and 1,10-Phen; and (b) 4-Me_2N-Py, 4-Ph-Py, and 4,4'-bpy.

Reactions with Pyridines. The reactions of **PicH$^+$3$^-$** and **4** with pyridines produce MeReO(edt)Py, eq 6-7. The reactions of **PicH$^+$3$^-$** show a second-order dependence on the concentration of pyridines (Figure 2b). Two pyridines, 4-Me_2N-Py and 4-Ph-Py, gave third-order rate constants, $1.02(2) \times 10^6$ and $7.4(1) \times 10^3$ L^2 mol^{-2} s^{-1} respectively. The two order of magnitude difference between these rate constants indicates a substantial electronic effect from the substituents on pyridine. The electronic effect is cumulative because two molecules of pyridine are involved in the third-order reactions. No reaction has been observed with the less basic pyridine, 4-cyano pyridine (4-NC-Py), or with the sterically hindered pyridine, 2-Me-Py. Unlike the case of **PicH$^+$3$^-$**, first-order kinetics was observed when **4** reacts with excess 4-Me_2N-Py, giving k = 20.1(2) L mol^{-1} s^{-1}. To rule out the involvement of the dimer, an experiment with $\{MeReO(edt)\}_2$ (**2**) and 4-Ph-Py was carried out; the reaction shows a second-order dependence on [Py], with $k = 2.76(3) \times 10^4$ L^2 mol^{-2} s^{-1}, which is four times bigger than the rate constant for **PicH$^+$3$^-$**.

$$\textbf{PicH}^+\textbf{3}^- + Py \rightarrow MeReO(edt)Py + PhSH + 2\text{-}Pic \quad (6)$$

$$\textbf{4} + Py \rightarrow MeReO(edt)Py + tmtu \quad (7)$$

Reactions with Bidentate Ligands. The chelating ligands, 2,2'-bpy and 1,10-phen react with **PicH$^+$3$^-$** to produce six-coordinate complexes with first-order dependences on the concentrations of **PicH$^+$3$^-$** and the ligand (Figure 2a). Second-order rate are k = 0.84(2) L mol^{-1} s^{-1} for 2,2'-bpy and 3.14(3) L mol^{-1} s^{-1} for 1,10-phen. Reaction of **PicH$^+$3$^-$** with the nonchelating ligand 4,4'-bipyridine follows second-order kinetics with respect to ligand concentration, Figure 2b, with $k = 1.53(2) \times 10^3$ L^2 mol^{-2} s^{-1}.

Base Assistance in Ligand Displacement. Although the Brønsted bases (**B**) 4-NC-Py and 2-Pic do not react with **PicH$^+$3$^-$**, they do accelerate the reaction of **PicH$^+$3$^-$** with PPh_3. It is important to point out that MeReO(edt)**B** was not observed. When [PPh_3] was kept constant at 10 mM, the pseudo-first order rate constant rises with [**B**] and saturates at the high concentration, Figure 3. The data, including that of the reactions without Brønsted bases, were fitted to eq 8 by using the computer program Scientist,[19] affording K = 240(40), k_2 = 3.1(1) L mol^{-1} s^{-1} for 4-NC-Py, and K = 23(8), k_2 = 1.7(9) L mol^{-1} s^{-1} for 2-Pic, and k_1 = 2.58(5) L mol^{-1} s^{-1}, the same for both. The latter agrees with the directly-determined value, 2.57(2) L mol^{-1} s^{-1}.

$$k_{\psi} = k_1[PPh_3] + \frac{k_2K[B]}{1+K[B]}[PPh_3] \quad (8)$$

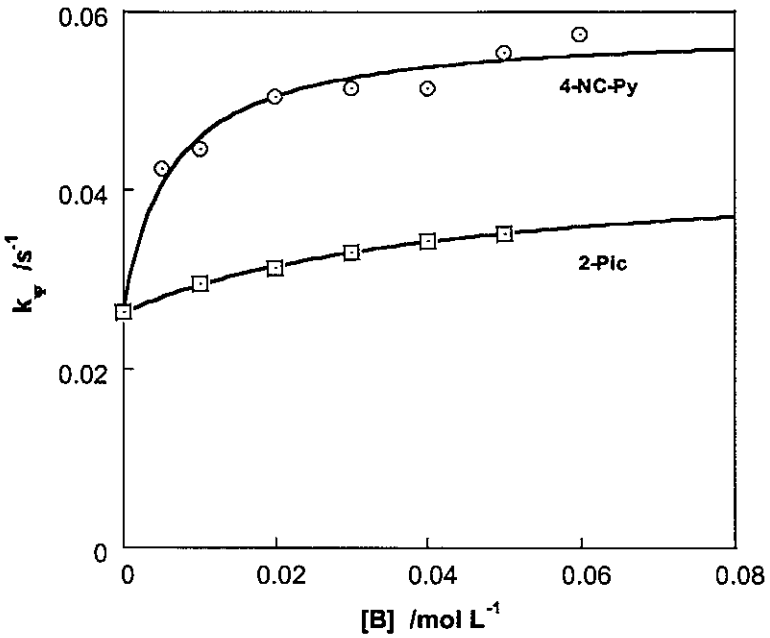

Figure 3. Plots of the pseudo-first-order rate constants for reactions of **PicH$^+$3$^-$** with PPh_3 in the presence of the added Brønsted bases 4-NC-Py and 2-Me-Pic against [**B**] in $CHCl_3$ at 25 °C.

Similarly, 4-NC-Py and 2-Pic accelerated the reaction of **PicH$^+$3$^-$** with 4-Me_2N-Py, but without rate saturation was even at high [**B**]. The rate is given by

$$v = k_m \cdot [\mathbf{3}\text{-Pic}] \cdot [Me_2NPy] \cdot [\mathbf{B}] \quad (9)$$

with $k_m = 5.8(1) \times 10^4$ (4-NC-Py) and 88(18) $L^2\ mol^{-2}\ s^{-1}$ (2-Me-Py).

Brønsted bases like 4-Ph-Py, that react with **PicH$^+$3$^-$** with $k = 7.37(5) \times 10^3\ L^2\ mol^{-2}\ s^{-1}$, show an additional effect when added to the PPh_3 reaction, where biphasic kinetics was observed. The intermediate MeReO(edt)(4-Ph-Py) formed and vanished during the course of the reaction. With excess 4-Ph-Py and PPh_3, the two-phase absorbance change could be fitted to eq 3, giving pseudo-first –order rate constants, k_α for the formation of MeReO(edt)(4-Ph-

Py) and k_β for its disappearance. Keeping [PPh_3] constant (10 mmol/L) during the course of the reaction, k_α shows a second-order dependence on [4-Ph-Py], giving $k_1 = 6.8(1) \times 10^3$ L^2 mol^{-2} s^{-1}; similarly, with [4-Ph-Py] = 30 mM, k_β depends linearly on [PPh_3], giving $k_2 = 98(1)$ L mol^{-1} s^{-1}. Both rate constants agree with the independent values from the direct study of the two steps, $k_\alpha = 7.4(1) \times 10^3$ L^2 mol^{-2} s^{-1} and $k_\beta = 96(1)$ L mol^{-1} s^{-1}.

Again, the acceleration was observed when pyridines were introduced into the reaction of **4** with PPh_3. When [PPh_3] was kept constant, the rate varied linear according to [4-NC-Py] and [2-Pic], giving the second-order rate constants 0.095(1) and 0.0103(3) L mol^{-1} s^{-1} for 4-NC-Py and 2-Pic respectively. With the most basic pyridine, 4-Me_2N-Py, biphasic kinetics was observed and intermediate MeReO(edt)(4-Me_2N-Py) formed and disappeared during the course of the reaction. The rate constants for the two phases were obtained by fitting the kinetic trace to eq 3, giving k_α and k_β, which are linearly dependent on [4-Me_2N-Py] and [PPh_3] respectively, $k_\alpha = k_1$[4-Me_2N-Py] and $k_\beta = k_2$[PPh_3], with $k_1 = 19.2(3)$ and $k_2 = 33(1)$ L mol^{-1} s^{-1}. The consistency of these rate constants is acceptable, compared with the independent values, 20.1(2) L mol^{-1} s^{-1} and 28.0(5) L mol^{-1} s^{-1}.

Influence of the Cation. This factor was investigated by using $LutH^+\mathbf{3}^-$ in reactions with Ph_3P and 4-Ph-Py. The results are identical with those for $\mathbf{PicH^+3^-}$, with k = 2.53(3) L mol^{-1} s^{-1} and 7.14(9) $\times 10^3$ L^2 mol^{-2} s^{-1} for $LutH^+\mathbf{3}^-$, as compared with 2.57(2) and 7.37(5) $\times 10^3$ for $\mathbf{PicH^+3^-}$. An excess of pyridinium ions was added to the reaction system and it had no effect on the kinetics. This clearly indicates that the counter-cation is not involved.

The reactions and rate constants are summarized in Table 4.

Table 4. Summary of Kinetic Data for $\mathbf{PicH^+3^-}$ and **4**

		$\mathbf{PicH^+3^-}$	**4**
L	$[L]^n$	$k/L^{n-1}\ mol^{1-n}\ s^{-1}$	$k/L^{n-1}\ mol^{1-n}\ s^{-1}$
	n =		
4,4'-Bpy	1	$1.53(2) \times 10^3$	
1,10-Phen	1	3.14(3)	
PPh_3	1	2.57(2)	$8.20(6) \times 10^{-2}$
2,2'-Bpy	1	0.84(2)	
4-Me_2N-Py	2	$1.02(6) \times 10^6$	20.1(2), n = 1
4-Ph-Py	2	$7.4(1) \times 10^3$	
4-NC-Py	–	NR	
2-Me-Py	–	NR	
4-Me_2N-Py + 4-NC-Py	1+ 1	$5.8(1) \times 10^4$	
4-Me_2N-Py + 2-Me-Py	1 + 1	88(2)	
PPh_3 + 4-NC-Py	eq 8	$K = 2.4(4) \times 10^2$, $k_2 = 3.1(1)$	
PPh_3 + 2-Me-Py	eq 8	K = 23.8(1), $k_2 = 1.7(9)$	

Reactions with Pyridine N-oxides. When $\mathbf{PicH^+3^-}$ reacts with pyridine N-oxides, a three-stage absorbance change was observed. Those changes are consistent with the scheme: (1) the first pyridine N-oxide replaces the SPh^- ligand to form MeReO(edt)OPy; (2) a second pyridine N-oxide coordinates to rhenium trans to the oxo group, where it assists the cleavage of the N–O bond of the first pyridine N-oxide to yield a Re(VII) intermediate, $MeRe(O)_2$(edt)OPy; (3) the slow decomposition of that intermediate completes the sequence. The UV/Vis spectra of these species are given in Figure 4.

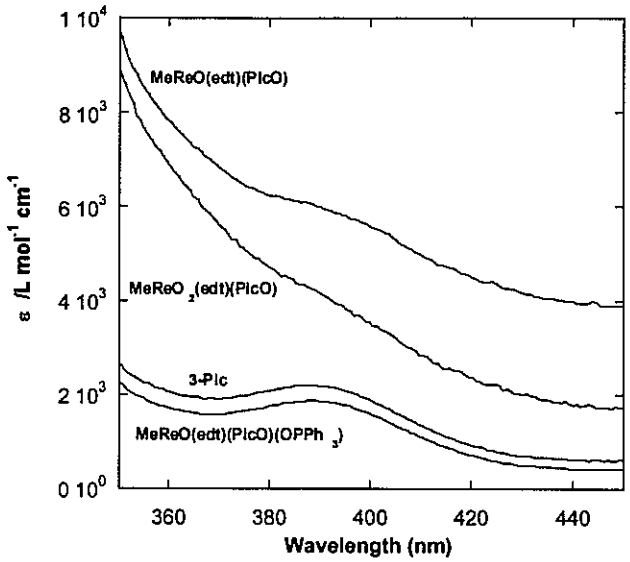

Figure 4. Spectra of $\mathbf{PicH^+3^-}$ and the intermediates MeReO(edt)(OPic) and $MeRe(O)_2(edt)$, and the product from the reaction of the latter with PPh_3, MeReO(edt)(OPic)($OPPh_3$).

The last stage of decomposition was too sluggish for kinetic study. The first two stages of absorbance change were fitted to eq 3, giving two pseudo-first-order rate constants, designated k_α and k_β ($k_\alpha > k_\beta$). Figure 5 depicts the plots of the pseudo-first-order rate constants for oxidation of $\mathbf{PicH^+3^-}$ against concentrations of pyridine N-oxides.

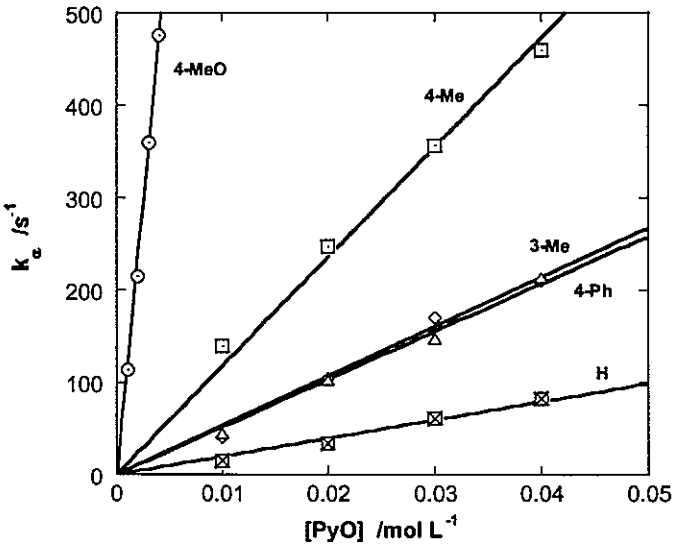

(a)

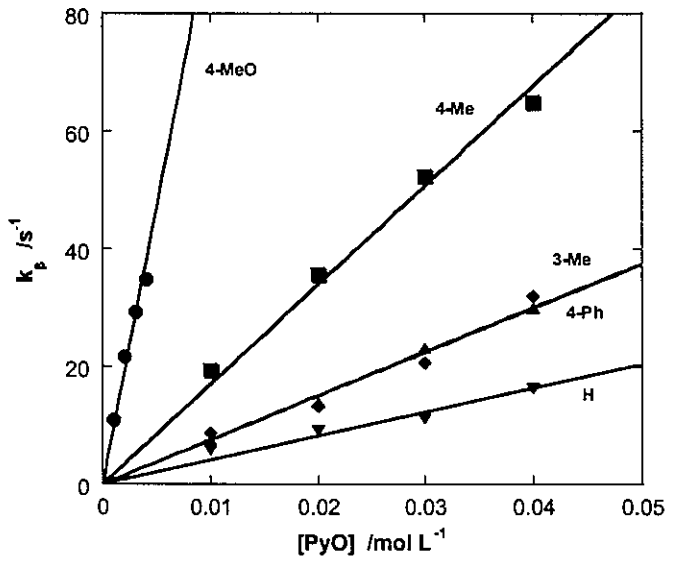

(b)

Figure 5. Plots of (a) k_α, (b) k_β against [PyO] for the reaction between **PicH$^+$3$^-$** and pyridine N-oxides in $CHCl_3$ at 25 °C.

Both rate constants vary linearly with [PyO]. Rate constants of oxidation of **PicH$^+$3$^-$** by pyridine N-oxides are summarized in Table 5. The rate constants of the first stage span a range of 2.3×10^3 - 1.2×10^5 L mol^{-1} s^{-1}; those of the second stage lie in the range of 3×10^2 - 8×10^3 L mol^{-1} s^{-1}. The Hammett analysis for **PicH$^+$3$^-$** shows large reaction constants, $\rho_1 = -5.3$ and $\rho_2 = -4.3$, as illustrated in Figure 6.

Table 5. Rate constants for the oxidation of **PicH$^+$3$^-$** and **4** by pyridine N-oxides.

X-C_5H_4NO	**PicH$^+$3$^-$**		**4**
X =	k_1 / 10^3 L mol^{-1} s^{-1}	k_2 / 10^3 L mol^{-1} s^{-1}	k_1 / L mol^{-1} s^{-1}
4-MeO	123(6)	7.9(8)	20.5(5)
4-Me	10.7(1)	1.53(6)	3.58(3)
3-Me	5.8(4)	0.78(11)	1.27(2)
4-Ph	5.5(3)	0.77(4)	1.34(2)
H	2.3(1)	0.34(4)	0.84(1)

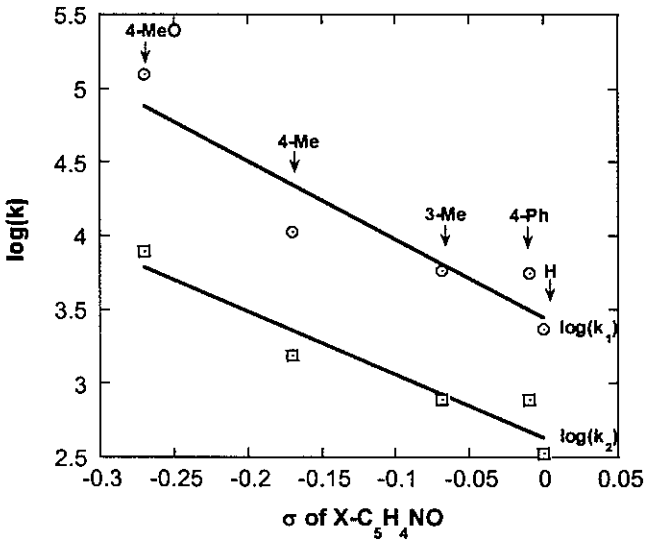

Figure 6. Analysis of the kinetic effects of pyridine N-oxide substituents on the rate constants for oxidation of **PicH$^+$3$^-$** by the Hammett equation.

To identify the rate constant for the first two steps, **2** was used to react with 4-MeO-PyO and 4-Ph-PyO. Three-stage absorbance changes were observed, like those for **PicH$^+$3$^-$**. The first two stages were fitted to eq 3, affording k_α and k_β. Varying the concentrations of two PyO, k_α shows mixed first-order and second-order dependences on [PyO], $k_\alpha = k_{1a}[PyO] + k_{1b}[PyO]^2$, affording $k_{1a} = 1.27(8) \times 10^4$ L mol^{-1} s^{-1} and $k_{1a} = 8(6) \times 10^4$ L^2 mol^{-2} s^{-1} for 4-MeO-PyO and $k_{1a} = 6.5(3) \times 10^3$ L mol^{-1} s^{-1} and $k_{1a} = 1.4(2) \times 10^5$ L^2 mol^{-2} s^{-1} for 4-Ph-PyO. Unlike k_α, k_β varies linearly with [PyO], giving second-order rate constants, $1.70(3) \times 10^4$ L mol^{-1} s^{-1} for 4-MeO-PyO and $1.32(1) \times 10^3$ for 4-Ph-PyO. The monomerization of **2** follows mixed first-order and second-order kinetics.[11,20] Although the complexity of the reaction of **2** with pyridine N-oxides causes the difference between the second-order rate constants from k_β and that of **3**, we can assign k_α to ligand displacement and k_β to oxidation.

The reaction of **4** with PyO is much slower than that of **PicH$^+$3$^-$**; the absorbance change occurs in two stages, the second corresponds to the third stage of the **PicH$^+$3$^-$** reaction, namely the decomposition of $MeRe(O)_2(edt)OPy$. The first stage shows a first-order dependence on [PyO], affording second-order rate constants in the range of 0.8-23 L mol^{-1} s^{-1}, as listed in Table 4. A Hammett analysis gave $\rho = -4.7 \pm 0.7$, indicative of an unusually large substituent effect.

Although the decomposition of $MeRe(O)_2(edt)OPy$ is too sluggish for kinetics, the relative rate can be estimated by the time for complete reaction. The rate did not depend on [PyO], but did depend on the identity of pyridine N-oxides. The rate for 4-Ph-PyO is about two times slower than that for 4-PicO. When PPh_3 was added to the solution of $MeReO_2(edt)OPy$, the absorbance changed instantaneously, as the catalytic cycle transfers an oxygen atom from PyO to PPh_3 according to the stoichiometric reaction of eq 1. Figure 4 depicts the spectrum of $MeReO(edt)(4\text{-}OPic)(OPPh_3)$, the product from this reaction. The weak ligand Ph_3PO can be readily replaced by PyO in the system. Although this metastable species was not structurally characterized, certain comparison compounds has been found in the literature, involving Re-$OPPh_3$ interaction..[21-24] $Re(O)Cl_3(OPPh_3)(Me_2S)$ was used as a catalyst for oxygenation of thiols.[21] $[(HCpz_3)ReCl_2(OPPh_3)]Cl$ and $(HBpz_3)ReCl2(OPPh_3)$ was formed from the oxygen abstraction of PPh_3 from corresponding rhenium(V) complexes, $(HCpz_3)ReOCl_2$ and $(HBpz_3)ReOCl_2$.[24] Analogous Mo and W compounds were also found

and structurally characterized, such as $[LMo^{IV}(OPR_3)(p\text{-}OC_6H_4\text{-}OC_2H_5)_2]^+$ and anti-$Cl_2O(Ph_3PO)W(\mu\text{-}S\text{-}i\text{-}Bu)_2W(Ph_3PO)Cl_2O$.[22,23] The reaction of $MeRe(O)_2(edt)OPy$ with PPh_3 is too fast for stopped-flow kinetics, giving a conservative limit on the second-order rate constant $k > 6\times10^5$ L mol^{-1} s^{-1}.

Discussion

The N–H···S Hydrogen Bond. This interaction has been recognized in metalloproteins, electron-transfer iron-sulfur proteins,[25-29] and cytochrome P450 compounds containing thiolate-metal coordination.[30-32] This weak interaction plays an important role in maintaining structures and modulating redox potentials of metal centers. Model compounds containing Fe, Co, Mo were synthesized and a variety of N–H···S hydrogen bonds were discovered and characterized.[33-37] Most of them contain a bent hydrogen bond with an N–H···S angle <180°.[33-36] In only a few cases has an angle close to 180° been observed.[37] To our knowledge, the N–H···S hydrogen bond in $\mathbf{PicH^+3^-}$ is the first case of this interaction in a rhenium complex. Another point of significance can be seen from the crystal structure of $\mathbf{PicH^+3^-}$: the N–H···S hydrogen bond could arise from the reaction of partially protonated $edtH^-$ with the Brϕnsted base 2-Pic. This reaction enters into the interpretation of the Brϕnsted base-assisted ligand displacement.

Ligand Displacement. First-order kinetics with respect to the concentration of entering ligand is a common feature of well-known ligand displacement reactions of methyl(oxo)rhenium(V) complexes.[38-40] The reaction of $\mathbf{PicH^+3^-}$ with PPh_3 and the reactions of **4** with PPh_3 and pyridines exactly follow this behavior. Strikingly, the reactions of $\mathbf{PicH^+3^-}$ with pyridines displayed second-order dependences on [Py]. Noting that the monomerization of dimeric methyl(oxo)rhenium(V) complexes with pyridine also shows a second-order dependence on [Py] owing to their two metal centers,[11,20] we presumed that $\mathbf{PicH^+3^-}$ in solution has two reaction centers. One can be attacked by PPh_3 and Py, another can be attacked only by the Brønsted base, Py. This proposal was confirmed by the finding that the added Brønsted bases, 4-NC-Py and 2-Pic, which themselves are not able to replace the SPh^- ligand, accelerate the reactions of $\mathbf{PicH^+3^-}$ with PPh_3 and Py. Again, the first-order kinetic dependence on the entering ligand for $\mathbf{PicH^+3^-}$ with the chelating bidentate ligands

2,2'-bpy and 1,10-phen confirms the existence of two reaction centers and further indicates that those two centers are relatively rigid and close to one another, because the reaction with 4,4'-bpy, which does not have two N atoms close to one another, is second-order with respect to [4,4'-bpy].

Thus, we presume that the resulting species that exists in chloroform is MeReO(edtH)SPh, **5**, with the structural formula

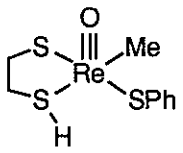

5

This is a neutral complex that contains two reaction centers: a rhenium atom that can be attacked by a Lewis base, PPh_3 and Py, and a proton attached to sulfur that can be abstracted by a Brønsted base. This proposal was also based on the fact that the same rate constants were obtained for **PicH$^+$3$^-$**, LutH$^+$**3**$^-$, and **PicH$^+$3$^-$** + PyH$^+$.

The Lewis base PPh_3 can attack only the rhenium atom of **PicH$^+$3$^-$** to yield MeReO(edt)PPh_3. This reaction is first-order with respect to [PPh_3]. This mechanism was displayed in Scheme **1**, pathway **a**. In the presence of a Brønsted base **B**, = 4-NC-Py or 2-Me-Py, the reaction was accelerated to a saturation level in [**B**], clearly indicating that a prior equilibrium between **PicH$^+$3$^-$** and pyridine was established before the replacement of SPh^- with PPh_3 (pathway **b**). An intermediate with the same structure, containing an N–H···S hydrogen bond, was proposed in accord with the kinetic observations.

Scheme 1. Alternative pathways **a-c** for displacement of SPh^- by PPh_3, assisted by Py

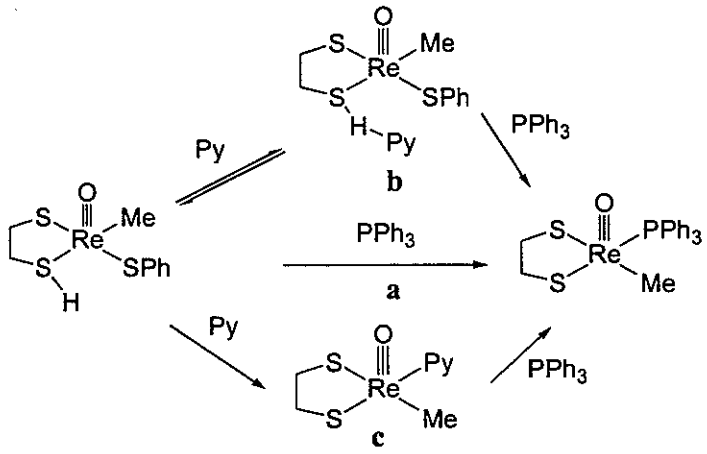

Given that Py can react with $\mathbf{PicH^+3^-}$ to form MeReO(edt)Py, it seems plausible that there will be yet another possible pathway (**c**) by which 4-NC-Py and 2-Pic might assist ligand displacement from $\mathbf{PicH^+3^-}$ with PPh_3. It is through an intermediate, MeReO(edt)Py, which might be formed from more basic and less sterically hindered pyridines. But in the cases of 4-NC-Py and 2-Pic, there is no direct reaction between these pyridines and $\mathbf{PicH^+3^-}$; one can presume that the equilibrium between $\mathbf{PicH^+3^-}$ and MeReO(edt)Py is unfavorable with K<<1. This is totally opposite to the data obtained from the kinetic study, K = 240 ± 40 for 4-NC-Py and K = 23 ± 8 for 2-Me-Py. For 4-Ph-Py, however, which is capable of replacing SPh^-, pathway **c** becomes available, especially at a high (30 mM) concentration of 4-Ph-Py; indeed, MeReO(edt)(4-Ph-Py) was detected spectrophotometrically and the rate constants for the biphasic kinetics were obtained. These values were in good agreement with those from the independently-studied reactions between $\mathbf{PicH^+3^-}$ with 4-Ph-Py and MeReO(edt)(4-Ph-Py) with PPh_3.

As was already mentioned, pyridine, both a Brønsted and a Lewis base, can attack both reaction sites in $\mathbf{PicH^+3^-}$, affording the second-order kinetics with respect to [Py]. The two pathways in Scheme 2 are potentially consistent with the kinetic data. In pathway **d**, a prior equilibrium was proposed as in **b**, followed by an attack of second Py on rhenium from the position trans to oxo group. In **e**, Py approaches rhenium from the lower empty position and

equilibrates quickly; then second Py attacks the proton on sulfur, followed by a fast step to yield the final product MeReO(edt)Py.

Pathway **d** can be ruled out by the following analysis. Since the prior equilibrium in **d** is as same as that in scheme 1 pathway **b**, the same rate saturation should be observed as that in the Py assisted reaction of $\mathbf{PicH^+3^-}$ with PPh_3. But in experiments no saturation was ever observed with single or mixed pyridines. To the contrary, for **e**, the prior equilibrium for formation of six-coordinate rhenium species is unfavorable. Indeed, no $MeReO(edt)L_2$, where L is a monodentate ligand, has ever been observed. The clear implication is that the equilibrium constant is small and can not lead to saturation. On the other hand, it is reasonable to postulate the formation of intermediate six-coordinate rhenium species because they are known with chelating ligands.[39] The reason for requirement of the second Py possibly lies on that the abstraction of proton from sulfur increases the electron density on sulfur, and further on rhenium; the scission of Re–S bond requires the shift of electron from Re to S.

Scheme 2. Alternative pathways **d-e** for the two-stage displacement of SPh^- by Py

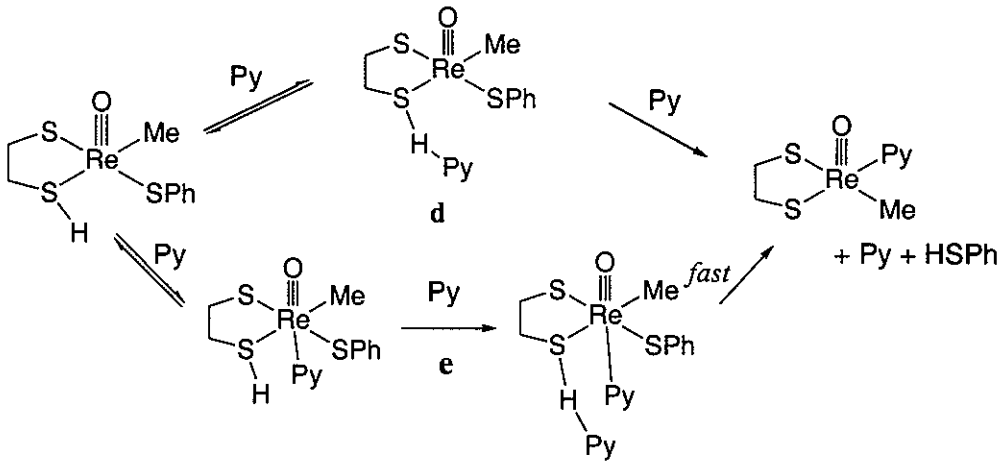

In contrast to **3**, **4** only has one reaction site, the rhenium atom. Displacement of tmtu in **4** by Py and PPh_3 is a simplified version of the reactions of **3**. Since there is no proton on the sulfur atom of **4**, pathway **b, d** and **e** are not suitable for the reactions of **4** any more. But pathways **a** and **c** are adaptable. Scheme 3 depicts two pathways for the reactions of **4** which can account for of the kinetic data. Pathway **f** stands for a common ligand displacement mechanism, affording a second-order kinetics, first-order dependence on both rhenium

complex and the entering ligand. Pathway **g** is a two-step scheme. For 4-Me_2N-Py, the reaction stops at the first step. For the Py assisted reaction of **4** with PPh_3, the reaction goes through two steps, the formation of intermediate MeReO(edt)Py and the generation of final product MeReO(edt)PPh_3. For the case of 4-Me_2N-Py, the formation and disappearance of MeReO(edt)(4-Me_2N-Py) was observed and the kinetic curve was fitted to the biphasic kinetics. When 4-NC-Py and 2-Pic were used, the first step becomes very slow compared the rate of the second step. Thus the biphasic kinetics changes to a single-phase kinetics. That is, the first step becomes the rate-controlling step, which is first-order dependence on [4-NC-Py] and [2-Pic].

Scheme 3. Alternative pathways **f, g** for displacement of tmtu by PPh_3, assisted by Py

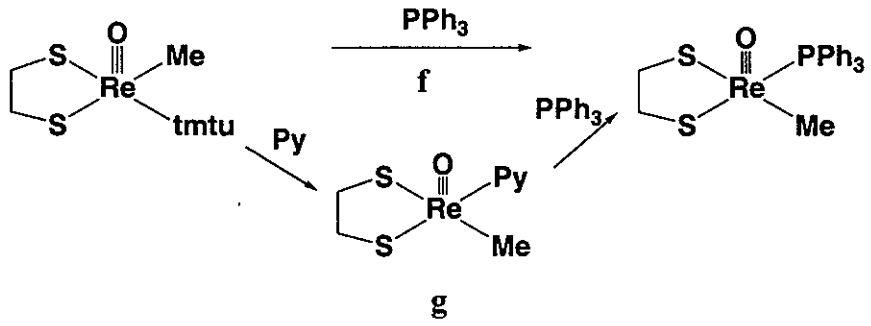

Oxidation of Rhenium Complexes. The nucleophilic assistance on the severing of the O–Py bond was first discovered in the reduction of pyridine N-oxides with the catalyst MeReO(mtp)PPh_3.[6,7] In the case of oxidation of **PicH$^+$3$^-$**, the three-stage absorbance change corresponded to the mechanism proposed in Scheme 4. The first stage is a common ligand displacement since pyridine N-oxide acts well as Lewis base,[41-44] showed first-order dependence on [PyO]. By using series of substituted pyridine N-oxides, a large substituent effect, $\rho = -5.3$, was found, which is possibly caused by the change of the charge on rhenium during the first step.

Scheme 4. Oxidation of $\mathbf{PiCH^{+}3^{-}}$

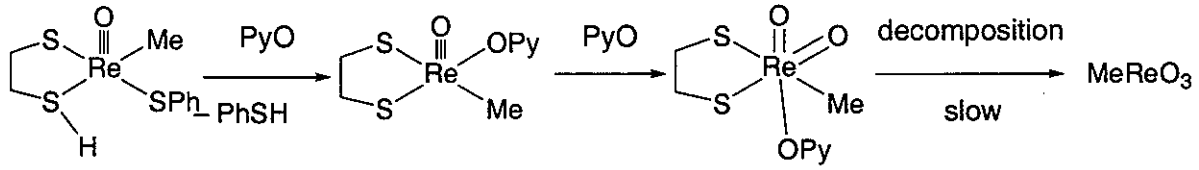

The scission of the O–N bond of PyO coordinated to rhenium occurs in the second step with the assistance of a second PyO. Two reasonable species can be assigned as the transient oxidation product, $MeRe(O)_2(edt)$ and $MeRe(O)_2(edt)OPy$. The former is a five coordinated rhenium(VII) complex with two terminal oxo groups. An analogous compound, $\{MeRe(O)_2\}_2\{SCH_2CH(O)CH(O)CH_2S\}$, was discovered with a distorted trigonal bipyramidal structure that contained two identical oxo groups.[11] The reaction of $MeRe(O)_2(OCH_2CH_2S)$ with PPh_3 occurs at relatively slow rate.[1] Similar to these rhenium compounds, five-coordinate Mo(VI) complexes with two terminal oxo groups were recognized as key models for sulfite oxidase, which has been widely studied and characterized.[45-49] The later species is a six-coordinate rhenium complex containing one PyO trans to one of the oxo groups. With 8-hydroxyqulinoline as ligand, a six-coordinate dirhenium complex was synthesized from the condensation of methyltrioxorhenium(VII) with free ligands.[50] Similarly, the condensation of methyltrioxorhenium(VII) with diols and diamines affords dioxorhenium(VII) complexes with an extra Lewis base as the sixth ligand.[12,51,52] Both of these compounds have two oxo groups cis to each other. In the catalytic OAT reaction, six-coordinate dioxorhenium species were proposed as the immediate oxidation product.[4,53] The dependence on the identity of PyO of the decomposition of this species indicates that PyO is coordinated. Thus $MeRe(O)_2(edt)OPy$ is the product from the scission of the O–N bond.

As to why nucleophilic assistance is necessary, we note that the scission of O-N bond requires electron transfer from O to N. With coordination of another PyO, the electron density on rhenium is enriched; as is it on the O atom. Another possibility is that the coordinated PyO stabilizes the oxidation product, dioxorhenium(VII), which would direct the

reaction through a nucleophile-assisted pathway. Electron-rich ligands are known to stabilize and lower the reactivity of Re=O bond.[54]

The first step of the oxidation of **4** by pyridine N-oxides is much slower than the second, which is as same as the second step of oxidation of $\mathbf{PicH^+3^-}$. So the reactions simplify into two stages, ligand displacement and decomposition of $MeRe(O)_2(edt)OPy$.

Conclusion

Two ionic and one neutral methyl(oxo)rhenium(V) compounds were synthesized and structurally characterized. They were compared in reactivity towards the ligands triphenylphosphane, pyridines, pyridine N-oxides. Assistance from Brønsted bases was found on ligand displacement of ionic rhenium compounds as well as nucleophile assistance on oxidation of all of compounds. From the kinetic data, crystal structures, and an analysis of the intermediates, a structural formula of $\mathbf{PicH^+3^-}$ and mechanisms of ligand displacement and oxidation were proposed.

Acknowledgment. This research was supported by the U.S. Department of Energy, Office of Basic Energy Sciences, Division of Chemical Sciences under Contract W-7405-Eng-82 with Iowa State University of Science and Technology.

Supporting Information Available: X-ray crystallographic tables and plots of kinetic data. This material is available free of charge via the Internet at http://pubs.acs.org.

References

(1) Dixon, J.; Espenson, J. H. *Inorg. Chem.* **2002**, *41*, 4727-4731.

(2) Espenson, J. H. *Chem. Commun.* **1999**, 479-488.

(3) Lente, G.; Espenson, J. H. *Inorg. Chem.* **2000**, *39*, 4809-4814.

(4) Shan, X.; Ellern, A.; Espenson, J. H. *Inorg. Chem.* **2002**, *41*, 7136-7142.

(5) Shan, X.; Ellern, A.; Guzei, I. A.; Espenson, J. H. *Inorg. Chem.* **2003**, *42*, 2362-2367.

(6) Wang, Y.; Espenson, J. H. *Organic Letters* **2000**, *2*, 3525-3526.

(7) Wang, Y.; Espenson, J. H. *Inorg. Chem.* **2002**, *41*, 2266-2274.

(8) Coucouvanis, D. *Acc. Chem. Res.* **1991**, *24*, 1-8.

(9) Holm, R. H.; Berg, J. M. *Acc. Chem. Res.* **1986**, *19*, 363-370.

(10) Holm, R. H. *Coord. Chem. Rev.* **1990**, *100*, 183-221.

(11) Espenson, J. H.; Shan, X.; Wang, Y.; Huang, R.; Lahti, D. W.; Dixon, J.; Lente, G.; Ellern, A.; Guzei, I. A. *Inorg. Chem.* **2002**, *41*, 2583-2591.

(12) Takacs, J.; Cook, M. R.; Kiprof, P.; Kuchler, J. G.; Herrmann, W. A. *Organometallics* **1991**, *10*, 316-320.

(13) Blessing, R. H. *Acta Cryst.* **1995**, *51*, 33-38.

(14) All software and sources of the scattering factors are contained in SHELXTL (version 5.1) program library (Sheldrick, G. M. S., Version 5.1; Bruker Analytical X-ray Systems: Madison, WI, 1997)..

(15) Raper, E. S.; Creighton, J. R.; Clegg, W.; Cucurull-Sanchez, L.; Hill, M. N. S.; Akrivos, P. D. *Inorg. Chim. Acta* **1998**, *271*, 57-64.

(16) Francois, S.; Rohmer, M.-M.; Benard, M.; Moreland, A. C.; Rauchfuss, T. B. *J. Amer. Chem. Soc.* **2000**, *122*, 12743-12750.

(17) Lente, G.; Shan, X.; Guzei, I. A.; Espenson, J. H. *Inorg. Chem.* **2000**, *39*, 3572-3576.

(18) Shan, X.; Espenson, J. H.,, Unpublished information.

(19) Scientist; 2.0 ed.; Micromath Software: 1995.

(20) Lente, G.; Guzei, I. A.; Espenson, J. H. *Inorg. Chem.* **2000**, *39*, 1311-1319.

(21) Abu-Omar, M. M.; Khan, S. I. *Inorg. Chem.* **1998**, *37*, 4979-4985.

(22) Ball, J. M.; Boorman, P. M.; Richardson, J. F. *Inorg. Chem.* **1986**, *25*, 3325-3327.

(23) Nemykin, V. N.; Davie, S. R.; Mondal, S.; Rubie, N.; Kirk, M. L.; Somogyi, A.; Basu, P. *J. Amer. Chem. Soc.* **2002**, *124*, 756-757.

(24) Seymore, S. B.; Brown, S. N. *Inorg. Chem.* **2000**, *39*, 325-332.

(25) Bertini, I.; Felli, I.; Kastrau, D. H. W.; Luchinat, C.; Piccioli, M.; Viezzoli, M. S. *European Journal of Biochemistry* **1994**, *225*, 703-714.

(26) Blake, P. R.; Park, J. B.; Adams, M. W. W.; Summers, M. F. *J. Amer. Chem. Soc.* **1992**, *114*, 4931-4933.

(27) Denke, E.; Merbitz-Zahradnik, T.; Hatzfeld, O. M.; Snyder, C. H.; Link, T. A.; Trumpower, B. L. *J. Biol. Chem.* **1998**, *273*, 9085-9093.

(28) Nakamura, A.; Ueyama, N. *Adv. Inorg. Chem.* **1989**, *33*, 39-67.

(29) Sheridan, R. P.; Allen, L. C.; Carter, C. W., Jr. *J. Biol. Chem.* **1981**, *256*, 5052-5057.

(30) Sundaramoorthy, M.; Terner, J.; Poulos, T. L. *Structure* **1995**, *3*, 1367-1377.

(31) Crane, B. R.; Arvai, A. S.; Gachhui, R.; Wu, C.; Ghosh, D. K.; Getzoff, E. D.; Stuehr, D. J.; Tainer, J. A. *Science* **1997**, *278*, 425-431.

(32) Cupp-Vickery, J. R.; Poulos, T. L. *Nature Structural Biology* **1995**, *2*, 144-153.

(33) Huang, J.; Ostrander, R. L.; Rheingold, A. L.; Leung, Y.; Walters, M. A. *J. Amer. Chem. Soc.* **1994**, *116*, 6769-6776.

(34) Walters, M. A.; Dewan, J. C.; Min, C.; Pinto, S. *Inorg. Chem.* **1991**, *30*, 2656-2662.

(35) Okamura, T.-A.; Takamizawa, S.; Ueyama, N.; Nakamura, A. *Inorg. Chem.* **1998**, *37*, 18-28.

(36) Ueyama, N.; Nishikawa, N.; Yamada, Y.; Okamura, T.-a.; Nakamura, A. *J. Amer. Chem. Soc.* **1996**, *118*, 12826-12827.

(37) Suzuki, N.; Higuchi, T.; Urano, Y.; Kikuchi, K.; Uekusa, H.; Ohashi, Y.; Uchida, T.; Kitagawa, T.; Nagano, T. *J. Amer. Chem. Soc.* **1999**, *121*, 11571-11572.

(38) Shan, X.; Espenson, J. H. *Organometallics* **2003**, *22*, 1250-1254.

(39) Espenson, J. H.; Shan, X.; Lahti, D. W.; Rockey, T. M.; Saha, B.; Ellern, A. *Inorg. Chem.* **2001**, *40*, 6717-6724.

(40) Lahti, D. W.; Espenson, J. H. *J. Amer. Chem. Soc.* **2001**, *123*, 6014-6024.

(41) Batigalhia, F.; Zaldini-Hernandes, M.; Ferreira, A. G.; Malvestiti, I.; Cass, Q. B. *Tetrahedron* **2001**, *57*, 9669-9676.

(42) Herrmann, W. A.; Correia, J. D. G.; Rauch, M. U.; Artus, G. R. J.; Kuehn, F. E. *J. Mol. Catal. A:* **1997**, *118*, 33-45.

(43) Lichtenhan, J. D.; Ziller, J. W.; Doherty, N. M. *Inorg. Chem.* **1992**, *31*, 4210-4212.

(44) Sensato, F. R.; Cass, Q. B.; Longo, E.; Zukerman-Schpector, J.; Custodio, R.; Andres, J.; Hernandes, M. Z.; Longo, R. L. *Inorg. Chem.* **2001**, *40*, 6022-6025.

(45) Garrett, R. M.; Rajagopalan, K. V. *J. Biol. Chem.* **1996**, *271*, 7387-7391.

(46) George, G. N.; Garrett, R. M.; Prince, R. C.; Rajagopalan, K. V. *J. Amer. Chem. Soc.* **1996**, *118*, 8588-8592.

(47) George, G. N.; Kipke, C. A.; Prince, R. C.; Sunde, R. A.; Enemark, J. H.; Cramer, S. P. *Biochemistry* **1989**, *28*, 5075-5080.

(48) Kisker, C.; Schindelin, H.; Pacheco, A.; Wehbi, W. A.; Garrett, R. M.; Rajagopalan, K. V.; Enemark, J. H.; Rees, D. C. *Cell* **1997**, *91*, 973-983.

(49) Peariso, K.; McNaughton, R. L.; Kirk, M. L. *J. Amer. Chem. Soc.* **2002**, *124*, 9006-9007.

(50) Takacs, J.; Kiprof, P.; Kuchler, J. G.; Herrmann, W. A. *J. Organomet. Chem.* **1989**, *369*, C1-C5.

(51) Takacs, J.; Kiprof, P.; Riede, J.; Herrmann, W. A. *Organometallics* **1990**, *9*, 782-787.

(52) Wang, W.-D.; Ellern, A.; Guzei, I. A.; Espenson, J. H. *Organometallics* **2002**, *21*, 5576-5582.

(53) Arias, J.; Newlands, C. R.; Abu-Omar, M. M. *Inorg. Chem.* **2001**, *40*, 2185-2192.

(54) Gangopadhyay, J.; Sengupta, S.; Bhattacharyya, S.; Chakraborty, I.; Chakravorty, A. *Inorg. Chem.* **2002**, *41*, 2616-2622.

Supporting Information

Table of contents:

S-1. Plot of k_Ψ against the Concentration of Triphenylphosphine (10~50 mM) with 0.1 mM **4** in $CHCl_3$ at 25 °C.

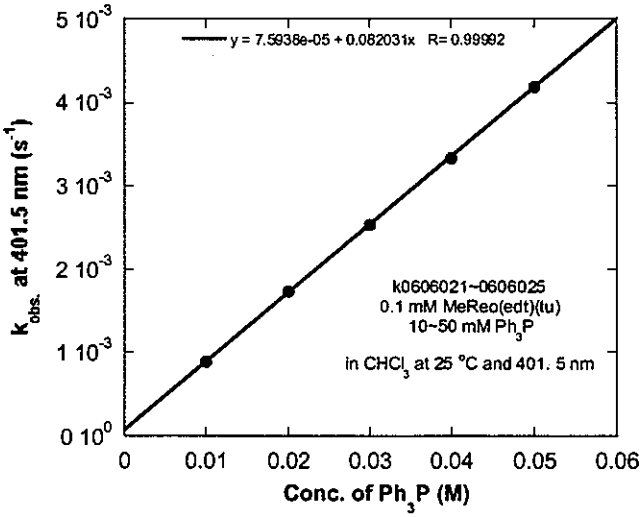

S-2. Plot of k_Ψ against the Concentrations of 4-Picoline N-oxide (5~25 mM) in the Reaction with 0.1 mM **4** in $CHCl_3$ at 25 °C.

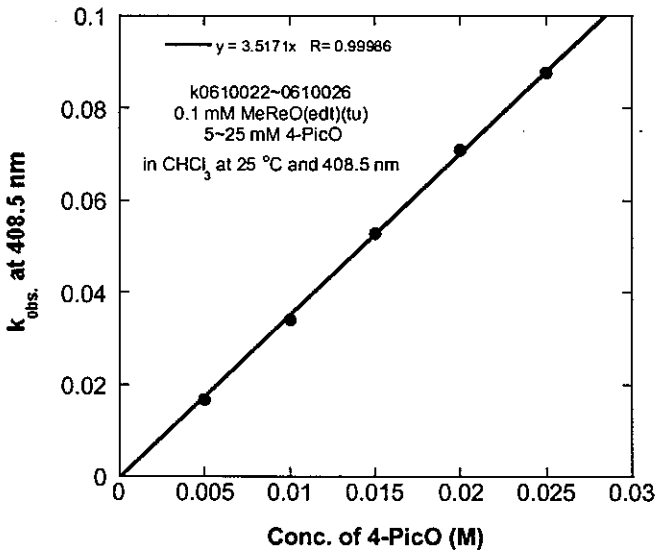

S-3. Plot of k_Ψ against the Concentrations of 4-Phenylpyridine (5~30 mM) in the Reaction with 0.025 mM **2** in $CHCl_3$ at 25 °C.

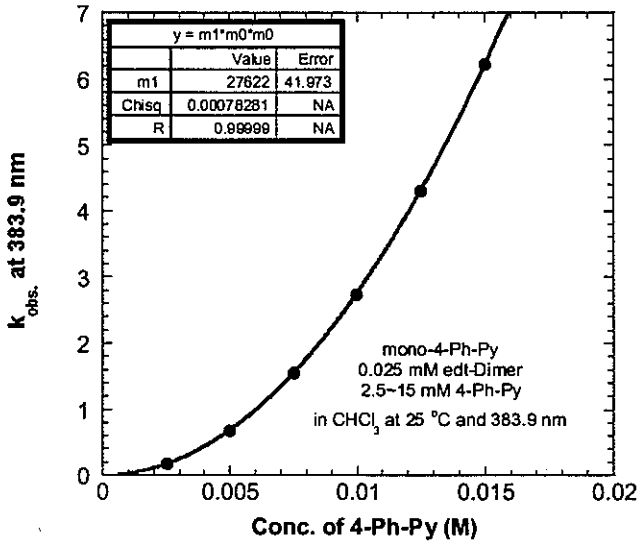

S-4. Plot of k_Ψ against the Concentrations of 4-Phenylpyridine N-oxide (2.5~15 mM) in the Reaction with 0.025 mM **2** in $CHCl_3$ at 25 °C.

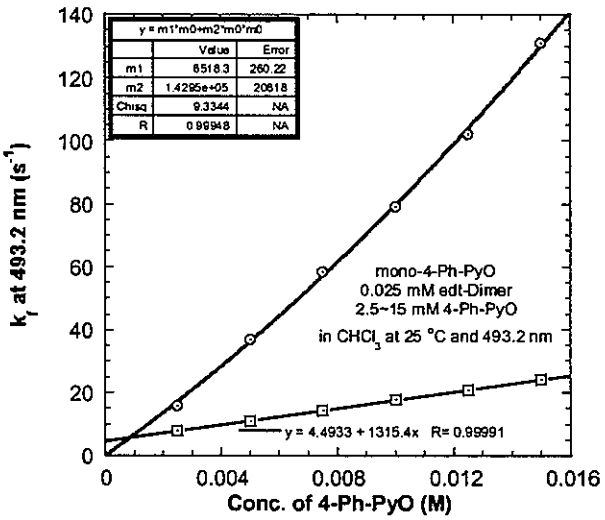

S-5. Plot of k_ψ against the Concentrations of 4-Picoline N-oxide (2.5~15 mM) in the Reaction with 0.025 mM **2** in $CHCl_3$ at 25 °C.

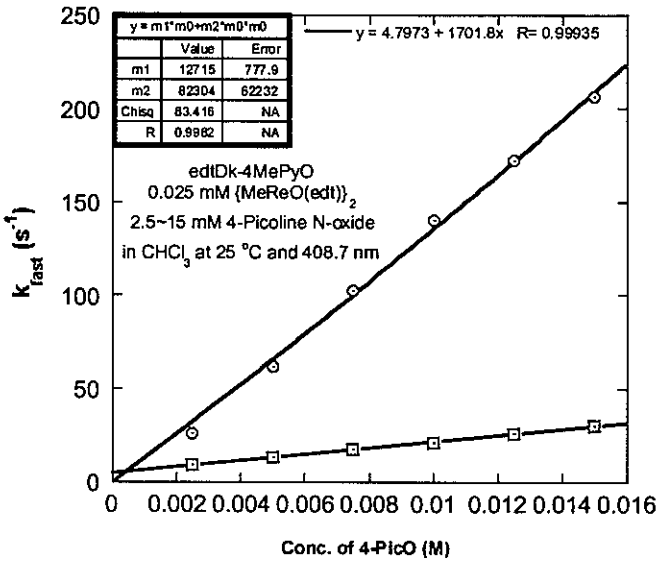

S-6. Crystal data of compound **3**.

A. Crystal data and structure refinement for **3**.

Identification code	**$PicH^+$ 3^-**	
Empirical formula	$C_{15}H_{20}NOPReS_3$	
Formula weight	512.70	
Temperature	173(2) K	
Wavelength	0.71073 Å	
Crystal system	Triclinic	
Space group	$P\bar{1}$	
Unit cell dimensions	a = 7.3826(5) Å	α= 94.362(1)°.
	b = 9.7701(6) Å	β= 102.414(1)°.
	c = 12.8309(8) Å	γ = 99.639(1)°.
Volume	885.02(10) $Å^3$	
Z	2	
Density (calculated)	1.924 Mg/m^3	
Absorption coefficient	7.216 mm^{-1}	

F(000)	496
Crystal size	$0.38 \times 0.35 \times 0.15\ mm^3$
Theta range for data collection	2.13 to 26.37°.
Index ranges	-9<=h<=8, -12<=k<=12, 0<=l<=16
Reflections collected	7878
Independent reflections	3581 [R(int) = 0.0226]
Completeness to theta = 26.37°	99.0 %
Absorption correction	Empirical with SADABS
Max. and min. transmission	0.4107 and 0.1702
Refinement method	Full-matrix least-squares on F^2
Data / restraints / parameters	3581 / 0 / 203
Goodness-of-fit on F^2	1.020
Final R indices [I>2sigma(I)]	R1 = 0.0219, wR2 = 0.0567
R indices (all data)	R1 = 0.0237, wR2 = 0.0575
Largest diff. peak and hole	1.489 and –1.227 e.$Å^{-3}$

B. Atomic coordinates ($\times 10^4$) and equivalent isotropic displacement parameters ($Å^2 \times 10^3$) for **3**. U(eq) is defined as one third of the trace of the orthogonalized U_{ij} tensor.

	x	y	z	U(eq)
Re	841(1)	2795(1)	7240(1)	23(1)
S(1)	-478(1)	4719(1)	6719(1)	35(1)
S(2)	3193(1)	4311(1)	8505(1)	27(1)
S(3)	3231(1)	1660(1)	7002(1)	33(1)
O	-657(4)	1743(3)	7797(2)	35(1)
N	4468(4)	6609(3)	7034(3)	33(1)
C(1)	-28(6)	2229(5)	5527(3)	45(1)
C(2)	5400(5)	3625(5)	8628(3)	39(1)
C(3)	4995(5)	2087(5)	8277(3)	39(1)

C(4)	37(5)	6156(4)	7740(3)	27(1)
C(5)	-75(5)	6014(4)	8790(3)	31(1)
C(6)	328(5)	7175(4)	9549(3)	36(1)
C(7)	814(6)	8482(4)	9276(4)	41(1)
C(8)	913(6)	8666(4)	8246(4)	42(1)
C(9)	531(5)	7510(4)	7467(3)	35(1)
C(10)	5693(7)	8117(5)	8718(4)	48(1)
C(11)	5491(5)	7846(4)	7542(3)	34(1)
C(12)	6261(6)	8756(4)	6909(4)	45(1)
C(13)	5974(7)	8407(5)	5826(4)	49(1)
C(14)	4897(6)	7121(5)	5343(4)	48(1)
C(15)	4142(5)	6233(4)	5967(3)	41(1)

C. Bond lengths [Å] and angles [°] for **3**.

Re-O	1.692(3)	C(4)-C(5)	1.384(5)
Re-C(1)	2.154(4)	C(4)-C(9)	1.404(5)
Re-S(3)	2.2965(9)	C(5)-C(6)	1.386(5)
Re-S(2)	2.3249(9)	C(6)-C(7)	1.360(6)
Re-S(1)	2.3349(10)	C(7)-C(8)	1.363(6)
S(1)-C(4)	1.777(4)	C(8)-C(9)	1.398(6)
S(2)-C(2)	1.844(4)	C(10)-C(11)	1.482(6)
S(3)-C(3)	1.829(4)	C(11)-C(12)	1.383(6)
N-C(15)	1.349(5)	C(12)-C(13)	1.367(7)
N-C(11)	1.846(5)	C(13)-C(14)	1.389(7)
C(2)-C(3)	1.496(6)	C(14)-C(15)	1.356(6)

O-Re-C(1)	107.14(16)	C(5)-C(4)-C(9)	118.0(3)
O-Re-S(3)	108.59(10)	C(5)-C(4)-S(1)	123.3(3)
C(1)-Re-S(3)	80.80(12)	C(9)-C(4)-S(1)	118.7(3)
O-Re-S(2)	113.10(10)	C(4)-C(5)-C(6)	120.7(4)

C(1)-Re-S(2)	139.72(14)	C(7)-C(6)-C(5)	120.8(4)
S(3)-Re-S(2)	84.83(3)	C(6)-C(7)-C(8)	120.3(4)
O-Re-S(1)	109.48(10)	C(7)-C(8)-C(9)	120.1(4)
C(1)-Re-S(1)	79.71(12)	C(8)-C(9)-C(4)	120.2(4)
S(3)-Re-S(1)	140.85(4)	N-C(11)-C(12)	116.4(4)
S(2)-Re-S(1)	88.55(3)	N-C(11)-C(10)	117.9(4)
C(4)-S(1)-Re	114.43(12)	C(12)-C(11)-C(10)	125.7(4)
C(2)-S(2)-Re	107.97(14)	C(13)-C(12)-C(11)	121.0(4)
C(3)-S(3)-Re	104.70(13)	C(12)-C(13)-C(14)	120.1(4)
C(15)-N-C(11)	124.2(3)	C(15)-C(14)-C(13)	118.6(4)
C(3)-C(2)-S(2)	111.0(3)	N-C(15)-C(14)	119.6(4)
C(2)-C(3)-S(3)	110.8(3)		

D. Anisotropic displacement parameters ($Å^2 \times 10^3$) for **3**. The anisotropic displacement factor exponent takes the form: $-2\pi^2[h^2 a^{*2} U_{11} + ... + 2 h k a^* b^* U_{12}]$

	U_{11}	U_{22}	U_{33}	U_{23}	U_{13}	U_{12}
Re	23(1)	21(1)	23(1)	-2(1)	4(1)	2(1)
S(1)	39(1)	33(1)	28(1)	-3(1)	-6(1)	12(1)
S(2)	26(1)	26(1)	27(1)	-1(1)	0(1)	2(1)
S(3)	33(1)	37(1)	30(1)	-2(1)	10(1)	10(1)
O	35(1)	24(1)	46(2)	-1(1)	14(1)	-2(1)
N	33(2)	26(2)	38(2)	1(1)	10(1)	3(1)
C(1)	49(2)	50(3)	29(2)	-11(2)	-2(2)	15(2)
C(2)	26(2)	50(3)	36(2)	0(2)	0(2)	7(2)
C(3)	31(2)	50(3)	37(2)	2(2)	3(2)	19(2)
C(4)	25(2)	26(2)	29(2)	2(1)	0(1)	10(1)
C(5)	31(2)	28(2)	35(2)	7(2)	9(2)	7(2)
C(6)	36(2)	37(2)	36(2)	-4(2)	9(2)	12(2)
C(7)	34(2)	35(2)	52(3)	-10(2)	5(2)	11(2)

C(8)	34(2)	24(2)	68(3)	8(2)	10(2)	8(2)
C(9)	36(2)	35(2)	36(2)	10(2)	7(2)	11(2)
C(10)	41(2)	49(3)	47(3)	-12(2)	-2(2)	7(2)
C(11)	24(2)	34(2)	44(2)	-4(2)	6(2)	7(2)
C(12)	32(2)	30(2)	72(3)	2(2)	15(2)	3(2)
C(13)	50(3)	41(30	69(3)	18(2)	32(2)	13(2)
C(14)	45(3)	59(3)	45(3)	5(2)	16(2)	15(2)
C(15)	45(2)	39(2)	38(2)	-1(2)	13(2)	3(2)

E. Hydrogen coordinates ($\times 10^4$) and isotropic displacement parameters ($Å^2 \times 10^3$) for**3**.

	x	y	z	U(eq)
H(1A)	386	1360	5337	67
H(1B)	542	2977	5164	67
H(1C)	-1407	2092	5299	67
H	3981	6008	7424	39
H(2A)	6180	4114	8181	46
H(2B)	6128	3810	9385	46
H(3A)	4526	1578	8834	47
H(3B)	6174	1782	8194	47
H(5)	-432	5110	8993	37
H(6)	263	7058	10270	43
H(7)	1086	9269	9804	49
H(8)	1242	9581	8057	50
H(9)	607	7641	6750	42
H(10A)	4482	7778	8895	73
H(10B)	6080	9124	8945	73
H(10C)	6652	7630	9092	73
H(12)	7002	9637	7232	54
H(13)	6512	9045	5403	59

H(14)	4693	6869	4592	58
H(15)	3389	5352	5655	49

S-7. Crystal data of Compound **4**.

A. Crystal data and structure refinement for **4**.

Identification code	**4**	
Empirical formula	$C_8H_{19}N_2ORES_3$	
Formula weight	441.63	
Temperature	293(2) K	
Wavelength	0.71073 Å	
Crystal system	Monoclinic	
Space group	P2(1)	
Unit cell dimensions	a = 8.7615(12) Å	α= 90°.
	b = 16.426(3) Å	β= 93.768(4)°.
	c = 10.0210(15) Å	γ = 90°.
Volume	1439.1(4) $Å^3$	
Z	4	
Density (calculated)	2.038 Mg/m^3	
Absorption coefficient	8.859 mm^{-1}	
F(000)	848	
Crystal size	0.22 × 0.18 × 0.08 mm^3	
Theta range for data collection	2.04 to 24.72°.	
Index ranges	$-10 \le h \le 3, -18 \le k \le 15, -8 \le l \le 11$	
Reflections collected	4488	
Independent reflections	3787 [R(int) = 0.0233]	
Completeness to theta = 24.72°	89.4 %	
Absorption correction	Empirical	
Max. and min. transmission	0.68 and 0.26	

Refinement method	Full-matrix least-squares on F^2
Data / restraints / parameters	3787 / 1 / 271
Goodness-of-fit on F^2	0.962
Final R indices [I>2sigma(I)]	R1 = 0.0303, wR2 = 0.0698
R indices (all data)	R1 = 0.0340, wR2 = 0.0711
Absolute structure parameter	0.003(12)
Largest diff. peak and hole	1.805 and -1.062 e.$Å^{-3}$

$R1 = \Sigma \, | \, |F_o| - |F_c| \, | \, / \, \Sigma \, |F_o|$ and $wR2 = \{ \, \Sigma \, [\, w(F_o^2 - F_c^2)^2 \,] \, / \, \Sigma \, [\, w(F_o^2)^2 \,] \, \}^{1/2}$

B. Atomic coordinates ($\times 10^4$) and equivalent isotropic displacement parameters ($Å^2 \times 10^3$) for **4**. U(eq) is defined as one third of the trace of the orthogonalized U_{ij} tensor.

	x	y	z	U(eq)
Re(1)	8331(1)	989(1)	9873(1)	32(1)
Re(2)	4183(1)	9011(1)	5076(1)	38(1)
S(1)	9233(4)	-44(2)	8587(3)	55(1)
S(2)	8741(4)	99(2)	11583(3)	48(1)
S(3)	9602(3)	1907(2)	8503(3)	40(1)
S(4)	2758(4)	8197(2)	6356(3)	49(1)
S(5)	2023(3)	9086(2)	3650(3)	46(1)
S(6)	5614(3)	8976(2)	3164(3)	47(1)
C(1)	9252(14)	1840(7)	11311(11)	43(3)
C(2)	8768(17)	-918(7)	10839(13)	60(4)
C(3)	9360(30)	-963(9)	9608(15)	120(9)
C(4)	9744(13)	1469(6)	6918(12)	38(3)
C(5)	12515(15)	1426(9)	7309(15)	70(4)
C(6)	11364(15)	1384(9)	5018(13)	65(4)
C(7)	8493(17)	554(8)	5226(14)	60(4)
C(8)	6935(13)	1544(8)	6414(14)	55(4)
C(9)	5944(16)	8180(9)	5738(17)	79(5)

C(10)	794(14)	8513(7)	5941(13)	50(3)
C(11)	465(13)	8597(7)	4498(14)	50(3)
C(12)	4661(13)	9477(7)	1804(12)	42(3)
C(13)	5038(14)	10803(7)	2863(12)	51(3)
C(14)	2967(16)	10621(9)	1122(15)	72(4)
C(15)	4256(19)	9437(9)	-676(12)	70(5)
C(16)	4220(20)	8168(8)	596(17)	89(5)
N(1)	11114(11)	1393(6)	6450(10)	44(3)
N(2)	8487(11)	1238(5)	6196(10)	40(2)
N(3)	4295(10)	10261(6)	1863(10)	45(2)
N(4)	4328(12)	9067(7)	684(10)	50(3)
O(1)	4589(10)	9891(5)	5957(9)	60(2)
O(2)	6447(9)	1174(5)	9636(9)	49(2)

C. Bond lengths [Å] and angles [°] for **4**.

Re(1)-O(2)	1.680(8)	S(6)-C(12)	1.756(13)
Re(1)-C(1)	2.128(11)	C(2)-C(3)	1.372(18)
Re(1)-S(2)	2.264(3)	C(4)-N(1)	1.323(14)
Re(1)-S(1)	2.302(3)	C(4)-N(2)	1.333(14)
Re(1)-S(3)	2.366(3)	C(5)-N(1)	1.453(16)
Re(2)-O(1)	1.718(8)	C(6)-N(1)	1.465(14)
Re(2)-C(9)	2.133(14)	C(7)-N(2)	1.486(14)
Re(2)-S(4)	2.281(3)	C(8)-N(2)	1.479(14)
Re(2)-S(5)	2.298(3)	C(10)-C(11)	1.463(18)
Re(2)-S(6)	2.359(3)	C(12)-N(4)	1.325(15)
S(1)-C(3)	1.823(14)	C(12)-N(3)	1.330(14)
S(2)-C(2)	1.830(13)	C(13)-N(3)	1.460(14)
S(3)-C(4)	1.756(12)	C(14)-N(3)	1.463(15)
S(4)-C(10)	1.819(13)	C(15)-N(4)	1.491(16)
S(5)-C(11)	1.839(11)	C(16)-N(4)	1.481(17)

O(2)-Re(1)-C(1)	107.6(4)	C(11)-S(5)-Re(2)	107.2(5)
O(2)-Re(1)-S(2)	109.2(3)	C(12)-S(6)-Re(2)	111.6(4)
C(1)-Re(1)-S(2)	83.0(3)	C(3)-C(2)-S(2)	115.5(10)
O(2)-Re(1)-S(1)	115.1(3)	C(2)-C(3)-S(1)	116.5(11)
C(1)-Re(1)-S(1)	137.3(3)	N(1)-C(4)-N(2)	121.1(11)
S(2)-Re(1)-S(1)	84.51(12)	N(1)-C(4)-S(3)	118.7(10)
O(2)-Re(1)-S(3)	107.4(3)	N(2)-C(4)-S(3)	120.2(8)
C(1)-Re(1)-S(3)	78.6(3)	C(11)-C(10)-S(4)	112.0(8)
S(2)-Re(1)-S(3)	142.54(11)	C(10)-C(11)-S(5)	113.2(9)
S(1)-Re(1)-S(3)	87.35(10)	N(4)-C(12)-N(3)	119.4(12)
O(1)-Re(2)-C(9)	104.9(6)	N(4)-C(12)-S(6)	119.1(10)
O(1)-Re(2)-S(4)	107.8(3)	N(3)-C(12)-S(6)	121.6(10)
C(9)-Re(2)-S(4)	82.1(4)	C(4)-N(1)-C(5)	122.4(10)
O(1)-Re(2)-S(5)	114.1(3)	C(4)-N(1)-C(6)	123.0(11)
C(9)-Re(2)-S(5)	141.0(5)	C(5)-N(1)-C(6)	114.0(10)
S(4)-Re(2)-S(5)	85.54(12)	C(4)-N(2)-C(8)	123.9(10)
O(1)-Re(2)-S(6)	109.6(3)	C(4)-N(2)-C(7)	122.1(10)
C(9)-Re(2)-S(6)	79.9(4)	C(8)-N(2)-C(7)	113.4(10)
S(4)-Re(2)-S(6)	141.48(12)	C(12)-N(3)-C(13)	121.5(10)
S(5)-Re(2)-S(6)	87.49(10)	C(12)-N(3)-C(14)	123.7(11)
C(3)-S(1)-Re(1)	107.9(5)	C(13)-N(3)-C(14)	114.0(10)
C(2)-S(2)-Re(1)	106.7(4)	C(12)-N(4)-C(16)	124.6(12)
C(4)-S(3)-Re(1)	109.1(4)	C(12)-N(4)-C(15)	124.1(11)
C(10)-S(4)-Re(2)	104.4(4)	C(16)-N(4)-C(15)	110.7(12)

D. Anisotropic displacement parameters ($Å^2 \times 10^3$) for **4**. The anisotropic displacement factor exponent takes the form: $-2\pi^2[\, h^2 a^{*2} U_{11} + \ldots + 2\, h\, k\, a^*\, b^*\, U_{12}\,]$

	U_{11}	U_{22}	U_{33}	U_{23}	U_{13}	U_{12}